RECOVERY OF METAL CYANIDES USING A FLUIDIZED BED OF RESIN

ALLAN BERNARD NESBITT

A THESIS SUBMITTED IN FULFILMENT OF THE REQUIREMENTS
FOR THE MASTERS DEGREE IN TECHNOLOGY
(CHEMICAL ENGINEERING)
AT THE CAPE TECHNIKON

SUPERVISOR : PROF. F. W. PETERSEN

THE CAPE TECHNIKON
DECEMBER 1996

DECLARATION

I, the undersigned, hereby declare that the work contained in this thesis is my own original work and has not previously in its entirety or in part been submitted for a degree at any other institution.

A. B. Nesbitt

1 November 1996

PAMIECI PIOTRA

IN MEMORY OF PETER

ACKNOWLEDGEMENTS

Most of the research work contained in this thesis was performed at the Department of Chemical Engineering attached to the University of Stellenbosch. I would like to thank all the technical staff of this Department for their assistance and in particular, Aubrey Atkins and Leander Brand for their technical input into the building of the fluidization plant.

Part of the fluidization test-work was carried out at the Department of Physical Sciences at the Cape Technikon. I owe a deed of thanks to Gamieda Mustapha for her prompt completion of this technical effort undertaken with a great deal of dedication and accuracy.

Finally, I would like to thank my promoter Professor Francis Petersen for his technical input and assistance in acquiring a study bursary from the Foundation for Research and Development.

SYNOPSIS

Metal cyanide complexes are a toxic pollutant in wastewater originating from various industrial and mining activities. The removal/retrieval of cyanide and metal cyanide complexes has been studied by researches for many years, leading to the establishment of a variety of patents. The mechanisms used by these patents vary from purely chemical techniques to those using ion exchange resins.

In this thesis, the feasibility of the recovery of metal cyanide complexes by using a strong base macroreticular resin, in a fluidized bed configuration, has been investigated. The resin in question is presently used in the sugar industry where its main application is the recovery of large organic molecules similar in nature to metal cyanides.

The selected resin was contacted with synthetic solutions of various metal cyanide complexes, for the purposes of evaluating performance in the adsorption thereof. It was found that polyvalent metal cyanide molecules were adsorbed efficiently, while divalent metal cyanide molecules were adsorbed satisfactorily.

The loaded resin was also evaluated for the ease with which the metal cyanides could be removed. It was discovered that a brine solution of pH 7, could effectively remove all metal cyanide complexes. This test-work was of particular importance as it is well known that the removal of metal cyanides from strong base metals is not easily achieved.

To distinguish the fluidization characteristics of the selected resin (or any resin for that matter), a method of modelling the expansion of a fluidized resin bed was proposed, that takes into account the difficulties associated with the hydrodynamic characteristics of a macroporous resin of this nature. The technique is based on the *Serial Model* which is a discretised application of the Zaki and Richardson equation. From the interpretation of the results of a matrix of fluidization tests, it was found that the algorithm proposed could effectively model the expansion of a fluidized bed of ion exchange resin, independently of the dimensions of the accomodating receptical.

Finally, it was shown that the change in the fluidization characteristics of the selected resin, between its chloride and metal cyanide states, could clearly be modelled by the technique referred to above.

CONTENTS

LIST OF FIGURES

LIST OF TABLES

INTRODUCTION

SOUTH AFRICA, THE ENVIRONMENTAL ISSUE AND CYANIDE

The environmental issue in South Africa has developed somewhat differently to international trends. Local legislation concerning the disposal of effluent into the environment has been sluggish in following the world trend towards greater stringency[56]. The politics of the last four decades has been polarised around issues of social aspirations and security, to such an extent, that the national depate on the "green issue" seemed altogether feeble by comparison. The pre 1994 South African government may have rationalised that the added cost of effective environmental management, in terms of industrial development, would have strained an economy already suffering the effects of legislation borne out of the policy of increased national security and sanctions. A further short-fall of South African environmental policy is the ineffective mechanisms, within existing legislation, for dealing with gross offenders. One example of this is the imposition of fines so disproportionately small when compared to the cash flow of an offending industrial plant that it becomes more cost effective for the organisation to simply budget for this fine rather than actually do something about the problem. A pertinent example of this is the 1989 spill of soap skimmings and black liquor into the Ngodwana river from the local Sappi plant, causing the death of thousands of fish as a result of the increased oxygen demand to the system. For this violation Sappi was fined R2000.00.

One can be certain however that the environmental issue will grow in South Africa and given the importants that the post-1994 government attaches to the rights of the individual, there will almost certainly be a move towards legislation designed to encourage stricter environmental management. The topical example of the proposed I.S.C.O.R. plant at Saldana bay which had to be relocated to

accommodate the vagaries of a public becoming more aware of environmental issues, is proof of the greater importance that will be placed on environmental issues in the future. It is notable that, only a few short years ago, the public outcry over the announcement of the construction of the Richards Bay Minerals project, on the Northern Natal coast in the middle of a wild life sanctuary, in very little[57]. Neither the government nor the project planners were moved to change perceived images of industry slowly encroaching into a nature reserve.[57]

Cyanide plays a role in many industries. Without cyanide the refining of minerals, a process upon which the South African economy depends heavily for its prosperity and development, would be enormously expensive. In the same way standard processes used in the galvanising and metal plating industries would also be far more costly. What is clear at this stage is that if the environment is to be protected, legislation controlling cyanide emissions needs to be revised and improved. When this happens industry will be forced to spend money in researching techniques to either destroy or recover cyanide from industrial effluent. The recovery of cyanide, clearly more desirable than destruction, is the subject of this thesis.

CHAPTER ONE
CYANIDE USEFUL AND DANGEROUS

1.1.1 Introduction

The chemistry of cyanide is such that it is able to bond with many different elements. Ford-Smith[1] has shown that at least twenty-eight elements are capable of forming complexes with cyanide with seventy-two metal cyanide complexes being possible. This characteristic makes cyanide a useful facilitator for the mass transport of those metals upon which the successful development of modern national economies depend.

1.1.2 Cyanide and the mineral processing industry.

In 1898[2] the cyanydation process for the extraction of gold from ore was first used in New Zealand and South Africa. So efficient was this process that it is still in use to this day and no doubt will remain an integral part of extraction metallurgy for many years to come. The principal reasons for the prominent place of cyanide in gold ore processing include its availability and the strength and solubility of its gold cyanide complex.

Elsner's equation effectively describes the reversible reaction by which gold is extracted from its ore:

$$4Au + 8NaCN + O_2 + 2H_2O = 4NaAu(CN)_2 + 4NaOH$$

Analogies can be drawn between this reaction which specifically features gold as the transition metal reacting with cyanide and reactions that feature other transition metals, e.g. silver, copper, zinc and nickel. Although it is during the leaching process that cyanide plays its major role, cyanide is also used in the carbon in pulp gold concentration process and in certain base metal flotation processes.

1.1.3 Leaching

The use of cyanide as a facilitator in the leaching of minerals is generally recognised. However, despite the completion of extensive test-work throughout the world, the mechanism of chemical leaching by cyanidation is not well understood. Nevertheless, technology acquired through empirical test-work, together with extensive practical application, have established this technique in mineral processing.

A typical leaching operation(pachuca) would consist of a mechanical or gas agitated mineral slurry, at controlled pH, having free cyanide added to it at a predetermined rate. To achieve this in practice a cyanided slurry, of high pH, would be passed through a train of leach tanks, their size being dictated by the required residence time and slurry through-put rate. As indicated by Elsner's equation oxygen plays a vital role in the leach reaction explaining the uncommon use of far more costly, yet chemically more efficient, air sparged pachucas at certain installations.

1.1.4 Carbon In Pulp

The Carbon In Pulp process (C.I.P.), which generally takes place after, or sometimes during the leach (Carbon-In-Leach/C.I.L.), is well established as the most effective technique for the concentration of the leached gold for the purposes of further refining. Initially, gold is adsorbed as the gold cyanide complex onto coconut shell activated carbon at ambient temperatures and high pH's. This is followed by the removal or elution of the complexes from the carbon, achieved in the presence of an excess amount of cyanide at high pressures and temperatures. The coconut carbon can, after regeneration, be reused a number of times making the Carbon-In- Pulp process suitable for continuous operation in a closed circuit. Carbon-In-Pulp is well understood and is presently in service at mineral processing installations throughout the world. Economic realities and the capital cost of plant modification, despite the recent technological advances in artificial substrates i.e. resin, will ensure that it remains in use for many years to come.

In the application of Carbon-In-Pulp "run of leach train" slurry is passed in series through an "adsorption train" of agitated vessels. Broadly speaking the activated carbon passes through the

same train in a counter current fashion before being separated from the slurry by screening. After separation from the adsorption train the carbon is eluted under pressure and in the presence of excess cyanide, before being returned to the adsorption circuit.

1.1.5 Cyanide in flotation

Another established, yet relatively uncommon process, uses cyanide as a depressant in the flotation of base metal sulphide ores. This leads to the formation of a variety of base metal cyanide complexes e.g. copper and iron cyanide.

1.1.6 The effluent of mineral processing plants

Several different waste-water streams may be produced at a mining/mineral processing operation resulting from run-off, acidic mine water generation, or metallurgical processing. These waste-waters exhibit different characteristics and may require different treatment approaches. However, for the purposes of this literature survey, we take a more general approach to describe the effluent makeup of waste streams. Run-off from the mill site is generally directed to the tailings pond which is the most common method of disposing of cyanide-containing waste in the mineral processing industry. The dumping of (cyanide in) plant tailings and waste streams containing cyanide is minimized by plant managment policy which seeks to improve cost efficiency and to a lesser extent for environmental reasons. Unfortunately, there is always an excess of "free" cyanide in the tailings of mineral processing plants accompanied by a variety of metal cyanide complexes. A further factor to consider is that dilutions with sasonal fluctuation in rainfall, alters the impact the effluent will have on the immediate environment. Fluctuation in effluent concentrations, present in tailing ponds, in tune with local seasonal cycles, is a recognizable phenomenon. Table 1 is a list of ions and their range of concentrations, together with other characteristics of mineral processing plant waste, collated from the results of a global survey.

PARAMETER	RANGE OF CONCENTRATIONS (mg/l)
Arsenic	<0.02 - 10.0
Cadmium	<0.005 - 0.02
Chromium	<0.02 - 0.1
Copper	0.1 - 400.0
Iron	0.50 - 40.0
Lead	<0.01 - 0.1
Manganese	0.1 - 20.0
Mercury	<0.0001 - 0.05
Nickel	0.02 - 10.0
Selenium	<0.02 - 6.0
Silver	<0.005 - 2.0
Zinc	0.05 - 100.0
Total Cyanide	0.5 - 1000.0
Weak Acid Dissociable (Wad) Cyanide	0.5 - 650.0
Free Cyanide	<0.01 - 200.0
Ammonia-N	<0.1 - 50.0
Thiocyanate	<1.0 - 2000.0
pH (in pH units)	2.0 - 11.5
Hardness (as ppm $CaCO_3$)	200 - 1500
Sulphate	5 - 20000
Temperature (in degC)	0 - 35

Table 1[2] Chemical Composition of Barren Decant/seepage solutions

It can be seen from Table 1 that cyanide concentrations in waste streams can reach as much as 1000ppm while copper, nickel, zinc and iron are generally the most prevalent transition metals.

Should there be an excess of free cyanide these transition metals will tend to form the associated cyanide metal complexes:

$$[Cu(CN)_2]^{-1}, [Cu(CN)_3]^{-2}, [Cu(CN)_4]^{-3}, [Ni(CN)_6]^{-2}, [Zn(CN)_4]^{-2}$$

These metal cyanide complexes are termed "Weak Acid Dissociable Cyanides" or WAD cyanide. The copper presented here is assumed to be in the cuprous state, and generally speaking, the copper cyanide complex formed is a function of the availability of cyanide in solution.

In the presence of excess cyanide free iron tends to form:

$$[Fe(CN)_6]^{-4} \textit{ for IRON of the valency [II] state}$$

$$[Fe(CN)_6]^{-3} \textit{ for IRON of the valency [III] state}$$

These cyanide complexes are more strongly bonded and are termed "Moderately Strong Cyanide Complexes" or "MSCC".

It is also clear from Table 1 that in addition to cyanide and metals, metallurgical solutions contain a variety of other compounds of secondary concern, including thiocyanate, ammonia, sulphate, nitrate and cyanate.

Internationally, the imposition of more stringent legislation governing cyanide effluent has come about partly as a result of political and social pressures, and as a result of numerous monitoring campaigns which have shown that the chemistry of cyanidation processes impacts on the characteristics of waste-water sources.

1.2 Cyanide in the electroplating/galvanizing industry

Another consumer of industrial cyanide is the galvanizing and electroplating industry. Zinc, generally consumed as the zinc cyanide ion, offers sacrificial protection of ferrous metals. Zinc's

high electro-negativity ensures that it will be anodic to the substrate, offering protection while there is still zinc remaining in contact with the substrate.

Until recently the cyanide bath for the plating of both zinc and cadmium was almost exclusively used for general plating, and will no doubt be in existence for many years to come. The "Alkaline Zinc Bath", the general term for this process equipment, usually contains a number of chemicals i.e. NaCN, NaOH, $NaCO_2$ and zinc, with the ratio of NaCN/Zn being 1:1.8 on average. Unfortunately, the electroplating process results in the production of highly poisonous byproducts, one of which is zinc cyanide. In countries where legislation governing effluent is strict, some effort is made to destroy or recycle zinc cyanide. Many novel techniques have been proposed mostly in the form of patents for the removal/retrieval/destruction of the zinc cyanide. It is notable that the chemistry of this particular type of cyanide complex is simpler than that of other transition metals. The removal of this complex by ion exchange resin or selective membranes, has been investigated by a number of authors[3, 4].

1.3.1 Dangers of cyanide

Despite the obvious advantages cyanide has in industrial application it is one of the most poisonous substances known to man due to it's asphyxiating properties. The mean lethal dosage for free cyanide for humans ranges from 50 to 200 mg, with death occurring within one hour[5].

By definition[6] a toxicant is a chemical, physical or biological agent which acts upon a living organism producing an undesirable of harmful effect. The level of toxicity measured is dependent upon the organism affected, and the dosage and form of the toxicant. Cyanide sits high on the list of environmentally unfriendly substances. Just as the chemistry of cyanide is complicated so to is the understanding of it's toxicity.

Hydrogen cyanide, a gaseous form prevalent in cyanide systems of low pH, is rapidly absorbed by an organism through ingestion or inhalation and carried into the plasma. It binds strongly to iron, copper and sulphur, the key constituents of many enzymes and proteins important to life processes. The principal compound affected is cytochrome oxidase, an enzyme contained within the cells of

the body and essential for the utilization of oxygen. Its inactivation leads to cellular asphyxiation and tissue death. Since the central nervous system of higher animals has the greatest oxygen requirement, it is they that are the most strongly affected. Suppression of the mechanism for oxygen transfer between cells leads to suspension of all vital functions and death of the organism. The evolution of hydrogen cyanide (gas) occurs when the pH of a system containing cyanide compounds drops. All process systems which contain some form of cyanide therefore are maintained at a high pH, preferably in excess of 10.

$$CN^{-}(soln) + H^{+} \rightarrow HCN(gas)$$

CHAPTER TWO
THE CHEMISTRY OF CYANIDE

2.1 Cyanide has a complex chemistry.

The chemistry of cyanide is extremely complex. The most recognisable form of cyanide is that of the carbon and nitrogen polyatomic anion containing a triple bond thus;

$$-C \equiv N$$

Cyanide is rarely found in this form, preferring to form complexes with transition metals, or ionic bonds with alkali metals and alkali earths. To bring some order to this seemingly vast array of possible combinations, researchers have categorised inorganic compounds of cyanide into subsets partitioned on the basis of similar chemical characteristics:

* *Free cyanide*
* *Simple cyanide compounds*
* *Weak acid dissociable (W.A.D.) cyanides*
* *Moderately strong cyanide complexes*

In addition to these subsets, it should be noted that cyanide can also attach to hydrocarbon chains resulting in a number of organic molecular combinations.

2.2 Free cyanide.

In its simplest form cyanide can be referred to as "free cyanide". Free cyanide has only two molecular forms or species,

$$\left(HCN, CN^{-}\right)$$

The hydrocyanic molecule or hydrogen cyanide and the anionic cyanide molecule. Free cyanide is defined as the forms of molecular and ionic cyanide released into aqueous solutions by the dissolution and dissociation of cyanide compounds and complexes. e.g. the potassium salt

$$KCN + H_2O \Rightarrow K^+ + CN^- \qquad pK_a \approx \infty$$

The reaction between cyanide ion and water is expressed by the following equation:

$$CN^- + H_2O \Rightarrow HCN + OH^- \qquad pK_a = 2.03E-10$$

Hydrocyanic "gas" is only slightly soluble in water and readily dissociates into hydrogen and anionic cyanide at low pHs. The relationship describing the dissociation of hydrocyanic acid vs pH is well known and is displayed in Figure 1. Note how at low pH's the tendency is towards the formation of hydrocyanic gas. As a general rule cyanide solutions should be maintained at a high pH so as to prevent the evolvement of hydrocyanic gas. In industrial practice plant operators, aware of the toxicity of hydrocyanic gas, are ever vigilant of the dangers of falling pH in cyanide solutions. It is also notable that the phenomenon of hydrocyanic gas evolvement at low pH's is used in many processes for the removal of cyanide from solution by acidification / volatilization. Hydrocyanic gas is colourless and has a distinctive almond smell which is readily detected when present in low quantities. However, at high concentrations a persons sense of smell becomes numbed to its presence resulting in a potentially dangerous situation.

2.3 Simple cyanide compounds

These are ionicaly bonded compounds of the cyanide polyatomic anion and alkali earth/metals. They are electrically neutral and are consequently capable of existing in solid form. When placed in an aqueous environment they dissociate into the alkali earth/metal and free cyanide. e.g.

$$NaCN \Rightarrow Na^+ + CN^-$$

$$Ca(CN)_2 \Rightarrow Ca^{+2} + 2CN^-$$

Cyanide produced for industrial purposes is normally supplied as a simple cyanide compound.

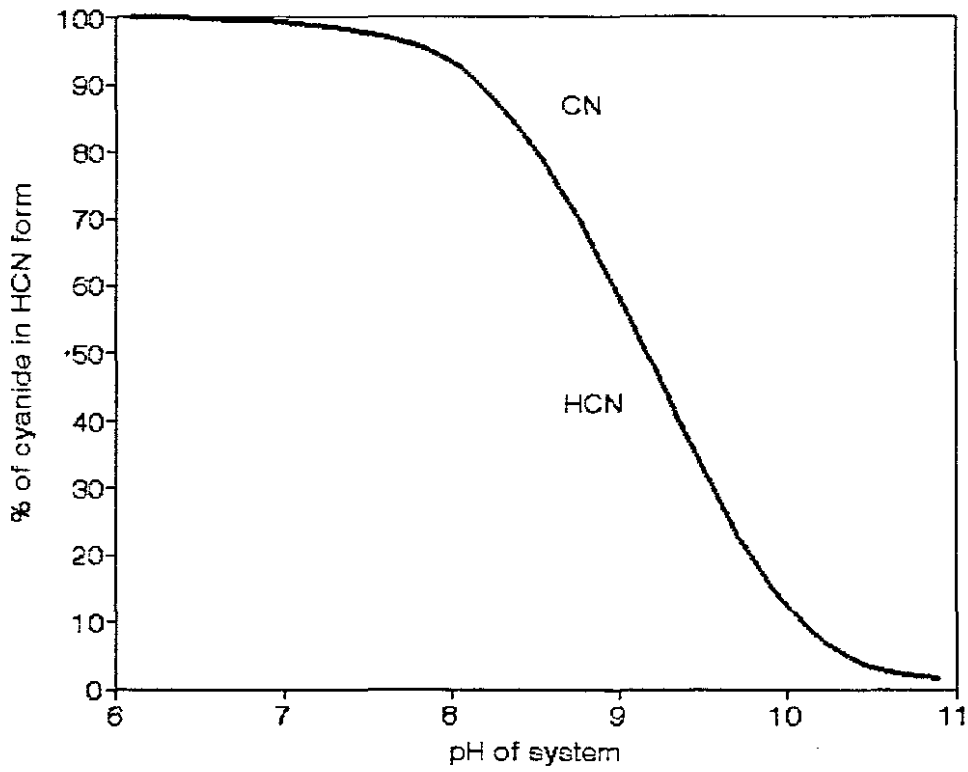

Figure 1[7] Relationship between HCN and CN^- with pH

2.4 Weak acid dissociable (W.A.D.) cyanides

As the name suggests these complex metal cyanides are discernable from others by their tendency to break down (into free cyanide and transition metal) when exposed to a weak acid environment. Examples of these shown in Table 2. Wet chemistry analytical methods for W.A.D. cyanide agree that these metal cyanide complexes are susceptible to breakdown when continuously refluxed for one hour with a pH buffer at 4.5[9]. It is also of note that the analytical techniques referred to include free cyanide in the W.A.D cyanide determination. To obtain an accurate value, the free cyanide should be determined separately and subtracted from the W.A.D. cyanide value obtained. The tendency of these metal cyanide complexes to dissoicate in the environment, readily producing toxic "free cyanide", indicates the degree of danger these complexes present. It is for this reason that W.A.D. cyanide content in a solution is considered to be a reasonable indicator of the toxicologically important complexed cyanides present.

NAME	FORMULA	DISSOCIATION CONST
Tricyanocuprate	$[Cu(CN)_3]^{-2}$	5.0×10^{-28}
Tetracyanonickelate	$[Ni(CN)_4]^{-2}$	1.0×10^{-22}
Dicyanosilverate	$[Ag(CN)_2]^{-1}$	1.0×10^{-21}
Tetracyanocadminate	$[Cd(CN)_4]^{-2}$	1.4×10^{-17}
Tetracyanozincate	$[Zn(CN)_4]^{-2}$	1.3×10^{-17}

Table 2[8] **Weak acid discernable metal cyanide complexes formulas and dissociation constants**

2.5 Moderately strong cyanide complexes

These metal cyanide complexes have higher dissociation constants than those of the weak acid discernable cyanides. Examples are the cyanide complexes of iron, mercury and cobalt (Table 3). These metal cyanides tend to be particularly stable in the absence of light. To analyze for these complexes, dissociation has to be achieved by lowering the pH of solution down to pH 1 and after a suitable reflux time, analysing the quantity of free cyanide produced. This presupposes quantitative knowledge of all W.A.D. and free cyanide present in solution.

NAME	FORMULA	DISSOCIATION CONS
Hecacyanoferrate(III) or Ferricyanide	$[Fe(CN)_6]^{-3}$	1.0×10^{-52}
Hexacyanoferrate(II) or Ferrocyanide	$[Fe(CN)_6]^{-4}$	1.0×10^{-47}
Tetracyanomercurate (I)	$[Hg(CN)_4]^{-2}$	4.0×10^{-42}

Table 3[8] **Strong cyanide complexes formulas and dissociation constants**

2.5.1 The chemistry of iron cyanide complexes

The above-average iron content(Table 1) in mining effluent together with the singular stability of the iron cyanide complex, presents a sound motivation for in-depth examination of iron cyanide chemistry.

As Table 3 indicates there are two possible iron cyanide metal complexes that can form, differing only in the valency state of the iron. Hexacyanoferrate(II) can be manufactured in the laboratory by addition of a soluble ferrous salt or freshly prepared ferrous hydroxide to a solution containing free cyanide. In practice, the reaction appears to be limited to the pH below about 9. The formation of hexacyanoferrate(III) normally occurs as a result of the further oxidation of iron in hexacyanoferrate(II).

Hexacyanoferrates are classified as "inert" complexes, in that their chemical stabilities result from extremely slow rates of dissociation. However, in the presence of ultraviolet light photolysis and hydrolysis occurs, in which a water molecule displaces one of the cyanide moieties in the complex. On prolonged exposure, hexacyanoferrate(II) and (III) have been shown to release up to 85% and 49% respectively of their cyanide respectively[10]. This in effect means that waste-waters containing ferrous or ferric cyanide ions that are exposed to UV light could very well evolve hydrocyanic gas, which in the event of bad ventilation could reach toxic levels.

The driving force for breakdown is the energy in ultraviolet radiation, although visible radiation contributes to the photolysis of iron cyanides to a minor degree. Only 6% of the total electromagnetic spectrum reaching the earth is ultraviolet and in reality the portion of this radiation which penetrates a water surface, in which iron complexed cyanides may be present, is limited. The limiting factors are reported to be attenuation of the UV at the water air interface aid the degree of turbulence present[11]. Only in controlled conditions, where strong solutions of ferrous, or ferric cyanide were subjected to intense amounts of UV radiation, have toxic concentrations of HCN been measured, and then only under circumstances where ventilation was kept to a minimum[12].

2.6 Cyanide bonding and cyanide as a pseudo-halogen[13]

As has already been stated, the cyanide ion is an anion which comprises one atom of carbon and one of nitrogen. It has one sigma bond, two pi bonds and two empty bonding orbitals. The first two orbitals in its structure are filled with the maximum number of electrons, the other orbitals are empty.

As all the "s" and "p" (i.e. 1 + 2) orbitals are filled with electrons the polyatomic ion tends to behave like a halogen (i.e. fluorine, chlorine, bromine and iodine). This behaviour can be seen in the similarity in chemical characteristics between sodium chloride and sodium cyanide.

However, the empty anti-bonding orbitals on the cyanide ion can form bonds with either partially or wholly filled "d" orbitals of transition series metals, which is where cyanide differs from halogen behaviour. The contribution of an electron pair, either from the cyanide ion to the metal or vice versa, is known as "back bonding" and explains the stability of the cyanide metal complexes.

The triple bond of cyanide makes cyanide a relatively reactive compound as these bonds are easily broken. It is the prominence and availability of the pi bond electrons which orbit outwards in a wide arc from the carbon and nitrogen nucleuses that account for its reactivity.

CHAPTER THREE
EXISTING PROCESSES FOR THE RECOVERY/DESTRUCTION OF CYANIDE

3.1 Philosophy behind cyanide retrieval/destruction[14]

Presently there are a number of processes which have been developed for the destruction / recovery of cyanides, some of which have operated industrially. Broadly speaking the current philosophy behind these processes is to retain as much cyanide as possible at minimal treatment cost per ton, by minimizing water consumption and maximizing water recycle and reuse. In addition reagent consumption, if any, should be kept to a minimum.

3.1.1 Processes for the destruction of cyanide

Here are a few examples of process which do not consider the recovery of cyanide but merely their destruction. These are described as processes which, despite being unable to recover cyanide for reuse, could prove economically viable.

3.1.2 Natural attenuation

In the late 1970's, attention was directed towards developing this process for primary treatment of cyanides containing tailings slurries and barren waters. Natural attenuation is a legitimate way of disposal which should be cautiously considered because of the disastrous consequences of misjudgment / mismanagement. It is the most economical method of cyanide destruction especially if tailings impoundment is already employed. Data acquisition, at existing tailing ponds world wide, have proved that cyanide and metal cyanide complexes undergo systematic decomposition when left exposed to the elements[15]. However, the major mechanism in the process of natural cyanide degradation in ponds is volatilization of HCN[16]. The pH of the pond is lowered by the natural uptake of carbon dioxide from the air and by the addition of low pH rainwater that is relatively

saturated with carbon dioxide. This drop in the pH induces a change in the CN^-/HCN balance increasing HCN concentration which then volatilizes.

Variables which affect cyanide decomposition are[15]:

* *pH,*
* *temperature,*
* *UV irradiation,*
* *aeration,*
* *initial cyanide concentration,*
* *metal content*
* *surface area/depth ratio.*

Temperature and aeration have the most significant effect on the volatilization rate of free cyanide in the hydrocyanic form. Data, recorded by Schmidt et al[15], indicates that cyanide decays irrespective of pond depth, although a greater decay time is needed for deep ponds. Smith *et al*[17] also report that surface effects contribute largely to cyanide loss in tailings systems in South Africa. Simovic *et al*[16] also discovered that ultra violet radiation has an effect on the stability and degradation of iron cyanide complexes in surface ponds.

Natural attenuation of cyanides present in tailings and decant waters is in extensive use in South African mineral processing plants.

The advantages of natural degradation of cyanides are:

* *The relatively inexpensive capital cost,*
* *the nonformation of any known toxic by-products, during the degradation process*
* *and it's simplicity and versatility.*

It should be borne in mind that although cyanide and some cyanide complexes decompose readily in the environment, certain cyanide complexes are resistant to natural attenuation or take an extremely long time to decompose and are able to exist for years in the environment e.g. iron and

cobalt cyanides. If such a cyanide complex were to remain dormant for many years it might, after temporary exposure to an oxidizing medium, decompose releasing highly toxic free cyanide into the environment. (e.g. the decomposition of ferricyanide into free cyanide and iron when exposed to UV.) In principle and practice however, present day wisdom holds natural attenuation to be a viable and cost-effective process for removal of free and complexed cyanides.

3.1.3 Alkaline Chlorination[14, 18]

Alkaline chlorination is the oldest and most widely recognized cyanide destruction process, based upon operational experience and engineering expertise. It is a chemical process involving the oxidation and destruction of free and W.A.D. forms of cyanide under alkaline conditions. The chlorine is administered as a solution or as a solid sodium or calcium hypochlorite. The first stage of destruction sees the formation of cyanogen chloride (CNCl) which is then rapidly hydrolysed to cyanate (CNO) assisted by the alkaline conditions. In the case of Cloride gas addition to sodium cyanide solution, the following reaction represents the first stage:

$$Na(CN) + Cl_2 \Rightarrow (CN)Cl + NaCl$$

Further hydrolysis of the cyanogen chloride (stage 2) to cyanate is represented by the following:

$$(CN)Cl + 2NaOH \Rightarrow NaCNO + NaCl + H_2O$$

Finally, the cyanate is hydrolised of the cyanate to ammonia and carbonate:

$$2NaCNO + 4H_2O \Rightarrow (NH_4)_2CO_3 + Na_2CO_3$$

If excess chlorine is used the ammonia will react further through the process of breakpoint chlorination to yield nitrogen gas thus:

$$(NH_4)_2CO_3 + 3Cl_2 + 6NaOH + 6NaOH + Na_2CO_3 \Rightarrow N_2 + 6NaCl + 2NaHCO_3 + 6H_2O$$

Exceeding breakpoint is not desirable, as an inefficient excess of chlorine is consumed.

The disadvantage of the alkaline chlorination process is that it is only effective on free cyanide and weak metal cyanide complexes. To effectively achieve the destruction of more stable metal cyanide compounds i.e. cobalt and ferric cyanide, addition of ultra violet light and/or an increase in temperature is necessary. As this is impractical in large operations, the alkaline chlorination process is said to be effective only on cyanide waste waters which have a low iron and cobalt content. The process has however been used at eight mining operations in the United States and Canada[55].

3.1.4 Copper Catalysed Hydrogen Peroxide Process[20]

This process was patented by DuPont in 1974 and involves the contacting of the waste solution with a 41% solution of hydrogen peroxide containing a few parts per million of formaldehyde and copper. A second, very similar, process was developed by Degussa Corporation which uses hydrogen peroxide and a few parts per million of copper sulphate. In essence the hydrogen peroxide oxidizes the cyanide in the W.A.D. metal cyanide complexes and free cyanide, in the presence of copper, to cyanate. In the case of the W.A.D metal cyanides the released metals are precipitated as hydroxides. The ferrous cyanide compounds combine with the free copper in solution to form an insoluble complex.

Oxidation of the cyanide to cyanate:

$$CN^- + H_2O_2 \Rightarrow OCN^- + H_2O \quad (copper)$$

Oxidation of the W.A.D. cyanide complexes:

$$M(CN)_4^{-2} + 4H_2O_2 + 2OH^- \Rightarrow M(OH)_2(\downarrow) + 4OCN^- + 4H_2O$$

where M is cadmium, copper, nickel or zinc

Reactions of the iron cyanides:

$$2Cu^{2+} + Fe(CN)_6^{-4} \Rightarrow Cu_2Fe(CN)_6(\downarrow)$$

Ditto the cyanate

$$OCN^- + 2H_2O \Rightarrow CO_3^{-2} + NH_4^+$$

This type of process is at present in operation at various installations throughout the world and has shown, through extensive toxicity testing, to yield environmentally acceptable effluents in the country on application.

The advantages of this process are;

* *Simplicity,*
* *low capital cost,*
* *the existence of an extensive body of knowledge, as a result of a number of operating plants, coupled with available technical support from Dupont and Degussa.*

The disadvantages of this process are

* *Excessive reagent costs, i.e. copper sulphate and hydrogen peroxide.*
* *cyanide is not recovered but merely destroyed while ammonia, thiocyanate and precipitated metals may require further treatment to satisfy environmental standards in the country of application..*

3.1.5 Sulphur Dioxide/air cyanide destruction process (INCO process)[19]

The "INCO" process is based upon conversion of W.A.D. cyanide to cyanate using mixtures of sulphur dioxide and oxygen in air, in the presence of elevated copper concentrations and in a controlled pH range.

This reaction is postulated to be:

$$CN^- + SO_2 + O_2 + H_2O \Rightarrow CNO^- + H_2SO_4 \quad (copper)$$

The iron complexed cyanides are reduced to the ferrous state and continuously precipitated as insoluble metal ferrocyanide salts of the general formula $M_2Fe(CN)_6$, where M can be copper, nickel of zinc.

Reduction:

$$2Fe^{3+} + SO_2 + 2H_2O \Rightarrow 2Fe^{2+} + 4H^+ + SO_4^{-2}$$

or

$$2Fe(CN)_6^{-3} + SO_2 + 2H_2O \Rightarrow 2Fe(CN)_6^{-4} + 4H^+ + SO_4^{-2}$$

Precipitation:

$$2M^{2+} + Fe(CN)_6^{-4} + H_2O \Rightarrow M_2Fe(CN)_6 \cdot H_2O(\downarrow)$$

where (M^{2+} is copper, nickel, or zinc)

The residual metals liberated from the cyanide complexes are precipitated as their hydroxides. Developed thiocyanate can be removed as well, but only after cyanide has been removed although this requires greater retention times and reagent usage. The sulphuric acid produced by this process is neutralized using lime or caustic.

The advantages of this process are:

* *Its proven success in treating pulps, clarified barren and decant solutions and heap leach rinse solutions,*
* *the availability of technical support from INCO personnel and its effectiveness at removal of all cyanides plus heavy metals by precipitation.*

The disadvantages of this process are;

* *The reagent costs,*
* *non recoverability of cyanide,*

* *excessive production of gypsum,*
* *requirement of a detailed study of the chemistry for any one particular application,*
* *royalty payments as a result of the world wide patent established by INCO on the process.*

This process can be closely compared to alkaline chlorination and the copper catalysed hydrogen peroxide processes. These three processes represent the preferred and most studied chemical treatment options.

3.1.6 Biological Treatment of cyanide wastes

Biological processes have been proven effective for treatment of solutions containing relatively high concentrations of free cyanide, it is only recently that they have been utilized in the treatment of mining effluents, containing metal cyanides[21]. Biological treatment of cyanide tailings result in the total removal of all cyanides including W.A.D. and stable metal cyanides. Cyanides and metal cyanide complexes are removed through a combination of oxidation and sorption into the biofilm. The metals present in the waste-water are removed through a combination of coagulant addition and adsorption onto the biofilm. Ammonia is converted to nitrate by the nitrification process. The organisms responsible for cyanide breakdown have been identified as various species of Pseudomonas which, during the course of many decades, have adapted to the elevated concentration of cyanides and thiocyanate they have been exposed to. The Biological process for the breakdown of metal and free cyanides involves the oxidative breakdown of cyanides and thiocyanate, and subsequent adsorption/precipitation of the free metals into the biofilm in a more general form thus;

$$M_xCN_y + 2H_2O + \frac{1}{2}O_2 \Rightarrow M\text{-}biofilm + HCO_3 + NH_3$$

where M = iron, copper, nickel or zinc

$$2SCN^- + 4H_2O + 5O_2 \Rightarrow 2SO_4^{2-} + 2HCO_3^- + 2NH_3$$

The second step of the assimilation converts ammonia to nitrate through conventional nitrification thus;

$$2NH_4^+ + 3O_2 \Rightarrow 2NO_2^- + 4H^+ + 2H_2O$$

$$2NO_2^- + O_2 \Rightarrow 2NO_3^-$$

The advantages of Biological cyanide degradation are:

* *The simplicity of the design,*
* *the environmentally acceptableness of the process,*
* *the relatively low cost of reagent consumption.*

The disadvantages are:

* *The higher capital costs,*
* *the lack of application in industry,*
* *that cyanide is not recovered.*

It should also be borne in mind that, unlike other chemical treatment processes, biological processes tend to be adversely affected by cold temperatures making biological treatment unwieldy in areas where ambient temperaturesare subject to large seasonal or even daily changes.

3.2 A chemical process for the recovery of cyanide

Metal cyanides characteristic breakdown on exposure to an acidic medium, followed by the volatilization of free cyanide makes total recovery possible.

3.2.1 Acidification, Volatilization and Re-adsorption (A.V,R.) [22]

The characteristic of cyanide and some metal cyanide complexes to decompose in an acid environment is used effectively in this process. The acidification of cyanide waters results in the generation of HCN which volatilizes off as a gas assisted by heating or air sparging. The volatility of free molecular cyanide (HCN) is related to its Henry's Law constant, which is affected by several factors including liquid medium viscosity, hydrogen bonding, pH and temperature. After volatilizing, the gas can be reabsorbed in an alkaline medium i.e. caustic or milk of lime spray. The acidification reaction for free and ionic cyanide is:

$$Ca(CN)_2 + H_2SO_4 \Rightarrow 2HCN + CaSO_4$$

and for metal cyanides (W.A.D.) is:

$$M(CN)_2 + H_2SO_4 \Rightarrow 2HCN + M^{2+}SO_4^{-2}$$

The volatilization of free cyanide proceeds thus:

$$HCN / H_2O \Rightarrow HCN / Air$$

There are several factors which affect the rate and extent of HCN removal from slurries or solutions through air stripping these are:

The pH of the solution
The form of cyanide
The concentration of cyanide
The temperature of the slurry or solution
The pressure maintained within the recovery system
The air-to-liquid ratio

The mechanical dispersion equipment

The viscosity of the solution or slurry

The liquid-to-air contact period

The absorption reaction proceeds thus:

$$HCN + NaOH / \frac{1}{2}Ca(OH)_2 \Rightarrow NaCN / \frac{1}{2}Ca(CN)_2 + H_2O$$

Precipitation / re-neutralization as hydroxide, with respect to all W.A.D. cyanide metal groups is as follows:

$$M^{2+} + 2OH \Rightarrow M(OH)_2$$

Precipitation of iron complexes is as follows:

$$Na_4Fe(CN)_6 + 2CuSO_4 \Rightarrow Cu_2Fe(CN)_6 + 2Na_2SO_4$$

The process saw extensive (50 years) use at the Flin Flon Mine operated by the Hudson Bay Smelting and Mining Company where it was used to recover cyanide from barren clarified solutions for economic reasons rather than environmental. Here the process was known by its original name i.e. the Mills Crow process[23]. The preferred reagents, because of the ease of procurement, were sulphuric acid for the acidification and lime for the adsorption.
One of the major faults of this process is the excessive build-up of mainly gypsum as well as copper and thiocyanate precipitates. This was observed during operations at Flin Flon mine which resulted in the generation of yet another environmental liability. The build up of precipitates within the plant workings required the Flin Flon plant to shut down every 2 to 4 months for manual cleaning.

Although, in the twenty years leading up to 1985, the process had been extensively studied and improved upon, researchers had not attempted to adapt the technology to the processing of

mineral slurries thereby effectively preventing application of the process in the mineral processing industry.

The Cyanisorb Process, which is loosely based on the Mille Crows process or A.V.R. and was invented in the years following 1985, claims that A.V.R. can be used on mineral slurries. Smith *et al*[14] report a number of successful pilot plant campaigns and that the first commercial full scale cyanisorb plant was due to come into operation at the Golden Cross Mine in New Zealand in 1991. The patent for the Cyanisorb Process is held by Cyprus Minerals of New Zealand[24].

The advantages of this process are:

* *Its efficiency in recovering all W.A.D. cyanide complexes and free cyanide for reuse,*
* *consumption of easily obtainable reagents,*
* *its robustness i.e. not effected by input variable fluctuations and able to process slurries as well as decant waters.*

The disadvantages are:

* *The hazards associated with the presence of hydrocyanic gas,*
* *high capital outlay,*
* *inability to remove stable metal cyanides.*

3.3.1 The recovery of cyanides using ion exchange resin

Many processes using ion exchange resins for the recovery of cyanide/cyanide metal complexes from unclarified/clarified solutions have been developed. Some of which have seen large scale industrial application especially in the plating and galvanizing industry. Some of these are described in the following sections which also contain pertinent comment.

The overall advantage of ion exchange processes is the ability of the resin to adsorb ions, such as cyanides that are present in small concentrations, quickly, thus facilitating the concentration

thereof. Another advantage is that, unlike with chemical techniques for the recovery of cyanides, there are no solution based toxic intermediaries produced e.g. cyanate and thiocyanate.

Concentration of cyanides is a necessity if the waste solution being processed is of a large flowrate and/or contains only a very small, yet toxic, quantity of cyanides. Chemical techniques are at a distinct disadvantage in this regard requiring excessive quantities of reagent to process an effluent of this nature.

3.3.2.1 Carlson process (pat. 1982)[4]

The Carlson process is a complicated process designed to remove toxic metals and cyanides from waste waters, especially the effluent of plating baths, by passing the contaminated liquid upward through three separate resin layers in succession. The physical characteristics of each resin group is such that clasification is easily achieved by hydrodynamic forces. The inventors suggest that the proportions of each of these resins will be dictated by the nature and quantitative character of the undesirables in the effluent.

The three resin types, in order of contact with the feed solution, are;

* *A strong base anion exchange resin,*
* *a weak acid cation exchange resin,*
* *a strong acid cation exchange resin.*

The strong base resin should preferably be a Type I, with quaternary ammonium functional group:

$$R - N^{+} - (CH)_3$$

or

$$R - N^{+} - (CH_2 - CH_3)_3$$

The weak acid resin is a carboxylic type:

$$R - COO^-$$

and the strong acid resin is the standard sulfonic type:

$$R - SO_3^-$$

The resins are regenerated in a two phase operation. Initially, a strong acid solution(i.e. hydrochloric acid) is used to put the cation resins into the hydrogen form and the strong base resin into the chloride form. The second stage is a caustic wash, where caustic solution is passed through at least a portion of the bed, converting the strong base resin to the hydroxyl form and the weak acid resin to the sodium form. The strong acid resin is unaffected by this.

A further aspect of this patent is the acidification of the product of resin regeneration resulting in the formation of hydrocyanic gas which in turn is contacted with a caustic solution in a gas liquid contactor for cyanide recovery.

3.3.2.2 Comments

It is of interest to note that, in it's published examples of effluent treatment, the patent release document concentrates on the effluent of plating baths rather than mining effluent and also gives no indication of the number of regeneration cycles that could be undertaken before the active sites become ineffective. This, combined with the reality that hydrochloric acid and caustic soda are relatively expensive reagents, could make the cost of this process too high for use in larger industrial installations, such as a large mineral processing plant. A number of authors have reported that one of the realities of metal cyanide removal from solution by adsorption onto strong base resin is that elution of the cyanide complex during the regeneration procedure is not easily achieved[26]. The report describing the Carlson patent makes no comment on this nor is it clear about how the strong acid resin is prevented from being converted to the sodium form during the caustic wash. Possibly the regenerant is only passed through a section of the bed.

3.3.3.1 Witteck Development (pat. 1986)[26]

This invention relates to the recovery of cyanide reagents for reuse, from waste solutions bearing soluble metal complexes. More particularly, the invention is directed to the recovery of cyanide from gold mill effluent solutions which contain a mixture of free cyanide and complex heavy metal cyanides.

The effluent is passed through a bed of anion exchange resin which may be of the weak or strong base type, but should have a macroporous structure and be in the sulphate form. The patent does not stipulate any specific functional group. All cyanide metal complexes i.e. zinc, copper, iron and nickel are readily absorbed, while free cyanide passes through the bed. The product of this ion exchange process can, after spiking with free cyanide, be readily reused in the further leaching of ores as it is devoid of most metal complexes and has some residual free cyanide in solution. The inventor suggests that the process be semi-batch, in that resin beds alternate between the loading and the regeneration stages, with the extent of resin loading being determined by monitoring for breakthrough.

Regeneration of the resin is achieved by passing a dilute solution of sulphuric acid is passed up-wards through the bed displacing the metal cyanide complexes and returning the resin to the sulphate form. The effluent of the regeneration process is then fed into a liquid-gas contactor, where air is used to assist in the volatilization of all the hydrocyanic gas. The hydrocyanic gas-rich air is then passed up-flow through a caustic scrubber, where the HCN is absorbed into solution. The caustic feed to the scrubber could either be an independantly made up solution of caustic, or more conveniently be the effluent solution of the loading cycle.

An important aspect that characterises this patent, is the spiking of the regenerant solution with an oxidant such as hydrogen peroxide, potassium peroxide, sodium peroxide, or ozone, so as to facilitate the controlled oxidation of the metal ion of the metal cyanide complex adsorbed under controlled oxidation conditions. The inventor also suggests that the regeneration process may be more efficiently achieved and controlled by the introduction of an oxidant at a rate sufficient to

maintain a redox potential of +500 mV (measured against a standard calomel electrode) in the regenerant solution.

3.3.3.2 Comments

What is not pointed out by the inventors of this patent is the importance that should be attributed to the controlled rate of injection of oxidants into the regenerant solution, as an excess of oxidant could well result in damage to the amines, of the active sites on the base resin, through chemical oxidation thereof. In addition there is no mention, in any of the listed examples of trial runs, of how many cycles a single quantity of resin can experience before permanent chemical degradation renders the resin useless.

3.3.4.1 The GM-IX process 1987[3]

This process advocates the use of an ion exchange resin in conjunction with a gas membrane module to selectively recover cyanide from the spent regenerant solution. The process is predominantly concerned with the recovery of cyanide from a solution where the cyanide is complexed with zinc. This effluent is found to be the by-product of a variety of industries such as, iron and steel manufacturing, photographic bleaching and metal plating and finishing, all of which generate substantial volumes of cyanide-bearing waste-water.

The waste-water solution is passed through a bed of strong base resin which is in the sulphate form. The anionic zinc cyanide complex and the free cyanide are readily adsorbed by the active sites on the resin, producing an effluent free of zinc cyanide complexes and free cyanide. The regeneration process is accomplished by continually circulating a dilute solution of sulphuric acid through the resin bed over a long period of time, a necessity, given the slow kinetics of desorption.

To remove the developed hydrocyanic acid from the desorption circuit, the acid is passed over a gas permeable membrane which has a solution of caustic soda circulating on the opposite side. Forces of diffusion cause the hydrocyanic gas to pass through the membrane, be readily absorbed

by the caustic and, with time, completely removed from the acid circuit. Once adsorbed in the caustic circuit the free cyanide can potentially be reused as sodium cyanide solution.

The authors give no indication of the type and nature of the active functional group to be used, although, according to the AMBERLITE GENERAL PRODUCT DATA SHEET, the resin used in the published example has the "tri-methyl ammonium" functional group.

3.3.4.2 Comments

Although being a highly efficient and novel technique for the removal of cyanide, a disadvantage of this process is the slow rate of elution kinetics. This is borne out by figures given in an example[3] which uses a strong base gel type resin IRA400. The researchers also limited their test-work to the zinc cyanide complex found in effluents produced by the listed industries. The mineral processing industry however, produces effluents with a great number of different metal cyanide complexes (i.e. Table 1). It is reasonable to assume that the outcome of further test-work may prove this process to be effective in the removal of metal cyanide complexes other than zinc. Further investigation into the type of resin and functional group will play a large role in defining potential possibilities for this process.

3.3.5.1 The Coltinari Process 1985[27]

This process uses a weak base anion exchange resin to remove cyanide metal complexes from dilute cyanide solution while the free cyanide is allowed to pass through and can ether be reused in the process, or sold as a useful by product. Although the author gives no indication of the functional group it is assumed that a di-methyl or -methy ammonium group is used:

$$R - N - (CH)_2 \qquad \text{or}$$

$$R - N - (CH_2 - CH_3)_2$$

The inventor moots the idea that if it is desirable to remove the free cyanide, the feed to the resin bed could be spiked by some metal salt so as to generate further metal complexes which in turn will be adsorbed. After adsorption onto the resin the cyanide complexes are then eluted from the resin using a milk- of-lime solution, producing a cyanide-rich eluate. Complete elution is accomplished by recycling the eluting fluid past a bed of solid calcium hydroxide, so as to maintain the eluting fluid in calcium hydroxide saturation. The recycling results in a high concentration of cyanide being attained in the eluate. This eluate is then subjected to an acidification / volatilization process, with acidification being achieved preferably with sulphuric acid. The inventer points out that those more stable cyanide complexes such as ferro- and cobaltocyanide will not be susceptible to acidification and despite not being recoverable will at least be concentrated in the acidified eluate for disposal. The hydrocyanic gas product of the acidification / volatilization step is effectively removed from solution by heating and air-sparging. The author does not indicate how the hydrocyanic-rich off- gas is to be further processed. However, it is assumed that it could be contacted with some sort of alkali solution in a liquid-gas contactor to facilitate the cyanide realizing a more useful form.

3.3.5.2 Comments

The inventor does not make any comment on how one is to dispose of the large quantities of gypsum that will be generated during the acidification process, that is if the suggested sulphuric acid is to be used. Further concerns could be voiced on heating large quantities of acidic solution. Even if utility steam were available, such action would represent a massive energy consumption seriously affecting the economic feasibility of this patent. In addition the author gives no indication about how to treat the iron cyanide complexes prevalent in the waste streams of mineral processing plants that will clearly not be removed by this process.

3.4.1 A short history of research into ion exchange technology for the recovery of cyanides from mining effluents

The use of anion exchange resins for the removal of free and complexed cyanides from solution was first scientifically investigated in detail in 1959[28]. Industrial trends in the seventies, towards more stringent effluent regulations, resulted in renewed interest in the treating of Canadian gold mining cyanide effluent[29]. It is well understood that the affinity of a resin for a specific ion increases with increasing charge on the resin and the anion being adsorbed. As a result, the di- and tri-valent negative metal cyanide complexes are removed in preference to free cyanide. Early investigations[28] found researchers removing cyanide by converting free cyanide into the copper cyanide complex by the addition of elemental copper and then adsorbing it onto strong base resin in this form.

Since the middle seventies most of the work done[4, 31, 32] on the recovery of metal cyanides has been performed using strong base quaternary amine resins in the Duolite and Amberlite range. However, a weak base resin has also been investigated[30].

The results of a substantial test program undertaken at the Homestake Mining Company from 1980 to 1983 demonstrate that strong base resins were by far the most effective for the removal of metal cyanides[35]. These tests also indicated problems with resin regeneration and with the evident trend of rapid loss in adsorption capacity with continuous loading and regeneration cycles. A further problem encountered was with competitive adsorption between thiocyanate and the metal cyanides. Despite these problems ion exchange was considered a good polishing process for the treatment of metal complex cyanides present at concentrations of only a few ppm but not for any greater ion exchange duties.

3.4.2 More recent developments

The last five years have seen a number of researchers studying the recovery of metal cyanide using strong base ion exchange resins such as IRA958[34], and GT-73 (Mudder unpublished data[35]).

3.4.2.1 The work of Smith and Mudder

Mudder et al[35] reported that IRA958 was ineffective in both metals and cyanide removal especially in the presence of high concentrations of sulphate and thiocyanate i.e. 1500 and 30 ppm correspondingly. Mudder reported GT-73 to perform excellently when exposed to the identical conditions. The results of this test work are given in Table 4. Further test work on regeneratability and possible poisoning trends were not done.

effluent parameters	influent conc. (mg/l)	effluent conc. after 48Hours	effluent conc. after 96Hours
total cyanide	1.7	0.19	0.49
WAD cyanide	1.2	0.19	0.11
Cu dissolved	0.39	0.01	0.01
Hg dissolved	0.014	<0.005	<0.005
Ag dissolved	0.9	0.01	0.01
Zn dissolved	0.09	0.02	0.04
Ammonia as N	18.6	———	16.7

Table 4[35] **Results of the ion exchange experiments employing ion exchange resin GT-73**

3.4.2.2 Results of work by this author

The test which forms the nucleus of this thesis, has shown IRA958 to be very effective in the adsorption of Polyvalent valent metal cyanide complexes even in the presence of a large concentration of sulphate i.e. 1000ppm. Effective regeneration was found to be straight forward

and could be achieved by a simple brine solution where the major solute component is industrial sodium chloride.

3.4.3.1 The Cy-tech exchange system[35]

This system is the most recent cyanide recovery process involving ion exchange. The company that operates this system is Cy-tech and to date only a single plant has been commissioned. This is a recovery unit in Quebec Canada[35] the capacity of which is five cubic meters of effluent per hour. No indication of the concentration of dissolved cyanides is given.

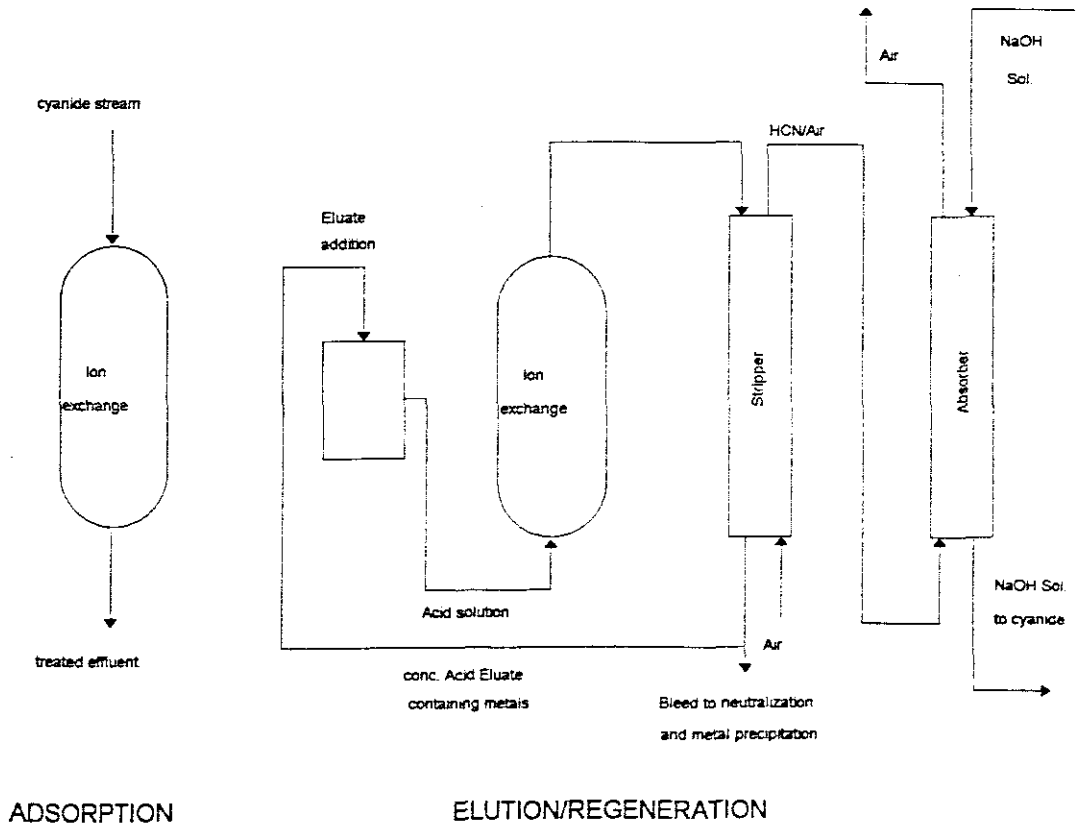

Figure 2[35] **Cy-Tech system for ion exchange recovery of cyanide**

Not much has been published about this system but a diagram of the plant is available which features an ion adsorption section, through which the treatable effluent passes, followed by a regeneration/elution section in which acid is used to remove the cyanide complexes.

The resin used is a strong base ion exchange resin which readily adsorbs the metal cyanides thus:

$$2(Resin^{+}X^{-}) + M(CN)_4^{-2} \Rightarrow (Resin^{+})_2 M(CN)_4^{-2} + 2X^{-}$$

Regeneration/elution with dilute sulphuric acid proceeds thus:

$$(Resin^{+})_2 M(CN)_{4-2} + 2H_2SO_4 \Rightarrow (Resin^{+})_2 SO_4^{2-} + 4HCN + MSO_4$$

The spent regenerant is treated in a stripping column producing a hydrocyanic-rich off gas which is then absorbed by a caustic solution in an absorber unit.

3.4.3.2 Comment

It is difficult to comment mainly due to lack of detailed information about the process. However Mudder *et al*[35] report that a company has been established which earns it keep directly from the profitability of this process.

CHAPTER 4

ION EXCHANGE TEST-WORK ON IRA958

4.1 Introduction to the ion exchange study

The rate of Ion exchange between solid and liquid phase, in a resin in solution application, is controlled by a number of factors:

* *Diffusion of ions through the liquid film surrounding the particle.*
* *Diffusion of ions through the pores of the polymeric matrix of the resin.*
* *Attachment to the functional groups on the resin matrix.*

In most instances one of the resistances above offers much greater resistance than the others, and hence becomes the rate controlling, or rate limiting step. There are standard techniques to discover which is the controlling step, for any particular set of circumstances:

* *Altered levels of agitation in the vicinity of the solid phase, (will increase/decrease film controlling resistance)*
* *The interruption test. (will indicate pore diffusion controlling resistance)*

In the initial stages of a kinetic study, the laminar layer is rate controlling and hence it is at this point that its resistance can be determined. In addition when convection in the solution is slight and/or the degree of polymer cross-linking within the resin structure is low i.e. large interstitial spaces(pores) in resin structure, the main resistance to mass transfer could also be in the laminar layer. Resin IRA958, the subject of this thesis, has very large interstitial spaces. So we expect low capacities and maximum allowance for large strongly negative molecules. The AMBERLITE GENERAL PRODUCT DATA SHEET reports the following for IRA958:

Capacity	0.50 eq/l (per litre of resin)
Density	1.08 kg/l (per litre of resin)

4.2 The history and development of resin IRA958

A strong base resin IRA958 was initially developed by Rohm and Haas specifically for the recovery of the iron cyanide complex[36], although there have been some reports of poor performance[35]. One of the existing problems with strong base resins, in the adsorption of iron cyanides, was the difficulty associated with the slow kinetics of desorption. To overcome this problem greater emphasis was placed on the size of the resin's pore structure and to the overall strength of the matrix. The sheer size of the iron cyanide molecule and the strength of its ionic charge requires attention to these characteristics of the resin. A further development was that sodium chloride was found to be an excellent elution reagent whereby the chloride ion with its strong electro-negativity effectively displaces the iron cyanide complex[36].

4.3.1 The porosity of IRA958 resin

IRA958 is a strong-base, macroporous resin which has a crosslinked acrylic copolymer matrix(very large pore sizes). Currently, it sees application in sugar refining plants, where its chief function is the adsorption of large organic molecules, similar in size and nature to metal cyanide complexes. As IRA958 presently has a confined application its production is limited. The active site of the IRA958 is the tri-methyl ammonium group.

4.3.2 Functional group of IRA958 resin

There is evidence that by varying the functional group of the adsorbent resin, selectivity can be achieved on the basis of ionic valency[37]. Resins with tri-ethyl ammonium groups (Figure 3) have been shown to be more selective towards the mono- and bi- valent metal cyanides. e.g. $Au(CN)_2^{1-}$ and $Ni(CN)_4^{-2}$, while, the tri-methyl ammonia functional group (Figure 4) tends to attract the multi-valent metal cyanide complexes e.g. $Fe(CN)_6^{-3}$, $Cu(CN)_4^{3-}$. Based on this it is reasonable to assume that IRA958 will have a greater affinity for the polyvalent metal cyanides than the mono- and bi-valent cyanides. As these complexes contain the greater quantity of cyanide molecules, there can

be no doubt that tri-methyl ammonia group is the more desirable for the purposes of cyanide recovery.

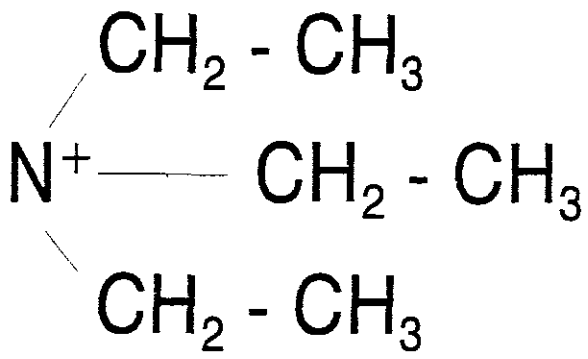

Figure 3. Tri-ethyl ammonium group

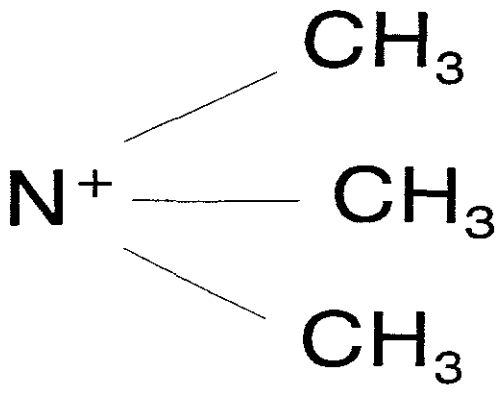

Figure 4. Tri-methyl ammonium group

4.4 The metal cyanides used for adsorption and desorption test-work

It was decided to evaluate the adsorption and desorption characteristics of strong base resin IRA958 by contacting the resin with solutions of specifically chosen metal cyanides in a contantly stirred batch reactor. The disappearance (in adsorption) and appearance (in regeneration) of these complexes would be observed for the purposes of evaluating the performance of IRA958. Four metal cyanide complexes were selected to represent the bulk of metal cyanides shown to be prevalent in the waste of mineral processing plants(Table 1). These were the cyanide complexes of nickel, iron, copper and cobalt.

4.4.1 Iron and copper

Iron and copper were chosen chiefly because of their reported above-average concentrations in the effluent of mineral processing plants and for their polyvalent character. It is also notable that iron cyanide solution has a distinctive yellow/green colour that alters in intensity with changing concentration. This phenomenon makes for easy visual qualitative evaluation. The iron and copper cyanide complex solutions are also relatively easy to obtain. The iron cyanide complex is acquirable as ferricyanide from potassium hexacyanoferrate(III), thus:

$$K_3Fe(III)(CN)_6 \Leftrightarrow 3K^- + [\ Fe(III)(CN)_6\ ]^{3-}$$

while the copper cyanide complex is manufactured from copper(II)cyanide and the addition of a stoichiometric quantity of potassium cyanide, thus:

$$Cu_2(CN)_2 + 6KCN \Leftrightarrow 6K^- + 2Cu(CN)_4^{3-}$$

4.4.2 Nickel

The nickel cyanide complex was chosen because of its prevalence in mineral processing waste and its divalency. Its divalency, it was expected, would result in the observation of the reported lesser affinity of IRA958 for this complex, as a result of the tri-methyl ammonium group active sites[37]. The nickel cyanide complex solution was also easily obtained by the dissolution of potassium tetracyanonicklate(II) hydrate, forming the tetracyanonickelate(II) complex, thus:

$$K_2Ni(CN)_4.H_2O \Leftrightarrow 2K^+ + Ni(CN)_4^{2-}$$

4.4.3 Cobalt

The cobalt cyanide complex was chosen because of a reported polymerization tendency, at pH below nine, once adsorbed onto strong base resin[38]. Such a phenomenon would seriously impede any regeneration of the resin, rendering it useless for further adsorption. It was postulated that, as a solution of brine / sodium chloride would be used for regeneration having a pH of not less than seven, the polymerization tendency may well not be severe. The preperation of the cobaltic-cyanide complex was achieved by reacting cobaltosulphate at room temperature with potassium cyanide in solution thereby producing the cobaltic hexacyanide complex, thus:

$$6CN + CoSO_4 \Leftrightarrow SO_4^{2-} + Co(CN)_6^{4-}$$

4.5 Adsorption test-work

The cyanide complexes of nickel, iron, copper and cobalt were adsorbed separately onto IRA958 in stirred batch reactors and in the presence of excess cyanide. The transition metal concentrations used in each test were similar to the average concentrations found in the effluent of mineral processing plants throughout the world and the amount of resin used was sufficient to adsorb approximately two thirds of the metal cyanides present. The reason for this was so that the kinetics at resin saturation could be observed. The four synthesised metal cyanided solutions described above were used in separate batch adsorption tests carried out a 1,5 litre baffled beakers, agitated by a magnetic stirrer. As the kinetics of adsorption for each of these complexes are compared, special attention was given to ensuring that the geometric configuration and agitation power input per unit volume, for each test, was identical. This was achieved by completing each test separately at identical stirring speed and temperature.

The adsorption test was started by adding a quantity of resin in the chloride form to each beaker calculated to adsorb two thirds of the metal cyanide present in solution at saturation. Eight grab samples were then taken at increasing time intervals, while a ninth sample extracted at twenty four

hours was concidered to give an equilibrium value, despite there being no percivable change in concentration at the 8 hours.

4.5.1 Adsorption in the presence of sulphate

All tests were then repeated under identical conditions with the addition of 2.22g sodium sulphate, so as to attain a concentration of 1000ppm sulphate in solution. Sulphate, like the metal cyanide complexes, is a polyatomic anion and according to data published by Smith and Mudder[2](Table 1), is present in high concentrations in mineral processing effluent. It was therefore considered pertinant to carry out this test as evidence of interference, during the adsorption of metal cyanides, caused by the presence of the sulphate ion, would be notable.

4.5.2 Results of adsorption test-work

The results of the first set of adsorption tests(Figure 5), where no competing anions were present, indicated that all of the cyanide complexes tested, are readily adsorbed onto IRA958. The second set of adsorption tests(Figure 6) demonstrated that even in the presence of a large excess of sulphate(1000ppm), all four metal cyanides were still found to be preferentially adsorbed. In both sets of tests rapid kinetics were observed while the equilibrium value of the $Ni(CN)_4^{-2}$ complex appeared to be affected by the presence of sulphate. This situation could be attributed to the bivalent state of the nickel cyanide complex for which the tri-methyl ammonium group has a lower affinity(See 4.3.2). It is interesting to note that almost 90% of equilibrium value is attained within one hour of the commencement of adsorption.

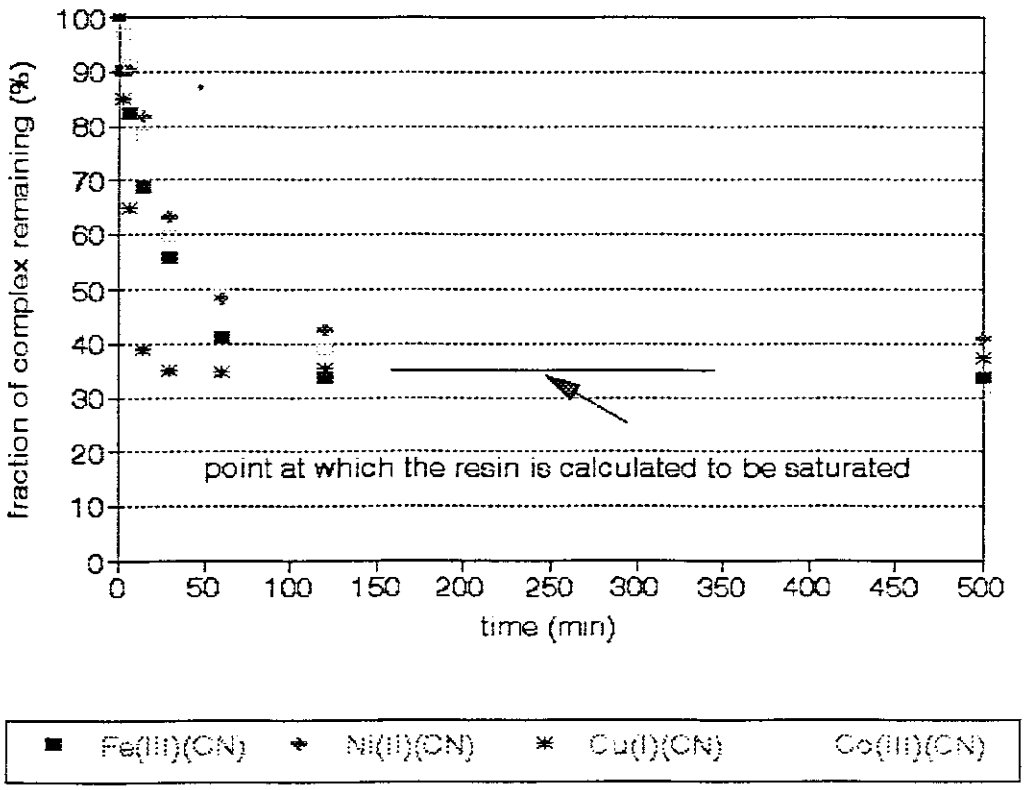

Figure 5 **Adsorption of four metal cyanides onto IRA958 strong base resin without competeing ions**

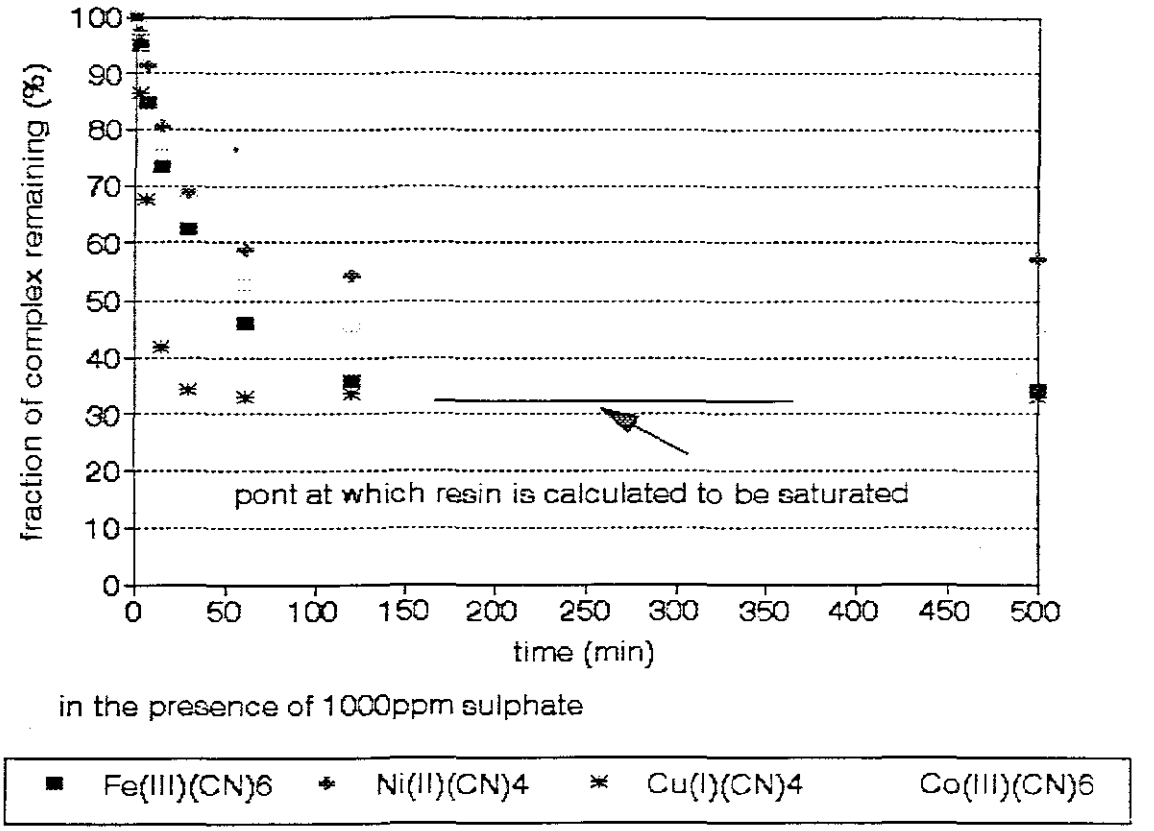

Figure 6 **Adsorption of four metal cyanides onto IRA958 strong base resin with 1000ppm sulphate competing**

4.6 Desorption test-work

A further matrix of tests were conducted in which analytical grade sodium chloride and brine solution were separately tested as regeneration agents. These tests were carried out in batch reactors of the same dimensions as those used in the adsorption tests. Standard solutions of sodium chloride were contacted with four separate quantities of resin, each saturated with one of the four metal cyanides. The saturated resin was achieved by submersing in an agitated soultion containing an excess of the applicable metal cyanide for 40 hours. Thereafter the resin was removed and washed with deionized water before preceeding with the test. These tests were conducted in the same manner as those of the adsorption tests, with samples being extracted from the batch reactor at increasing time intervals and an equilibrium value being taken at twenty four hours.

4.6.1 Desorption results and discussion

The results of the desorption tests are shown in Figure 7. The regeneration tests were repeated with brine solution of approximately the same ionic strength. The results are given in Figure 8. It is reasonable to assert that the results shown in Figures 7, 8 are satisfactory, if one considers that they were achieved after only a single "batch" contact with the regenerant. The tendency for the nickel cyanide complex to be easily dislodged from the resin, can once again be explained by the lower affinity the tri-methyl ammonium functional group has for this bivalent complex (See 4.3.2). As in the adsorption tests, the kinetics of resin regeneration are rapid, with ninety percent of the equilibrium values being reached within one hour. From Figure 8 it can be deduced that the quality of regeneration in brine solution is similar to that of analytical grade sodium chloride solution, with marginal improvements being observed in the removal of the iron and nickel cyanide complexes. An explanation for this is that impurities in the brine solution (anions) may be preferetially taken up by the resin in place of cloride. Futher test-work would shed light on this phenomenon.

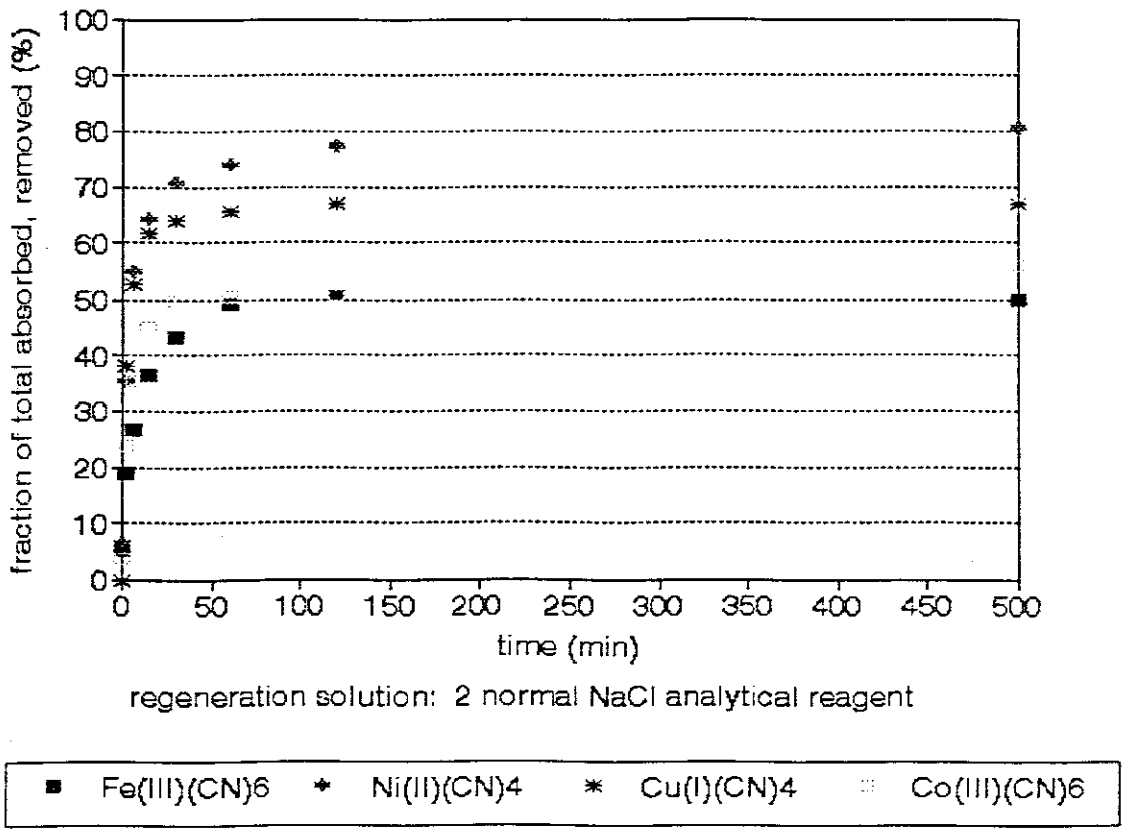

Figure 7 **Desorption of four metal cyanides from IRA958 strong base resin**

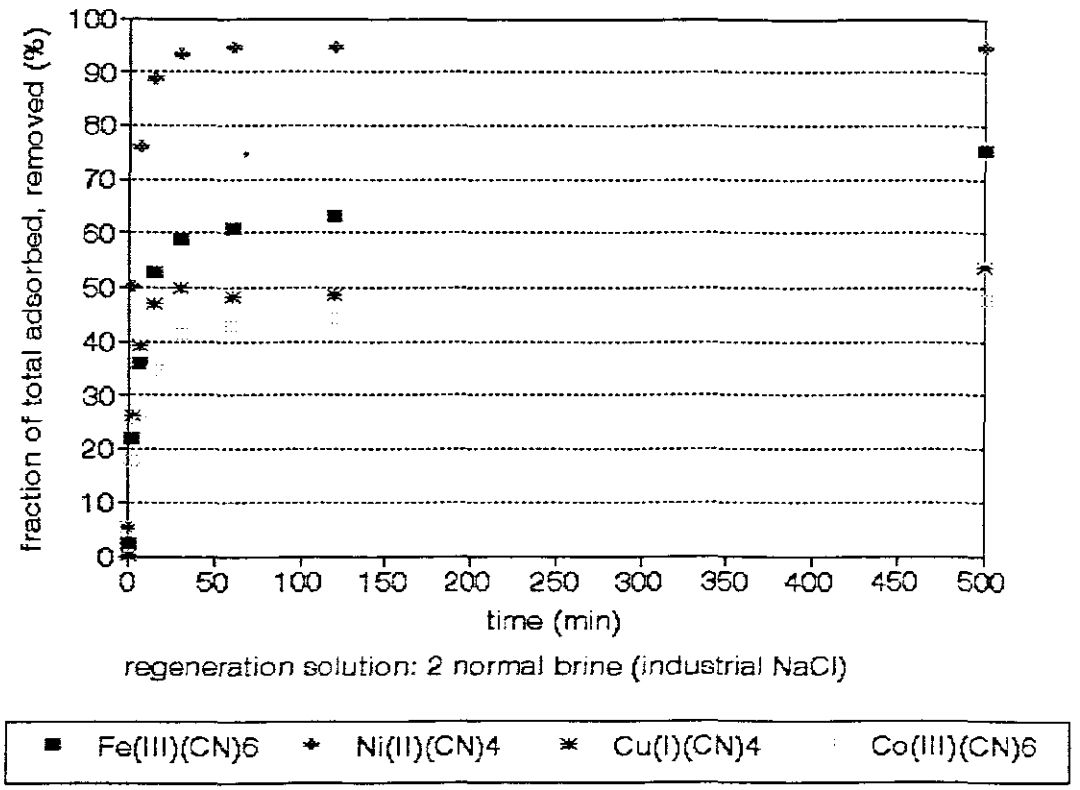

Figure 8 **Desorption of four metal cyanides from IRA958 strong base resin**

CHAPTER FIVE
LITERATURE SURVEY AND BACK GROUND STUDY INTO FLUIDIZATION TECHNOLOGY

5.1 Why the fluidized bed approach

The advantages of the fluidized bed route are the more efficient use of resin hold-up (as the fluidized bed concept loans itself to the possibilities of the plug flow reactor) and the typically lower pressure drop to that of a fixed bed of equivalent ion exchange duty. It is also notable that the fluidized bed configuration offers the means to employ a continuous process. The second part of this study constituted the development of a technique for the better understanding of the fluidization characteristics of ion exchange resin.

5.2 Fluidization and ion exchange resin

Since their development pseudo-continuous fluidized bed ion exchange reactors such as the Cloete/Streat[39] and NIMCIX columns have been used in many industrial ion exchange applications. However, a difficulty is encountered in designing fluidized bed ion exchange equipment, in the context of resin compartment dimensions optomization, when bed expansion is poorly predicted. Particularly in the instance where the difference between resin and fluidization solution density is small, and / or the inventary of resin in service at any one time is large. Not only do the recepticals dimensions affect the capital cost of construction, they also stricture the volume of resin in service at any one time which ultimately dictates plant capacity and performance.

A typical resin bead is a spherical porous structure which undergoes a slight change in volume, and a more substantial change in skeletal density, during the ion exchange process. Despite there being an abundance of information describing the particulate fluidization characteristics of particulate substances on the basis of physical characteristics all of which is based on the behaviour of solid spherical particls, the porous nature of ion exchange resin as an aqueously fluidized solid, makes applicability questionable.

Published mathematical correlations[40], for the prediction of expansion of a fluidized bed of particles require a particle density which, depending on its value can have a great effect on the final expansion prediction. Being of a porous nature, it might be more correct to refer to a resin bead's 'apparent density' of fluidization, a property which will only be significant when the resin is in a turbulent suspension, with the continuous phase intruding into the porous resin. It is evident therefore, that the physical characteristics of the continuous phase will play a substantial role in dictating the apparent density of a resin bead, clearly a difficult constant to measure gravimetrically. Akapo *et al*[41] have advocated the reverse notion suggesting that particle density of porous aeratable powders could be measured by observing the expansion characteristics of the solid, while Nicollella *et al*[42] apply the theory through to liquid fluidized beds.

A further problem is the poly-sized nature of manufactured resin, which in itself, and in its alteration as a result of minor adjustments in the resin manufacturing process, plays a significant role in the fluidization behaviour of the resin. Only recently have certain resin manufactures developed a process for manufacturing a mono-sized ion exchange resin, and this only for the most commonly consumed resins. Hartman *et al*[43] and Foscole *et al*[44] both reported that a wide range of particle size distribution, amongst other phenomenon, has a substantial effect on fluidization behaviour. Consider that there is approximately a four-fold difference in diameter from the smallest to the largest resin bead as supplied by most resin manufacturers, and that the particle size distribution between, varies some what from batch to batch.

Finally, empirical relationships which describe the expansion of a fluidized bed always correlate voidage to fluid velocity, and hence require the free wet settled voidage as a necessary base constant from which an expanded voidage, and hence a bed expansion, can be calculated. The free wet settled voidage, just as the apparent density of fluidization, will also be a difficult quantity to measure when using a porous discontinuous phase such as ion exchange resin. Another observation is that this value is not necessarily constant and depends chiefly on the manner in which the bed is allowed to settle.

In this study we attempt to see if existing fluidized bed technology, which requires these difficult to attain values for expansion prediction purposes, can be adapted and utilized for a bed of fluidized resin. It is suggested that given the particle size distribution, an adapted version of the *serial or*

incremental model can be fitted to measured expansion data by searching for, resin apparent density, and bed free wet settled voidage.

CHAPTER SIX

A FURTHER DEVELOPMENT OF THE *"SERIAL"* MODEL

A LOGICAL PROGRESSION

6.1 The Mono-sized particle bed

The Levenspiel criterion[45](i.e. small difference between density of discontinous and contionus phase) for determining fluidization stability, suggests that resin beads fluidized in an aqueous medium will tend to exhibit particulate or smooth fluidization over a large range of fluidization velocities. Particulate fluidization is defined as being a situation in which the bed continues to expand with increasing fluid velocity and maintaines its uniform character, with the amount of agitation of the particles increasing progressively. Under this circumstance one would expect the well established *Richardson and Zaki*[40] equation to satisfactorily dictate the relationship between voidage, and fluidization velocity for a fluidized, mono-sized bed of resin.

$$U = U_t \cdot e^n \qquad ..1$$

where:

$$n = \left[5.5 + 23\frac{dp}{D} \right] Ga^{-0.075} \qquad (21 < Ga < 2.4E4) \qquad ..2$$

$$Ga = \frac{dp^3 g(\rho_S - \rho_L)\rho_L}{\mu^2} \qquad ..3$$

To calculate the actual bed expansion (E), based on the change in voidage from the free wet settled condition, the following relationship can be used:

$$E = \frac{1 - e_{fws}}{1 - e} \qquad ..4$$

6.1.1 The poly-sized particle bed

Two theories have been presented, regarding the effective prediction of expansion, of constant density poly-sized particulately fluidized beds. The *averaging* model[46, 47], which assumes a single particle diameter to be representative of the entire bed, has been demonstrated by Epstein et al[48] to be inadequate at high voidages where the expansion contribution of the smaller sized particles tend to dominate. The averaging approach has also been proposed by Wen et al[47] for beds with a largest to smallest particle size ratio of not greater that 1.3, another limitation which effectively discounts this approximation technique as a possibility for resin beads, as on average there is a four-fold increase in particle size from smallest to largest size i.e. 300 - 1200 microns. The short comings of the averaging model seem to outweigh the advantageous lack of excessive calculation.

The *serial or incremental* model is proposed by a number of authors [40, 49] and assumes that the overall expansion of a particulately fluidized bed of particles is simply the sum of the individual expansions that each species would display, if fluidized separately, by the same parameters. The classification of particles in the axial dimension, a phenomenon which has been measured by Garside *et al*[50] has shown that the variation of local voidage can be predicted by assuming the bed to be totally classified even in the regions where classification is absent. This loans credence to the serial model as a semi-fundamental representation of the real condition which may be described as one in which each particle exerts a certain voidage envelope around itself dictated by its physical characteristics and that of the continuous phase. A three dimensional, more complicated approach to understanding fluidization characteristics, along these lines, is attempted by Patwardhan *et al*[51] in their *cell model*, for particulately fluidized beds. If the *serial model* is applied to a poly-sized fluidized bed, the overall bed expansion component should be equal to the sum of the individual expansion component's advanced by the various size fractions, thus:

$$E_t = I\sum_{dp_s}^{dp_l} V_i(E_i - 1)] + 1 \qquad ..5$$

If one accepts the volume fraction(V), and terminal velocity (U_t), to be a function of particle size(dp) thus:

$$V = G(dp) \qquad ..6$$

$$U_t = F(dp) \qquad ..7$$

then combining equations 1, 4, 6 and 7, and integrating for the entire bed in the domain of resin bead size, results in the following:

$$E_t = 1 + \int_{dp=0}^{dp=\infty} G(dp).\left(\frac{1 - e_{fws}}{1 - (U / F(dp))^{1/n}} - 1\right) d\,dp \qquad ..8$$

If the serial model is valid, equation 8 should effectively predict the expansion factor of a liquid fluidized bed of constant density poly-sized particles, such as resin.

6.1.2 Particle size distribution

It is clear that the relationship signified by equation 6 could take on any form, the only prerequisite being that each particle size has a singular volume fraction value. It is also reasonable to assume that in most applications, the particle size distribution of resin, will be a continuous function of particle size within two distinct particle diameters and above zero. For the purposes of this study a continuous functional relationship was developed by the application of an adapted spline routine algorithm to raw data. This adaption compensated for the unrealistic negative values reported by the developed spline function when the processing of raw particle size distribution data resulted in a spline curve that intersected the zero volume line (X axis) at high differential within the particle size domain. All sets of raw distribution data were normalized, before the adapted spline routine was applied, a process which is described, thus;

If V_i is the volume fraction of the resin in the ith of the in total N inter screen intervals,

and L_i is the extent of this interval in particle diameters then calculation of the size fraction is achieved thus:

$$S_i = \frac{V_i / L_i}{\sum_{i=1}^{N} V_i / L_i} \qquad ..9$$

The arithmetic mean of the screen fraction limits of the ith fraction was then paired with the calculated normalized volume fraction of the ith interval, before being "splined" for development into an algorithm based continuous function.

6.2 Terminal velocity

There are a number of published models (equation 7) describing terminal velocity of spherical particles in a continuous medium and as ion exchange resin beads can be assumed to have a near perfect spherical shape, the accuracy of these models could easily be tested. The apparent density of the resin beads applicable to the terminal velocity models was assumed to be the same as that in the *Zaki and Richardson* relationship (equation 1).

6.2.1 Terminal velocity model of Shiller *et al*

$$Ga = 18.Re_t + 2,7.Re_t^{1.687} \qquad ..10$$

Where:

$$Re_t = \frac{\rho_s.dp.U_t}{\mu} \qquad ..11$$

Note that the terminal velocity variable is present in both the right hand side terms which are each raised to different "real indices", requiring the use of a complicated iterative procedure(e.g. Rapson Newton) to solve for terminal velocity given all the other physical characteristics of the system.

6.2.2 Terminal velocity model of Hartman *et al*

$$log_{10} Re_t = P(A) + log_{10} R(A) \quad ..12$$

Where:

$$P(A) = [(0,0017795.A - 0,0573).A + 1,0315].A - 1,26222 \quad ..13$$

$$R(A) = 0,99947 + 0,01853.SIN(1,848.A - 3,14) \quad ..14$$

$$A = log_{10} Ga \quad ..15$$

6.2.3 The Ladenburg correction factor

$$Correction\ Factor = \left[1 + 2.4(dp / D)\right] \quad ..16$$

The Ladenburg correction factor gives the empirical relationship between, the ratio of partical diameter at terminal velocity to the radial dimentions of the finite medium, and the factor by which the terminal velocity of the particle will be altered as a result of it being in a finite medium.

6.2.4 Testing the terminal velocity models

The terminal velocities, of a number of randomly sized beads of the same resin in an identical chemical matrix solution, were measured in the laboratory. The diameters of these beads varied from 400 to 1000 microns with measurement being obtained as accurately as possible by using a micrometer. As the apparent density of the resin, a requirement of the terminal velocity models, could not be measured an iterative technique was used to check for parity between the measured terminal velocities and those predicted by the Hartman *et al* model[53]. The iterative technique proceeds as follows:

> *Each measured resin diameter is individually put into the Hartman model together with the other required and easily measurable characteristics of the continuous phase i.e. density and viscosity. The resin "apparent density" is located by iteration by performing the calculation for various assumed resin "apparent densities" until the measured terminal velocity of for that bead size is predicted by the model. The average density of the resin beads is then calculated. The calculated average apparent density is then used in both the Hartman and Shiller models to predict the terminal velocities for each resin diameter measured.*

The preceeding paragraph gives some indication of the importance of "apparent density" in predicting terminal velocity and also the difficulty sorrounding its accurate measurement.

A comparison of the Shiller *et al*[52] and Hartman *et al*[53] models in the applicable particle Reynolds No. range and their correspondence to the measured data are shown in Figure 9. The Ladenburg correction[54] factor was used to correct the model predictions for a finite medium.

6.2.5 Comment on the model fits

From Figure 9 it can be deduced that in the field of interest the models vary only marginally in their predictions, also of note is that the particle density achieved by iteration, is plausible. Given these

two observations, it was condoned that these results were sufficiently indicative to assume, with reasonable confidence, the accuracy of the models in predicting the terminal velocity of the resin.

Given these observations, and the fact that the model of Shiller *et al*, requires an iterative search when solving for terminal velocity for a stipulated resin density, it was decided to use the model of Hartman *et al*, in all fluidization calculations.

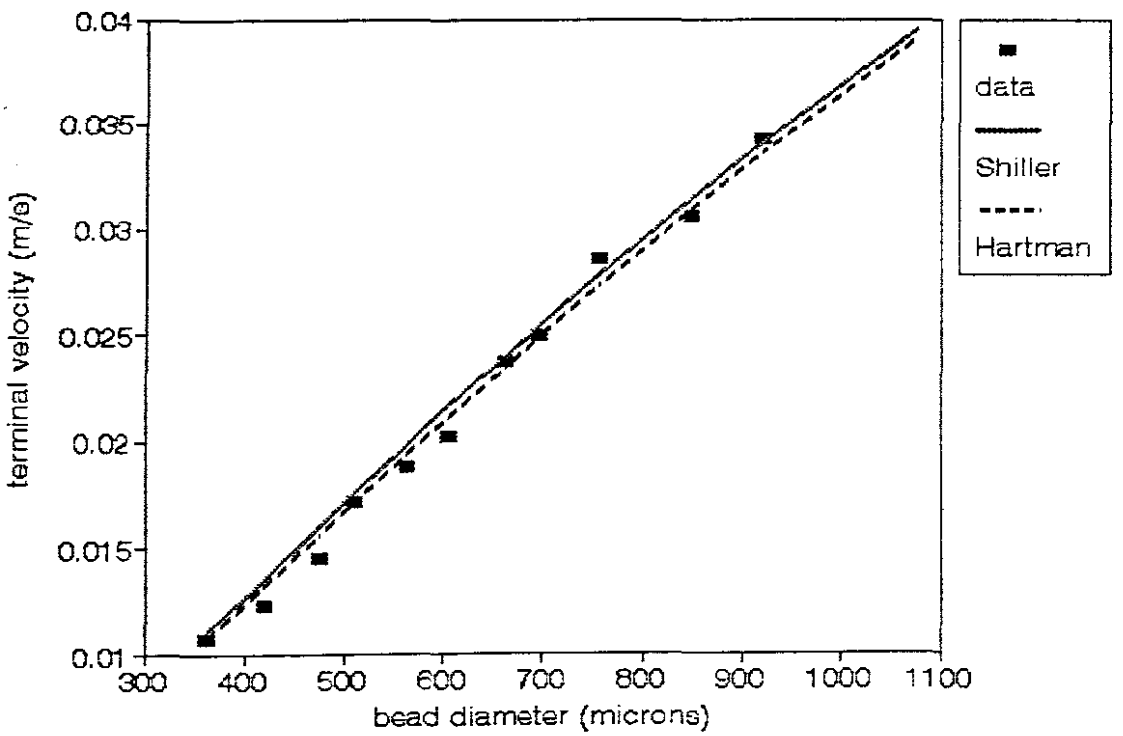

Figure 9 **A comparison between the models of Shiller and Hartman, including data measured by this author.**

CHAPTER SEVEN
STUDY OF FLUIDIZATION CHARACTERISTICS OF ION EXCHANGE RESIN.

7.1 Introduction

To prove the effectiveness of the model presented in equation 8, it was decided to conduct a matrix of expansion tests using two different resins, four columns and four system temperatures. The resins chosen where:

C26

* *A relatively dense, strong acid resin with a macroporous, styrene di-vinyl-benzene, co-polymer matrix and a sulphonic active site.(fluidized in the hydrogen form)*

IRA958

* *A relatively low density strong base resin with a macroporous crosslinked acrylic di-vinyl-benzene, copolymer matrix structure and an active site consisting of tri-methyl ammonium groups.(fluidized in the chloride form)*

The columns used had diameters of 30, 40, 50, and 60 mm. The temperatures used were between 11 and 26 degrees centigrade. The particle size distribution together with the expansion data were stored on computer disk using Turbo Pascal programs "PSDINPUT" and "EXPANINPUT" which are listed in appendixes A and B respectively. Once the data was stored on disk the Turbo Pascal program "HOOKJEEVESOPTOMIZER"(appendix C) was used to fit the proposed model in equation 8 to the data. The logic followed by the "HOOKJEEVESOPTOMIZER" program in calculating the overall expansion of the resin bed is displayed in Figure 10. On completion the program reported, the sum of square differences between data and model prediction, the average resin "apparent density" and the free wet settled voidage.

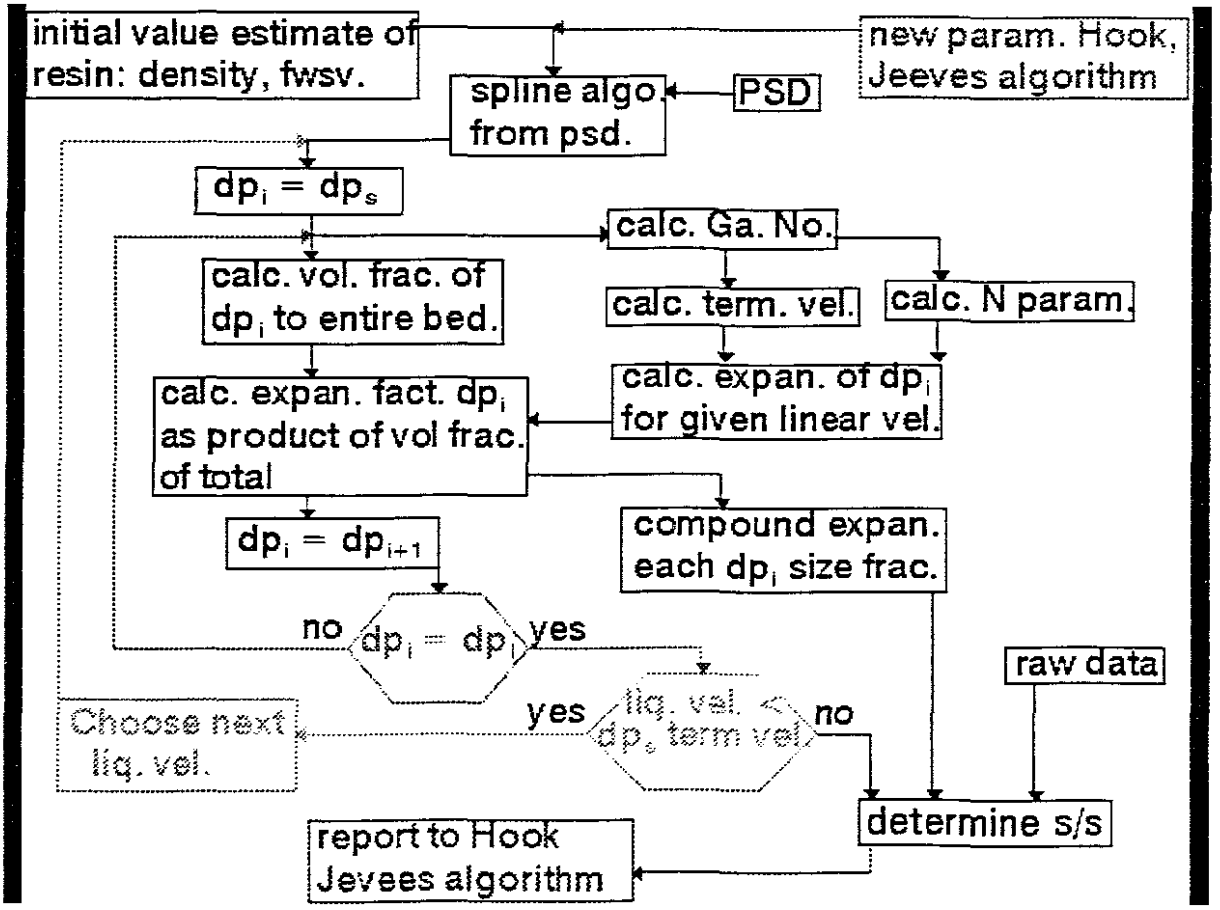

Figure 10 **Logic flow chart of the "Hookjeevesoptomizer" program**

7.2 Terminal velocity test-work

All terminal velocity tests were carried out in a two meter high glass tube with an internal diameter of about 40mm. The diameters of the resin beads were measured by micrometer. The fall speed was calculated by measuring the time taken for the bead to cover a predetermined vertical distance. To ensure there were no adverse effects due to surface proximity, only the terminal velocity of beads maintaining a preset distance from the side of the tube throughout their fall, were recorded. Calculation of the terminal velocity by using the model of Hartman *et al* was attempted by algebraic manipulation followed by substitution of the physical characteristics of the system.

Calculating the terminal velocity by means of the Shiller model required the use of a differential seek technique(Newtons method). The results of this test-work are shown graphically in Figure 9.

7.3 Expansion testwork

The columns used to measure the expansion of the fluidized beds of resin at various fluidization rates, were constructed of glass with an overall length of 1 meter, closed off at the bottom by a sintered glass fluid distributor with an average pore size of about 17 - 40 microns. Into these glass tubes varying quantities of each type of resin were placed and their fluidization characteristics observed. A turbulence settling zone was included below the sintered glass so as to allow for the calming of eddies created in the fluidizing liquid by the nozzle effect of the inlet, before reaching the sintered glass. In the larger diameter columns it was considered necessary to further reduce the jet action of the inlet by introducing solid baffles designed to distribute the nozzle effects of the incoming liquid.

To acquire raw, expansion vs specific liquid velocity data, distilled water was fed via a controlling gate valve to the bottom of the column from a header tank, so as to preclude any vibration. Deionized water leaving the top of the column ran into a reservoir from where it was pumped back to the header tank by a peristaltic pump in a closed loop. The temperature in both the header tank and the reservoir was maintained at constant temperature by a system of temperature controllers. The level of deionized water in the header tank was kept constant by a feed back controller which controlled the pumping rate of the peristaltic pump.

A vacuum breaker was installed at the fluid outlet of the column, so as to prevent siphoning action from causing a variation in the vertical pressure drop across the bed. A diagram of the test rig is displayed in Figure 11.

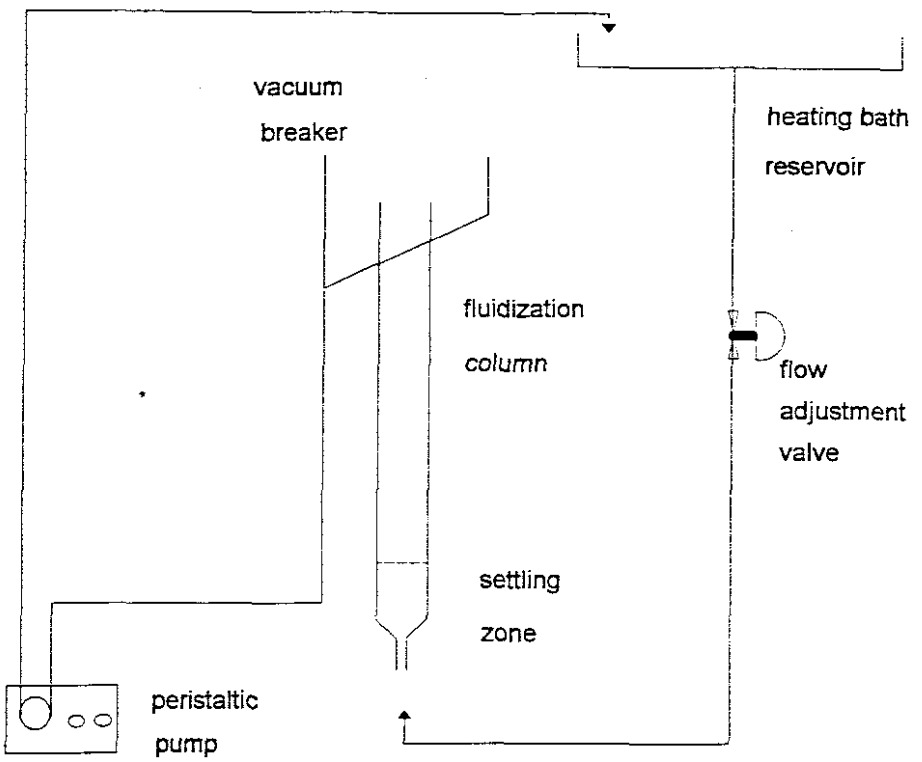

Figure 11 **Diagram of apparatus for observing bed expansion characteristics of resin**

Each resin was fluidized at various flow-rates tailored to elicit resin bed expansions of between 10 and 150 percent.

"100 percent = *a doubling in size"*

"200 percent = *a trebling in size"*

Wet sieve analysis was used to measure the particle size distributions. The density and viscosity of the deionized water was calculated from the temperature, using equations 17 and 18 respectively, where temperature (Temp) is in degrees centigrade, liquid density in kilograms per cubic meter and liquid viscosity in pascal seconds.

$$water\ density\ =$$

$$-4{,}604E-3.(Temp)^2\ -\ 9{,}783E-3.(Temp)\ +\ 1E3 \qquad ..17$$

$$water\ viscosity\ =$$

$$5{,}894E-7.(Temp)^2\ -\ 5{,}467E-5.(Temp)\ +\ 1{,}801E-3 \qquad ..18$$

7.4 Wet sieve analysis

As required by the model all resin had to be subjected to a wet screen analysis for the purposes of developing a particle size distribution. Deionized water was used for all sieving work so as to prevent any ion exchange activity which might very well have lead to resin expansion or matrix density alternation.

The following 20 centimetre diameter screens were used for the screening analysis:

* *300, 355, 425, 500, 600, 710, 850, 1000, 1180 (microns)*

This geometric progression grows by a factor more or less equivalent to the fourth root of two. The reason for using such a progression is to decrease the effect of the exponential increase in the volume of particles retained in each successive screen thus improving accuracy.

All resin beads passing the 300 micron screen were assumed to be nonspherical fragments of larger beads and hence were discarded. It was also assumed that all resin beads unable to pass the 1180 micron screen were smaller than 1200 microns. The resin manufacturer assured the author that all resin particles are in the size range of 300 to 1200 microns. All samples of resin were examined under a microscope so as to ensure that broken or partially fractured beads were kept to a minimum.

7.5 Fitting the model equation

Despite most of the parameters/variables in equation 8 being easily measurable, as previously explained the free wet settled voidage and apparent density still remained an effective obstacle in the application of the equation. To overcome this problem a technique was used, which comprised of fitting the *Serial model* to expansion vs linear velocity data, by searching for free wet settled voidage and apparent resin density, for an optimal sum of squares. The search technique used was that of Hook & Jeeves(appendix E). This particular search routine requires a large number of iterations to obtain its final optimum but this is compensated for by its intrinsic stability.

7.5.1 The nonlinear problem

An early observation, with respect to the model fitting, was that a proportional change, based on preset boundaries, of apparent density resulted in a far greater change in the sum of square errors than was the case when the identical change was made to free wet settled voidage. The optimization was therefore assumed to be of a highly nonlinear nature for which compensation was applied by adjusting the size of the Hook & Jeeves tentative increments for free wet settled voidage in relation to resin apparent density. Various ratios were experimented with until multiples were located that resulted in the "rate of change of the sum of squares" being similar in magnitude for an identical amplitude of tentative search in the each of the two variables.

The factors found to be suitable in the search algorithm were: a 1/10000 for the apparent density variable and 10 for the voidage.

7.6 Results and interpretations of fluidization testwork

The "Hookjeveesoptimizer" program took about 15 to 30 minutes to locate a global minimum when used on a "SAMPO" 486 66 MHz DX40 personal computer. The emulation mode was not used, ensuring the full use of the maths co-processor. The initial estimates of the "free wet settled

voidage" and "apparent density" were given as 0.5 and 1300 $kg.m^{-3}$ respectively. Figure 12 shows examples of the measured particles size distributions of the two resins used in the fluidization testwork and Figures 13 and 14 show the expansion data for the stipulated conditions together with the fitted model and parameters.

All apparent densities obtained by the program, for each of the two resins under the different circumstances were in good agreement, displaying effective independence from variation to system temperature and alteration in column diameter. All values obtained were also exceedingly plausible with all resin "apparent densities" being located in the 1050 $kg.m^{-3}$ to the 1200 $kg.m^{-3}$ range (Figures 15, 17) and voidages in the 0.3 to 0.4 range (Figures 16, 18).

It was concluded by the author that the facts presented in the previous paragraph constituted excellent circumstantial evidence, vindicating the argument on the effectiveness of the application of the resin fluidization characterisation technique described in this thesis.

Note that calculated apparent density and free wet settled voidage from data gleaned from the operations involving the smallest diameter column (30mm) (appendix F) were characterised by a greater scatter in the final values. This is attributed to the lack of a turbulence settler zone (section 7.3) below the sintered glass of this particular column. In addition this particular column was far older than the larger columns and hence the sintered glass was considered to be partially blocked resulting in channelling.

7.7 How ion exchange affects fluidization

In a further test to establish what effect the loading of resin IRA958 would have on it's fluidization characteristics. A quantity of this resin was initially fluidized in the chlorine form for the purposes of ascertaining an expansion curve and then loaded with hexacyanoferrate(III) ions after which a second expansion curve was assessed. The loading ion was formed from the dissolution of potassium hexacyanoferrate(III).

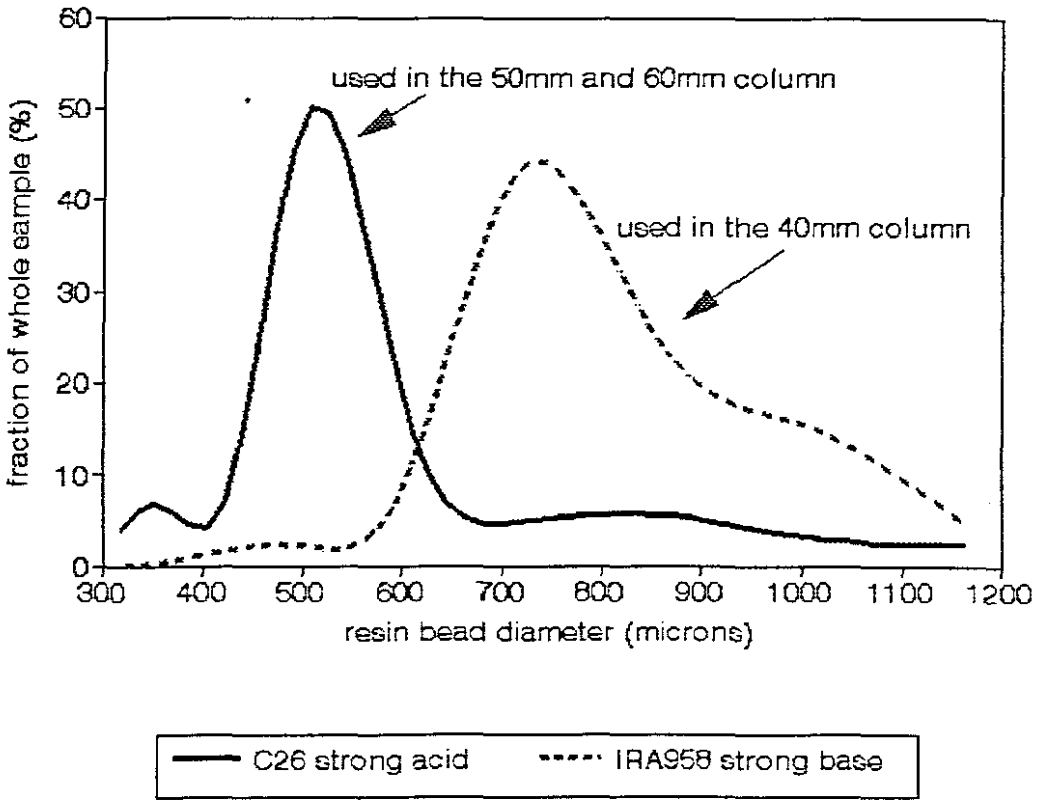

Figure 12 **An example of particle size distribution of two of the resins**

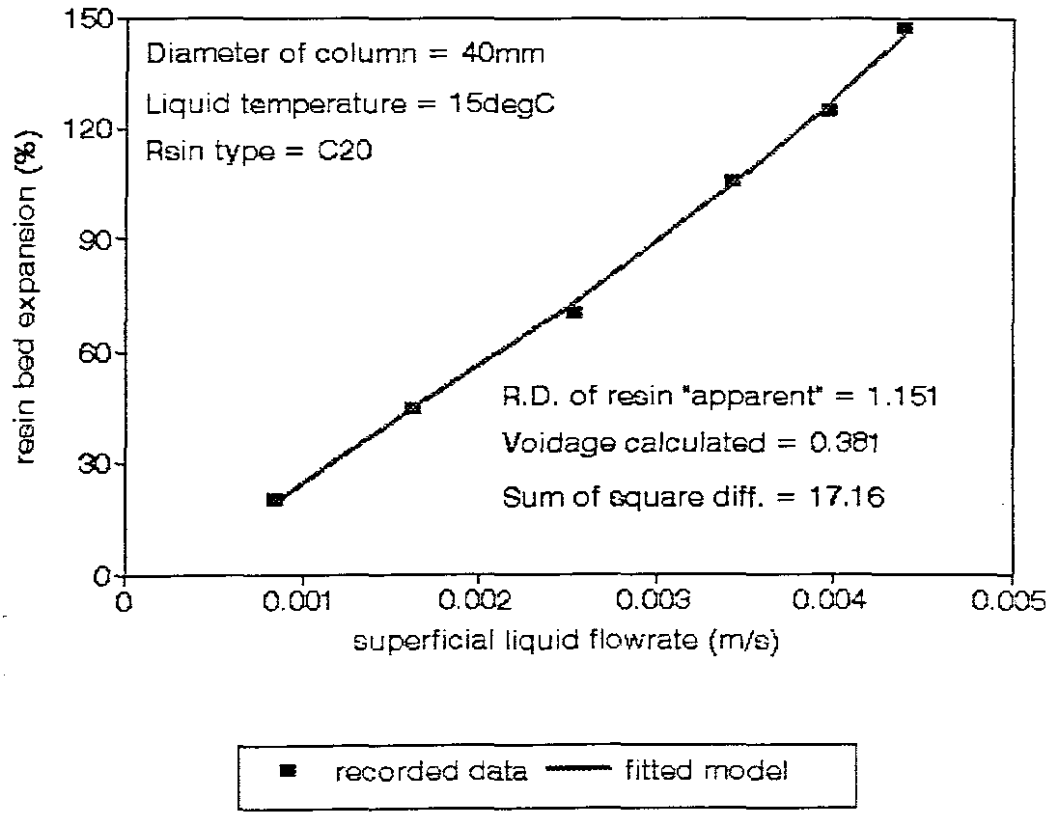

Figure 13 **Bed expansion data and fitted model for C26 resin**

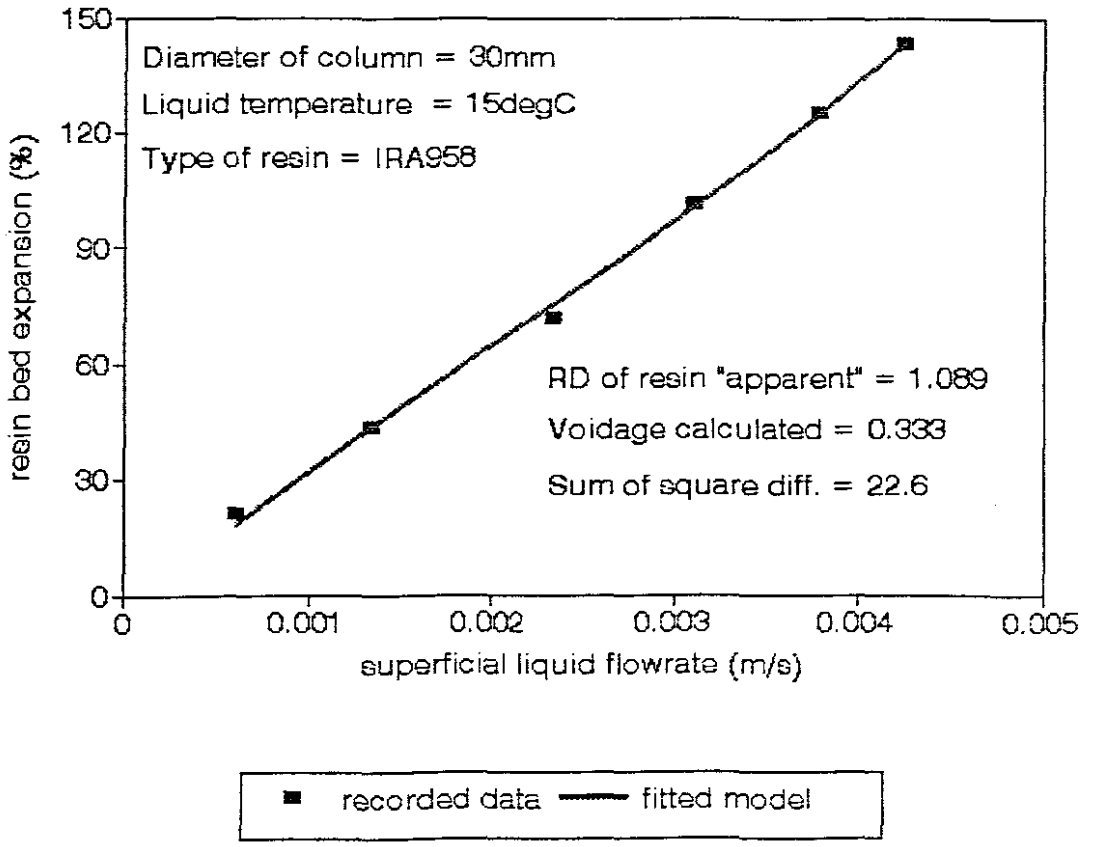

Figure 14 **Bed expansion data and fitted model for IRA958**

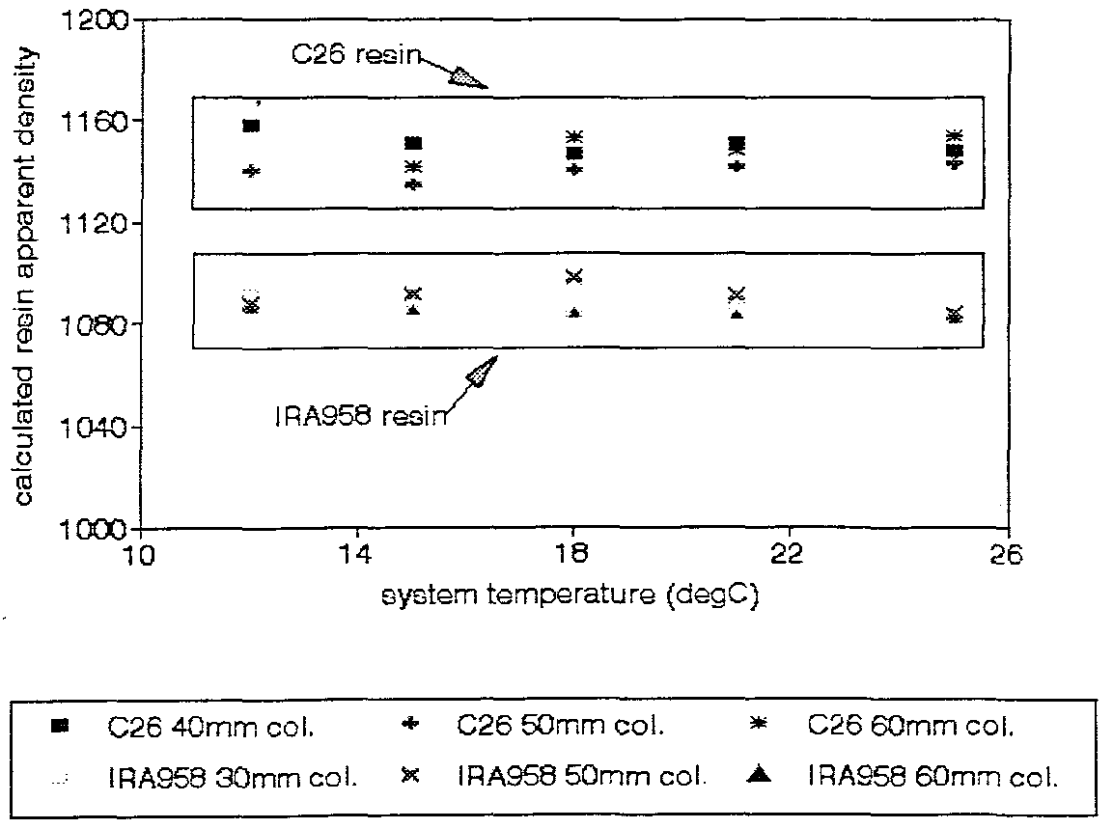

Figure 15 **Calculated apparent resin densities vs temperature**

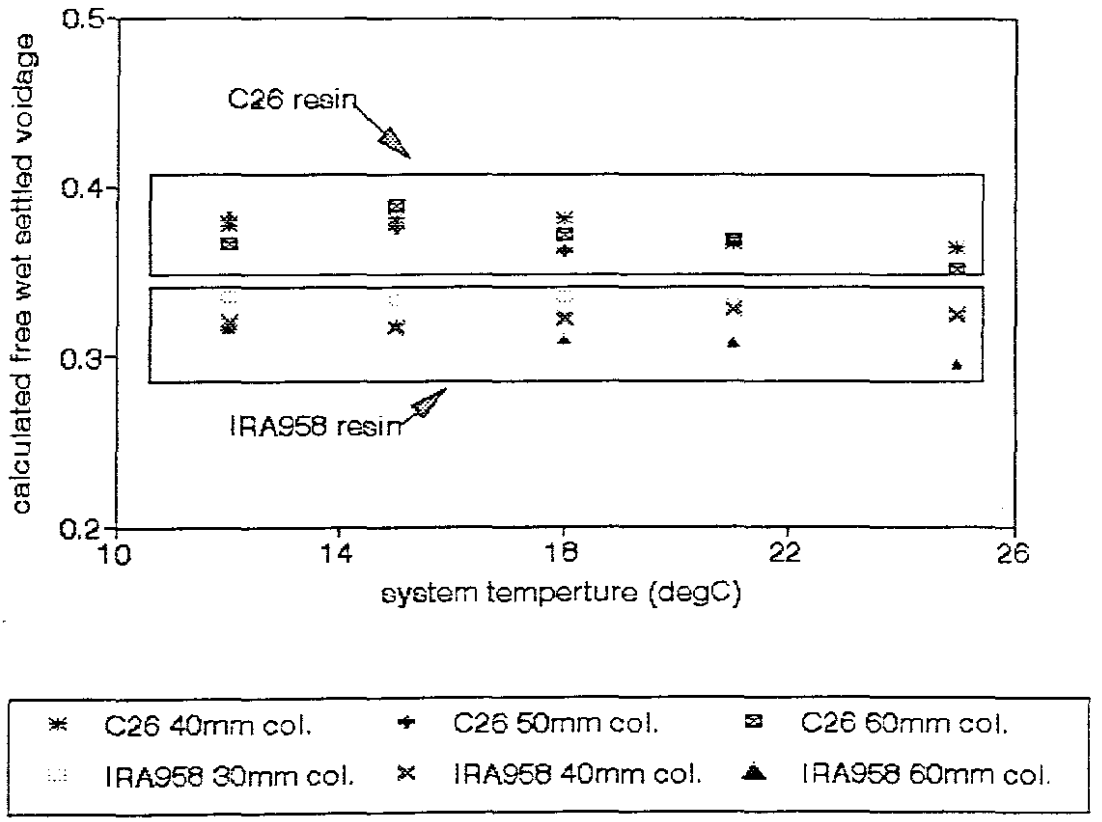

Figure 16 **Calculated resin bed free wet settled voidage vs temperature**

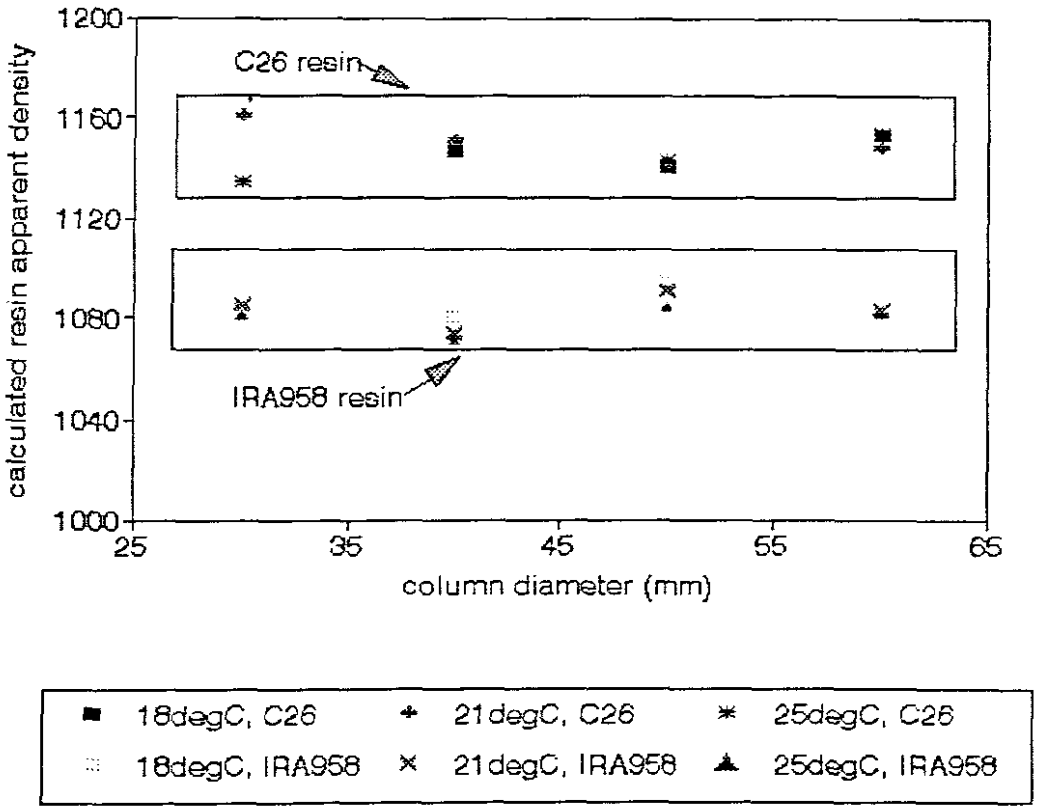

Figure 17 **Calculated apparent resin densities vs column diameter**

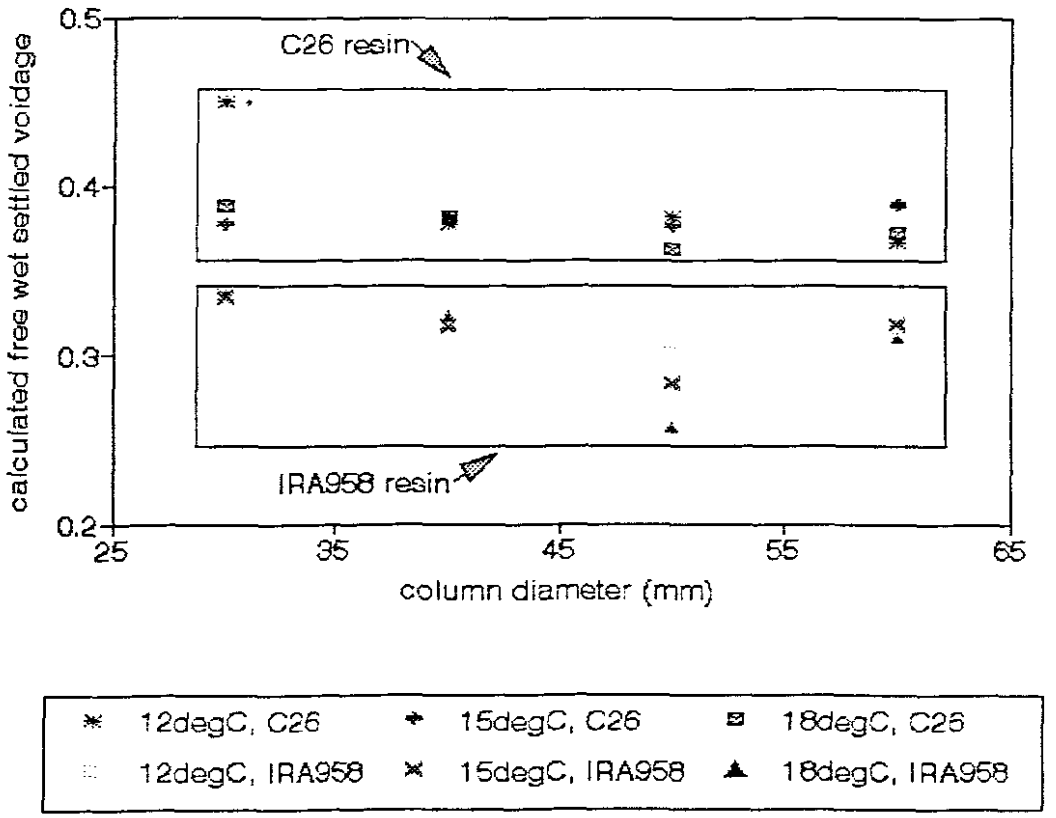

Figure 18 **Calculated resin bed free wet settled voidage vs column diameter**

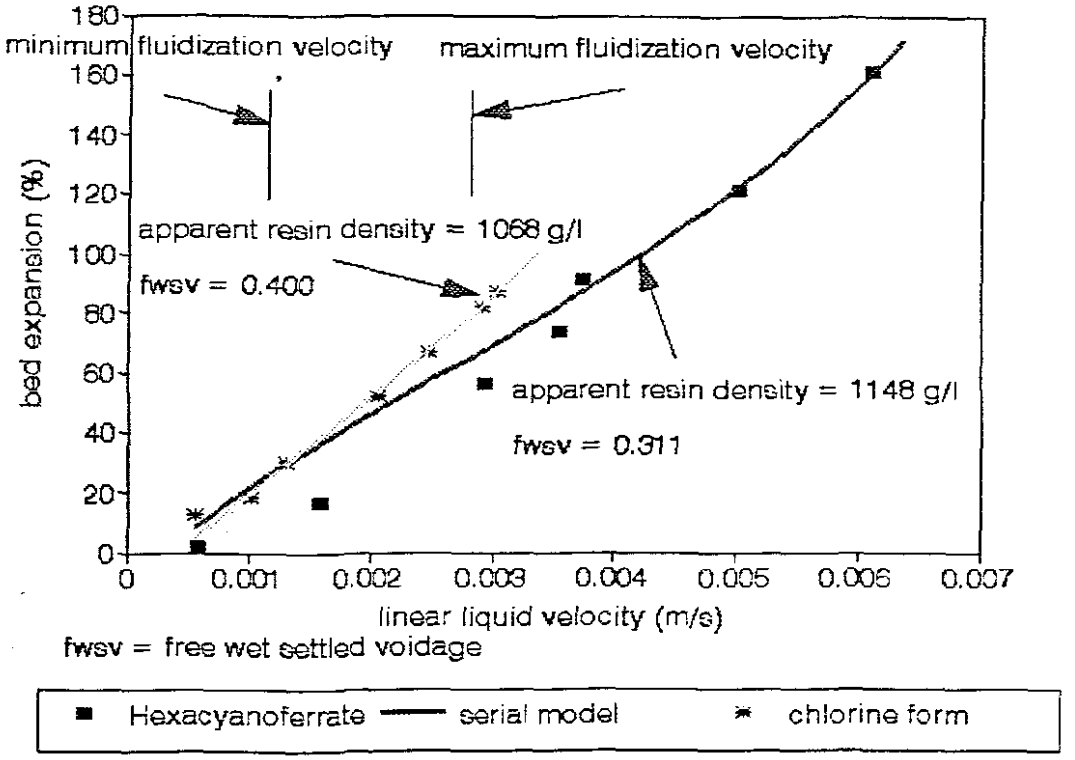

Figure 19 **Bed expansion vs liquid superficial velocity for different loadings of the resin IRA958**

The hexacyanoferrate(III) ion was chosen as the loading ion, primarily because of its abundance in effluents (Table 1) and secondly because of the ease with which its presence can be determined on the basis of solution colour. Furthermore, it has a higher mass per equivalent than tricyanocuprate, the other most abundant metal cyanide, which means that during loading the expected larger density change would result in greater variations to the fluidization characteristics of the resin. Figure 19 presents the results of the expansion behaviour of IRA958 in the chlorine and the hexacyanoferrate(III) forms, including the fitted *Serial model*. As can be predicted, there is a large difference in the curves mainly as a result of altered density and free wet settled voidage.

CHAPTER EIGHT
CONCLUSION

It is clear from the study presented in the thesis, that if the ion exchange route for the removal and/or recovery of metal cyanide ions is to be pursued, the use of "Amberlite" IRA958 resin may well be a feasible alternative. It is envisaged that a mineral plant effluent, preceded by semi-clarification (e.g. bank of hydro-cyclones), might then be contacted with IRA958 resin in a semi-continuous fluidized bed application, before disposal on the slimes dam, or tailing pond. Figure 20 is a tentative/ broad description of a possible cyanide recovery plant.

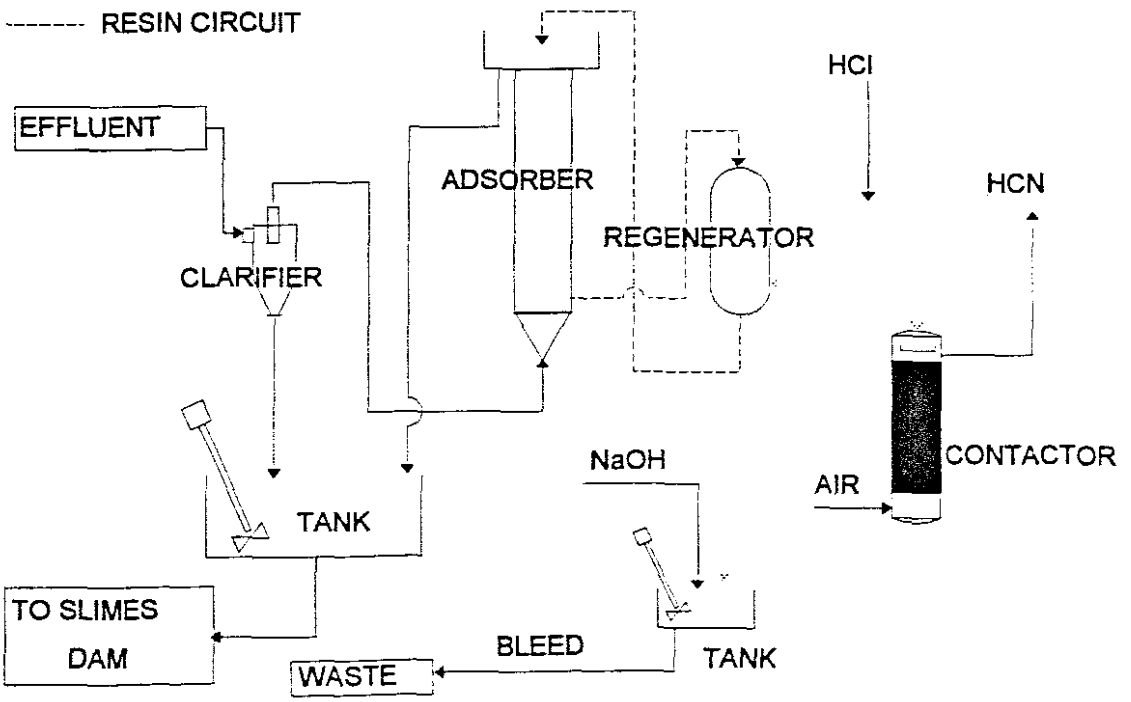

Figure 20 **A proposed cyanide recovery plant**

REFERENCES

1. Ford-Smith, M., "The Chemistry of Complex Cyanides: A Literature Survey", His Majesty's Stationery Office, London, (1964)

2. Smith, A., Mudder, T., "The chemistry and treatment of cyanidation wastes", pg(1..3, 180), Mining Journal books London (1991)

3. Semmens, M. J.; Kenfield, F. C., Qin R., Cussler, L. E. "The GM-IX Process: A novel metal cyanide treatment and recovery technique" (1987)

4. Carlson, L. G., "Ion exchange treatment for removing toxic metals and cyanide values form waste waters", U.S. Patent, 4,321,145 (1982)

5. Huiatt, J., Kerrigan, J., Olson, F., and Potter, G., Workshop of Cyanide from Mineral Processing, Utah Mining and Mineral Resources Research Institute, College of Mines and Mineral Industries, Salt Lake City, Utah, (1982)

6. Anderson, P.D. and Weber, L.J., "Toxic Response as a Quantitative Function of Body Size", Appl. Pharmacal, 33: 471-483, 1975

7. Smith, A., Mudder, T., "The Chemistry and Treatment of Cyanidation Wastes", pg (8..10) Mining Journal books London (1991)

8. Caruso, S. C., "The Chemistry of Cyanide Compounds and Their Behaviour in the Aquatic Environment", Carnegie Mellon Institute of Research, (1975).

9. Standard Methods (16th edition 1985, Method 412-H, pg. 344; 17th edition 1989, 4500-CN Methodei, pg. 4-38) and ASTM Method C.

10. Broderius, S. and Smith, L., USEPA, Grant NO. R805291, (1980).(As referenced by Smith and Mudder[2])

11. Wetzel, R., Limnology, W.A. Saunders Company Publishers, (1975).(As referenced by Smith and Mudder[2])

12. Meyn, E., Zajdel, R., and Thurston, V.,"Acute Toxicity of Ferrocyanide and Ferricyanide to Rainbow Trout:, Technical Report No. 84-1, Fisheries Bioassay Laboratory, Montana State University, work conducted for Homestake Mining company(1984) (As referenced by Smith and Mudder[2])

13. Baker, D. J., "Cyanide in the Environment", unpublished data, (1984) (As referenced by Smith and Mudder)

14. Smith, A., Mudder, T., "The Chemistry and Treatment of Cyanidation Wastes", pg (177..180), Mining Journal books London (1991)

15. Schmidt, J.W., Simovic, L. and Shannon, E., "Natural Degradation of Cyanides in Gold Milling Effluents", Proc. Sem. Cyanide and Gold Mining Industry Seminar: Environment Canada, Ottawa, Ontario, (1981)

16. Simovic, L., " Report on Natural Degradation of Cyanides from the Cullaton Lake Gold Mines Effluent", EPS Unpublished Manuscrip, Wastewater Technology Centre, Burlington, Ontario (1984) (As referenced by Smith and Mudder[2])

17. Smith, A., Dehrmann, A., and Pullen, R., "The Effects of cyanide-Bearing, Gold Tailings Disposal on Water Quality in Witwatersrand, South Africa", South Africa", cyanide and the Environment pp. 221-229, Van Zylm (Ed.), Tucson, Arizona, Pub. CSU, Fort Collins, Colorado, (1984)

18. Brodie, J. B., "Optimization of Cyanide Destruction by the Alkaline Chlorination Process as Related to Treatment of Gold Mill Effluents", Report prepared by Ker, Priestman and Associated Ltd., for the supply and services Canada and Environment Canada, Ottawa, (1983) (As referenced by Smith and Mudder[2])

19. Devuyst, E., Conard, B., Robbins, G., and Vergunst, R., "A Cyanide Removal Process Using Sulphur Dioxide and Air", Journal of Minerals, Metals and Materials, Vol. 41 12 (1989)

20. Mathre, O.B. and DeVries, F.W., "Destruction of Cyanide in Gold and Silver Mine Process Water", paper presented at the Annual Meeting of the Metallurgical Society of AIME, (1981) (As referenced by Smith and Mudder[2])

21. Mudder, T., and.Whitlock, J., "Biological Treatment of Cyanidation Wastewaters", Mineral and Metallurgical Processing pp. 161-165, (1984)

22. Avedesian, M., Spira, P., and Kanduth, H., "Stripping of HCN in A Packed Tower", Can. J. Chem. Engineering, Vol. 61, pp. 801-806 (1983)

23. Lawr, C.W., "Cyanide Regeneration or Recovery as Practised by the Compania Beneficiadore de Pachuca", Technical Report No. 208-B_20, American Institute of Min., Metall., and Pet. Engineers, (1929) (As referenced by Smith and Mudder[2])

24. Goldstone, A., Cyprus Minerals of New Zealand, personal communication, (1990) (As referenced by Smith and Mudder[2])

25. Trautman, L.L., and Ommen, F., "Cyanide Removal Testwork at Homestake Gold Mine", presented at the Cyanide In Gold Mining Seminar, Ottawa (1981) (As referenced by Smith and Mudder[2])

26. Witte, M., K., Frey, C., C., and Hatch, W., R., "Recovery of Cyanide from Waste Waters by an Ion Exchange Process", South African Patent ZA8607235 (1986)

27. Coltrinari, E. L., "Method for recovery of cyanide from waste streams", International Patent (PCT), WO 87/00072

28. Goldblatt, E., "Recovery of Cyanide From Waste Cyanide Solutions by Ion Exchange", Industrial and Engineering Chemistry, 51, No.3, 241-246 (1959)

29. Gilmore, A. J., "The Ion Exchange Removal of Cyanide From Gold Mill Waste for Environmental Benefit", Canmet, Mineral Sciences Laboratories Report MRP/MSL 76-26 (1976) (As referenced by Smith and Mudder[2])

30. Avery, N. L. and Fries, W., "Removal of Cyanide From Industrial Waste Effluents With Ion Exchange Resins", Rohm and Haas Co., Philadelphia, Pennsylvania., (1974)

31. Halbe, D., Trautman, L., Neville, R. G., Hart, L., and Ommen, R., "Destruction of Cyanide in Homestake Gold Mill Effluent - a Status Report", Homestake Gold Mine, Lead, South Dakota, (1979) (As referenced by Smith and Mudder[2])

32. Vachon, D., "Removal of Iron Cyanide From Gold Mill Effluents by Ion Exchange", Water Sci. Tech., 17 pp. 313-324, (1985)

33. Nesbitt, A. B., Petersen, F., W.,"Recovery of metal cyanides using a fluidized bed of resin" Proceedings of the 5th international mineral processing symposium held in Capadocia Turkey, (1994)

34. Whiteway, P., "Cyanide Technology could Save Gold Miners Thousands", Northern Miner, 72, No. 32, pg.(3), (1986)

35. Smith, A., Mudder, T., "The Chemistry and Treatment of Cyanidation Wastes", pg (284..289) Mining Journal books London (1991)

36. Smith, A., Mudder, T., "The Chemistry and Treatment of Cyanidation Wastes", pg (15..17) Mining Journal books London (1991)

37. Riveros, P. A., Molnar, R., NcNamara, V. M., "Alternative technology to decrease the environmental impact of gold milling a progress report on CANMET research activities in this field", pg (167..171) CIM Bulletin, March (1993).

38. Fleming, C. A., Hancock, R. D., "The mechanism in the poisoning of anion-exchange resin by cobalt cyanide.", pg(334..341) SAIMM Journal June (1979).

39. M., Streat, "Recent developments in continuous ion exchange." J. Separ. Proc. Technol. 1, 10-18. (1980)

40. Richardson, P. H., "Sedimentation and fluidization part 1" Trans. Inst. Chem. Eng. 32 (1954)

41. Akapo, S., Khong, T. M., Simpson, C. P., Toussaint, B., Yates, J. G., "A novel method for determining the particle density of porous aeratable powders" Powder Technol., 58 (1989)

42. Nicolella, C., Converti, A., Di Felice, R., Rovatti, M., "The estimation of the solid size and density in liquid fluidized-bed biological reactors" shorter communication Chem. Eng. Sci., 50 (1994)

43. Hartman, M., Havlin, V., Svoboda, K., "Predicting voidage for particulate fluidization of spheres by liquids" Chem. Eng. Sci., 44 (1989)

44. Foscolo, P. U., Di Felice, R., Gibilaro, "An experimental study of the expansion characteristics of gas fluidized beds of fine catalysts", Chem. Engng Process 22 (1987)

45. Levenspiel, O., Kunii, K., "Fluidization Engineering". John Wiley and Sons Inc. London (1969)

46. Amirtharajah, A., Cleasby, J. L., "Predicting expansion of filters during backwashing" J. Am. Water Works Assoc. 64 (1972)

47. Wen, C. Y., Yu, Y. H., "Mechanics of fluidization", Chem. Engng Progr. Symp. Series Chem 62 (1966)

48. Epstein, N., Leclair, B. P., Pruden, B. B., "Liquid Fluidization of binary particle mixtures-I" Chem. Eng. Sci., 36 (1981)

49. Lewis, E. W., Bowerman, E. W., "Fluidization of solid particles in liquids" Chem. Engng Progr. 48 (1952)

50. Al-Dibouni, M. R., Garside, J., "Particle mixing and classification in liquid fluidization beds", Trans IChemI., 57 (1979)

51. Patwardhan, V. S., Chi Tien, "Sedimentation and liquid fluidization of solid particles of different sizes and densities", Chem. Engng Sci. 34 (1979)

52. Schiller, L., Naumann, A, "Uber die grundlegenden Berechnungen bei der Schwerkraftaufbereitung", Ver. Deut. Ing. 77 (1933) (As referenced by Coulson and Richardson Volume 2)

53. Hartman, M., Havlin, V., Trinka, O., Casky, M., "Predicting the free-fall velocities of spheres", Chem. Engng. Sci. 44 (1989)

54. Ladenburg, R. A., "Uber den Eingluss von Wanden auf die Bewegung einer Kugel in einer reibenden Flussigkeit", Ann. Phys. 23 (1907) (As referenced by Coulson and Richardson Volume 2)

55. Smith, A., Mudder, T., "The Chemistry and Treatment of Cyanidation Wastes", pg (204) Mining Journal books London (1991)

56. Fourth high level sminar on cleaner Production. A United nations environment program Oxford (1996)

57. Barker, J., Weaver, A., "Alusaf smelter expansion project Richards Bay" UCT + CSIR Report 103 (1992)

NOMENCLATURE

D	=	empty fluidization tube diameter
dp	=	particle diameter
dp_i	=	particle size of the ith component
dp_l	=	largest diameter bead in sample
dp_s	=	smallest diameter bead in sample
E	=	expansion factor (1 = 0%, 2 = 100%)
E_i	=	expansion factor of the ith component
E_t	=	total expansion factor
e	=	voidage
e_{fws}	=	free wet settled voidage
g	=	gravitational constant (9.81 $m.s^{-2}$)
Ga	=	Galeleo number
i	=	integer
L_i	=	extent of inter screen interval (micron size of larger aperture screen less the micron size of smaller aperture screen)
N	=	number of interscreen intervals
n	=	Richardson and Zaki expansion indices
Re_t	=	Reynolds number
S_i	=	normalized volume fraction of the ith screen interval
U	=	superficial tube vertical liquid velocity
U_t	=	terminal velocity
V	=	volume fraction
V_i	=	volume fraction of ith component of resin

Greek symbols

ρ_L	=	density of liquid
ρ_S	=	apparent density of resin
μ	=	liquid viscosity

APPENDIX A

The following describes a data input program written in Turbo Pascal version 7. This program records particle size distributions (PSD's) collected as quantity of resin (volumetric) not passing stated resin screen size X (microns). The program normalizes the data and then stores it as an ASCII data file which has the general name "psd____.dat" the structure of which is as follows:

DATA FILE

e.g.

6	|	(number of screens)	
350 0.010	|	(diameter microns)	(normalized resin vol)
450 0.020	|	(diameter microns)	(normalized resin vol)
600 0.015	|	(diameter microns)	(normalized resin vol)
800 0.015	|	(diameter microns)	(normalized resin vol)
1000 0.010	|	(diameter microns)	(normalized resin vol)
1150 0.010	|	(diameter microns)	(normalized resin vol)

PROGRAM

```
program psdinput;

uses
  Crt;

const
  Maxi = 20;

var
      q, prefix, suffix, dat, psd:string;
      datpoipsd,i : integer;
      F: text;
```

```
    screen, resvol :  Array [1..maxi] of real;

begin
    ClrScr;
    {the following section sets up the data input}
    writeln('THIS PROGRAM IS FOR STORING PARTICLE SIZE DISTRIBUTION
    DATA');
    writeln('-----------------------------------');
    writeln('Remember the file will automatically');
    writeln('get the prefix "psd", and the suffix ".dat"');
    writeln('hence the outcome will be',' ','psd_____.dat');
    writeln('-----------------------------------');
    writeln('what do you what the file to be called, (5 digits only)');

    readln(q);
    prefix := 'psd';
    suffix := '.dat';
    q := (prefix) + (q) + (suffix);
    clrscr;
    writeln (q);
    writeln('how many data points are there(NUMBER OF SCREENS)');
    readln(datpoipsd);

        for i := 1 to datpoipsd do begin
            clrscr;
            writeln('during input of screen and resin volume
            data');
            writeln('remember to put the screen aperture size first, in microns');
            writeln('followed by the volume of resin found  there on in ccm or mls');
            writeln('start with the lowest screen size, and remember this');
            writeln('program assumes that there is nothing larger than 1200microns');
            writeln;
```

```
                writeln('enter the data like this..');
                writeln('screen aperture size data point No.1     <enter>');
                writeln('volume of resin found there on data point No.1 <enter>');
                writeln('screen aperture size data point No.2     <enter>');
                writeln('volume of resin found there on data point No.2 <enter>');
                writeln('etc, etc....');

                writeln('input screen aperture size',' ','data point',' ',i);
                read(screen[i]);
                writeln('volume of resin',' ','data point',' ',i);
                read(resvol[i]);
            end;
        clrscr;
        screen[datpoipsd + 1] := 1200;
{The following section normalizes the data.}
        writeln('No. of data points',' ',datpoipsd);
                for i := 1 to (datpoipsd) do begin
                 resvol[i] := (resvol[i])/(screen[i+1] - screen[i]);
                screen[i] := (screen[i+1] - screen[i])/2 + screen[i];
                writeln(screen[i]:0:0,' ',resvol[i]:0:3);
            end;
{The following section stores the data under file name given.}
                Assign(F, q);
                rewrite(F);
                writeln(F, datpoipsd);
                for i := 1 to datpoipsd do begin
                writeln(F, screen[i]:0:0,'  ',resvol[i]:0:3);
            end;
        close(F);
  writeln('file is now closed and;');
  writeln('stored on current drive as:',q);
```

```
    delay(3000);
end.
```

APPENDIX B

The following describes a data input program written in Turbo Pascal version 7. This program records all parameters surrounding a fluidization experiment, including a set of superficial liquid velocities vs resin bed expansions. The recorded parameters are; fluid temperature, resin bed diameter and free wet settled resin bed hight(fwsh). The superficial fluid velocity is calculated from inputed volumetric flowrates. The data is stored as an ASCII data file with the general name "exp___.dat" the structure of which is as follows:

DATA FILE

e.g

5		(number of fluidization velocities)
2.0000000E+0001		(temp of fluid, degC)
40		(diameter of bed, mm)
1.0000000E+0002		(fwsh of resin, mm)
9.9999999E-0004	44.9	(liquid velocity)(expansion %)
1.9999997E-0003	86.3	(liquid velocity)(expansion %)
3.0000002E-0003	133.8	(liquid velocity)(expansion %)
3.9999994E-0003	198.2	(liquid velocity)(expansion %)
4.9999999E-0003	316.6	(liquid velocity)(expansion %)

PROGRAM

```
program expaninput;

uses
  Crt;

const
   maxexpansions = 20;
```

```
var
        q, suffix, prefix, dat, exp : string;
        expansions, diameter, i : integer;
        fwsh, temp  : real;
        F : text;
        volflow, velflow, expan: Array [1..maxexpansions] of real;

begin
        clrscr;
        {this part of the program inputs the initial input}
        writeln('THIS PROGRAM WILL TAKE IN THE RECORDED EXPANSION
        DATA');
        writeln('AND WILL THEN STORE THIS DATA IN A FILE');
        writeln('-----------------------------------');
        writeln('remember the file will automatically');
        writeln('get the prefix "exp", and the suffix ".dat"');
        writeln('hence the outcome will be',' ','exp_____.dat');
        writeln('-----------------------------------');
        writeln('what is the name of the data?, (5 digits only)');
        readln(q);
        prefix := 'exp';
        suffix := '.dat';
        q := (prefix) + (q) + (suffix);
        clrscr;
        writeln (q);
        writeln('what is the diameter of the column in mm please?');
        readln(diameter);
        writeln('what is the temperature of the solution in the column in degC please?');
        readln(temp);
        writeln('excluding zero flows how many expansion were measured?');
        readln(expansions);
```

```
writeln('what was the free wet settled height of the bed, in mm ?');
readln(fwsh);
        for i := 1 to expansions do begin
        clrscr;
        writeln('THIS WILL BE FOR FILE',' ',q);
        writeln('column diameter',' ','(',diameter,'mm)');
        writeln('temperature of solution','                    ','(',temp:0:1,'degC)');
        writeln('free wet settled height of bed','             ','(',fwsh:0:2,'mm)');
        writeln('number of expansions excluding 0 flow','          ','(',expansions,'
        ','expansions)');
        writeln;
        writeln;

        writeln('enter the flowrates, and expansions');
        writeln('enter the data like this..');
        writeln('volflow in ml/min data point No.1 <enter>');
        writeln('height of resin bed in mm data point No.1          <enter>');
        writeln('volflow in ml/min data point No.2 <enter>');
        writeln('height of resin bed in mm data point No.2          <enter>');
        writeln('etc, etc....');
        writeln;
        writeln('START WITH THE LOWEST FLOWRATE');
        writeln('-------------------------------');
        writeln('input volflow',' ','data point',' ',i);
        read(volflow[i]);
        writeln('height of resin bed',' ','data point',' ',i);
        read(expan[i]);
        end;
```

{This section calculates liquid velocities and % expansions.}

```
        for i := 1 to expansions do begin
        velflow[i] :=    (volflow[i])/(((diameter/20)*
        (diameter/20))*3.14159) * (1/6000);
```

```
                expan[i] := ((expan[i]/fwsh)-1)*100
                end;
```

{This section of the program prints out the file information.}

```
        clrscr;
        writeln('    THIS WILL BE FOR FILE',' ',q);
        writeln;
        writeln;
        writeln;
        writeln('column diameter',' ','(',diameter,'mm)');
        writeln('temperature of solution','        ','(',temp:0:1,'degC)');
        writeln('free wet settled height of bed','        ','(',fwsh:0:2,'mm)');
        writeln('number of expansions excluding 0 flow','        ','(',expansions,' ','expansions)');
        writeln;
        writeln;
                for i := 1 to expansions do begin
                writeln('data point No.',i,' ','velocity','                    ',velflow[i]:0:5,' ','M/sec',',
                ','expansion','                ',expan[i]:0:1,'%');
                end;
```

{The next part of the program stores the expansion data in a file.}

```
    Assign(F, q);
    rewrite(F);
    writeln(F, expansions);
    writeln(F, temp);
    writeln(F, diameter);
    writeln(F, fwsh);
            for i := 1 to expansions do begin
            writeln(F, velflow[i],'  ',expan[i]:0:1);
            end;
    close(F);
```

```
    writeln;
    writeln;
    writeln;
    writeln('file is now closed and');
    writeln('stored on current drive as:',q);

    delay(3000);

end.
```

APPENDIX C

The following uncompiled computer software, written in Turbo Pascal version 7, simulates particulatly fluidized beds for a continuous medium of water i.e. resin fluidized by an aqueous medium. The program requires a particle size distribution to be stored in an ASCII file structured in the manner described in appendix A. This file can be generated manually by an editor, or can be generated by running the program described in appendix A. The program also requires some general inputs such as; temperature of the continuous medium (water temperature), free wet settled voidage, discontinuous medium density (resin density) and fluidized bed dimensions in the horizontal plane(fluidization tube diameter). Having processed these data and establishing the fluidization parameters the program then requires superficial vertical velocities of the continuous medium for which it then predicts a bed expansion. The program operator may input as many velocities as he requires. The program assumes the fluidized bed to be perfectly circular in the radial dimension i.e. at right angles to the average motion of fluidization liquid.

PROGRAM

```
program expansions;

uses
  Crt;

const
  MaxN = 500;

var
  qpsd, ex, dat, suffix, prefix : string;
  F,e, ELUTRIATION, FINE : text;
  i, datapoi, incno, q, j, number, check : integer;
  o, totfrac, temp, Ut, fvoidage, V, N, expan, expantot, fwsh,
```

```
  perexpan, diameter, dp, ga, liqvis, liqdens, Re,
  rdensity : real;
  dps  : Array[0..20] of integer;
  vols : Array[0..20] of real;
  d, u, w, p, inc, dx, dy, k, t, s :  Array [0..maxn] of real;
  a : Array[0..50, 0..50] of real;
```

Procedure vizdensity; .

{This procedure need's a "temp" in memory.}

```
begin
    liqvis := (temp*temp*6.894e-7)-(temp*5.467e-5)+(0.001801);
    liqdens := (-temp*temp*0.004604)-(temp*9.783e-3)+(1000);
end;
```

Procedure termvel;

{This procedure requires a particle diameter dp, resin density rdensity, liquid viscosity liqvis.}

```
var
  termvel, A, P, R : real;

begin

  Ga := ((dp/1000000)*(dp/1000000)*(dp/1000000)*9.81*
  (rdensity-liqdens)*liqdens)/(liqvis*liqvis);
  A := ln(ga)/ln(10);
```

```
    P := (((0.0017795 * A - 0.0573)*a + 1.0315)*a - 1.26222);
    R :=  ln(0.99947 + 0.01853*sin(1.848 *a - 3.14))/ln(10);
    RE := EXP(LN(10)*(P + R));
    Ut := Re * liqvis/(liqdens*(dp/1000000));

end;

begin
        clrscr;
```

{This part of the program obtains the previously stored psd information.}

```
        writeln('THIS PROGRAM WILL GIVE YOU EXPANSIONS FOR ANY SET OF
        GIVEN PARAMETERS');
        writeln('-----------------------------------');
        writeln('What is the name of the particle size distribution data?');
        writeln('(only the four letter code is important)');
        readln(qpsd);
        clrscr;
        prefix := 'PSD';
        suffix := '.DAT';
        qpsd := (prefix) + (qpsd) + (suffix);
        Assign(F, qpsd);
        reset(F);
        readln(F, datapoi);
        for i := 0 to datapoi-1 do begin
        readln(f, dps[i], vols[i]);
        end;
    writeln(datapoi);
    close(f);
```

{The next part of the program attempts to fit a spline to psd/volumes data the variables are: datapoi, number of data points; dps, particle sizes; vols, volumes attached to these sizes.}

```
ClrScr;
```

{This section determines the dps values which are going to be determined.}

```
incno := 500;

o := (dps[datapoi-1]-dps[0])/(incno+1);   {o=inc}
inc[1]  := dps[0] + o;
    for q := 2 to incno do begin
    inc[q] := inc[q-1] + o;
    end;
```

{This part of the program calculates dx, dy, d values.}

```
for i:=1 to datapoi-1 do begin
dx[i] := dps[i] - dps[i-1];
dy[i]:=vols[i]-vols[i-1];
d[i]:=dy[i]/dx[i];
end;
```

{This part of the program determines zspl values.}

```
A[1,1] := 2;
A[datapoi,datapoi] := 2;
for i := 2 to datapoi-1 do
A[i,i] := 2*(dx[i-1]+dx[i]);
```

{The next part of the program determines the w vectors.}

```
A[1,datapoi+1] := d[1]*3;
A[datapoi,datapoi+1] := d[datapoi-1]*3;
```

```
for i :=2 to datapoi-1 do
a[i,datapoi+1] := (d[i-1]*dx[i]+d[i]*dx[i-1])*3;
```

{Next part of program determines u values.}

```
a[1,2] := 1;
a[datapoi,datapoi-1] := 1;
for i := 2 to datapoi-1 do begin
a[i,i+1] := dx[i-1];
a[i,i-1] := dx[i];
end;
```

{The following part of the program solves the matrix for the k values.}

```
for i := 1 to datapoi-1 do begin
a[i+1,datapoi+1] := a[i+1,datapoi+1]-a[i,datapoi+1]*a[i+1,i]/a[i,i];
a[i+1,i+1] := a[i+1,i+1]-a[i,i+1]*a[i+1,i]/a[i,i];
end;


j := datapoi+1;
repeat
j := j-1;
k[j-1] := (a[j,datapoi+1]-a[j,j+1]*k[j])/a[j,j];
until j = 1;
```

{The next part of this program determines the applicable t value for each value of inc[i] chosen, the program calculates a t value.}

```
totfrac := 0;
for q := 1 to incno do begin
I := - 1;
```

```
repeat
I := i + 1;
until inc[q] <= dps[i+1];
t[q] := (inc[q]-dps[i])/dx[i+1];
```

{This part of the program determines the corresponding vols value for dps.}

```
s[q] := t[q]*vols[i+1]+(1-t[q])*vols[i]+dx[i+1]*
((k[i]-d[i+1])*t[q]*(1-t[q])*(1-t[q])-(k[i+1]-
D[i+1])*(t[q])*(t[q])*(1-t[q]));
{writeln(inc[q],' ',s[q]);}
TOTFRAC := totfrac + s[q];
end;
for q := 1 to incno do begin
s[q] := s[q]/totfrac;
end;
```

{At this point the psd data has been splined, and has been sorted out into 500 bits of data, the resin diameters are constituted as "inc" array, and the proportion of each size is stored as an array "s" i.e. sum of all s = 1.}

{————————————————————————————}

{The next part of the program takes in parameters that can be used to calculate expansions from estimated resin density and free wet settled voidage.}

```
clrscr;
writeln('THESE EXPANSIONS ARE FOR DATA STORED IN FILE ','  " ',QPSD,' " ');
writeln;
write('What is the diameter of the column, in mm please?,   ');
read(diameter);
```

```
diameter := diameter/1000;
write('What is the temperature of the fluidizing liquid in      degC ?, ');
read(temp);
write('Estimated resin density in kg/cubic meter ?, ');
read(rdensity);
write('Estimated free wet settled voidage?, ');
read(Fvoidage);
write('How many liquid velocities do you want?, ');
read(number);
    writeln('-------------------------------');
    For i := 1 to number do begin
    check := 1;
    writeln('give the',' No.',i,' velocity');
    read(V);
    expantot := 0;
        For q := 1 to incno do begin
        dp := inc[q];
```

{Ccalling on the calculation of liquid density and viscosity procedure.}

```
    vizdensity;
```

{Calling on the calculation of terminal velocity procedure.}

```
    termvel;
```

{Calculating Richardson and Zaki N parameter of fluidization.}

```
    n := (5.5+23*((dp/1000000)/diameter))
        *exp(ln(Ga)*(-0.075));
```

{Calculating individual expansions and adding.}

```
expan :=(((1-fvoidage)/(1-exp(ln(V/Ut)*(1/N)))-1)*s[q]);

                    if expan < 0 then
                    begin
                    check := 2;
                    end
                    else
                    begin
                    expantot := expantot + expan;
                    end;
    end;

                    if check = 2 then
                    begin
                    writeln('an error has been detected');
                    end
                    else
                    begin
                    perexpan := expantot*100;
```

{At this point the expansion is given for the inputed superficial velocity.}

```
                        writeln(perexpan:0:1,' % expansion');
                    end;
    end;
end.
```

APPENDIX D

The following uncompiled software, written in Turbo Pascal version 7, locates the apparent density of the discontinuous medium and voidage for a particularly fluidized bed of which the, particle size distribution, expansion parameters and all other characteristics are known. The particle size distribution data is retrieved from an ASCII data file structured as that described in appendix A. The fluidization parameters and superficial vertical continuous medium velocity vs expansion data is retrieved from a file as that described in appendix B. Both of these data files can be generated by an editor, or created by using the software described in appendix A or B respectively.

PROGRAM

```
program hookjeevesoptomizer;

uses
    Crt;

const
  MaxN = 500;
var
    F,e, exf :text;
    prefix, suffix, qpsd, dat, qexp : string;
    z, zz, h, k, zfi, zfb, o, totfrac, temp, fwsh, liqvis, liqdens, Re, Ga, dp, rdensity, aterm,
    pterm, rterm, Ut, expan, expantot, perexpan, N, diameter : SINGLE;
    incno, fe, par, i, j, flag, datapoi, q, js, expansions : integer;
    x, y, b, p, xmin, xmax, d, inc, dx, dz, dy, ks, t, s : Array [0..maxn] of SINGLE;
    dps : array[0..15] of integer;
    vols, velflow, expans : array[0..15] of SINGLE;
    a : array[0..50, 0..50] of SINGLE;
```

```
label
        200, 280, 290, 360, 420, 490, 540, 700, 3200;
```

Procedure vizdensity;

{This procedure need's a "temp" in memory.}

```
begin
    liqvis := (temp*temp*6.894e-7)-(temp*5.467e-5)+(0.001801);
    liqdens := (-temp*temp*0.004604)-(temp*9.783e-3)+(1000);
end;
```

Procedure termvel;

{This procedure requires a particle diameter dp, resin density X[1], liquid viscosity liqvis.}

```
begin
        x[1] := x[1] * 10000;
        Ga := ((dp / 1000000) * (dp / 1000000) * (dp / 1000000) *      9.81 * (x[1]-liqdens) *
        liqdens) / (liqvis * liqvis);
        aterm := ln(ga) / ln(10);
        pterm := (((0.0017795 * aterm - 0.0573) * aterm + 1.0315) * aterm - 1.26222);
        rterm :=  ln(0.99947 + 0.01853 * sin(1.848 * aterm - 3.14))/ln(10);
        re := exp(ln(10) * (pterm + rterm));
        Ut := Re * liqvis / (liqdens * (dp / 1000000));
        x[1] := x[1]/10000;
end;
```

procedure display;

{This procedure simply displays the variables during the search procedure and also the sum squares as it alters.}

```
begin
        ClrScr;
        gotoXY(40,11);
        writeln('q = ',zz:0:14);
        gotoXY(40,12);
        writeln('X[1] = ',X[1]:0:14);
        gotoXY(40,13);
        writeln('X[2] = ',X[2]:0:14);
end;
```

procedure detsumsqu;

{This procedure does two things; supplies a zz value which is the sum of squared differences between calculated velocities, and recorded velocities and also supplies an fe value which simply increments by 1 every time this procedure is called up.}

```
begin
        zz := 0;

                For i := 0 to expansions-1 do begin
                expantot := 0;
                For q := 1 to incno do begin
```

{Each resin diameter now to be referred to as dp.}

```
                dp := inc[q];
```

{Calling on the procedure that calculates the liquid density and viscosity.}

```
                vizdensity;

{Calling on the procedure that calculates the particle terminal velocity.}

                termvel;


{Calculating the Richardson and Zaki N parameter for fluidization.}


                N := (5.5+23*((dp/1000000)/(diameter/1000)))
                *exp(ln(Ga)*(-0.075));

{Calculating individual expansions and adding.}

                x[2] := x[2]/10;
                expan :=(((1-X[2])/(1-exp(ln(velflow[i]/Ut)*(1/N)))-1) * s[q]);
                x[2] := x[2]*10;
                expantot := expantot + expan;

                end;

                perexpan := expantot*100;
                z := (perexpan - expans[i]) * (perexpan - expans[i]);
                zz := zz + z;

  end;

fe := fe + 1;

end;
```

```
procedure eatheror;

{This procedure enforces the search boundaries.}

label 3200;

begin
    if x[j] > xmax[j] then begin
    x[j] := xmax[j];
    goto 3200;
    end;
    if x[j] < xmin[j] then x[j] := xmin[j];
    3200:
end;

{START OF MAIN PROGRAM}

begin
        ClrScr;
        writeln('optimization algorithm for the location of best fit parameters');
        writeln('            method of Hooke & Jeeves');
        {"par" is the number of variables}
        par := 2;

{The first search parameter is the resin apparent density, the second search parameter is
the free wet settled voidage.}

{At this point the psd data is retrieved.}
```

```
        writeln('What is the name of the particle size distribution data?');
        writeln('(only the name is important)');
        readln(qpsd);
        ClrScr;
        prefix := 'PSD';
        suffix := '.DAT';
        qpsd := (prefix) + (qpsd) + (suffix);
        assign(F, qpsd);
        reset(F);
        readln(F, datapoi);

        for i := 0 to datapoi-1 do begin
        readln(f, dps[i], vols[i]);
      end;

   close(f);
```

{The next part of the program attempts to fit a spline to PSD/VOLUME data the variables are : "datapoi", number of data points; "dps", particles sizes; "vols", volume of attached sizes.}

```
   ClrScr;
```

{This section determines the dp values which are going to be determined.}

```
   incno := 500;

   o := (dps[datapoi-1]-dps[0])/(incno+1);
   inc[1]  := dps[0] + o;

       for q := 2 to incno do begin
       inc[q] := inc[q-1] + o;
```

```
end;
```

{This part of the program calculates dx,dy,d values.}

```
for i:=1 to datapoi-1 do begin
dx[i] := dps[i] - dps[i-1];
dy[i]:=vols[i]-vols[i-1];
dz[i]:=dy[i]/dx[i];
end;
```

{This part of the program determines zspl values.}

```
A[1,1] := 2;
A[datapoi,datapoi] := 2;

for i := 2 to datapoi-1 do
A[i,i] := 2*(dx[i-1]+dx[i]);
```

{The next part of the program determines the w vectors.}

```
A[1,datapoi+1] := dz[1]*3;
A[datapoi,datapoi+1] := dz[datapoi-1]*3;

for i :=2 to datapoi-1 do
a[i,datapoi+1] := (dz[i-1]*dx[i]+dz[i]*dx[i-1])*3;
```

{Next part of program determines u values and puts them into the matrix.}

```
a[1,2] := 1;
a[datapoi,datapoi-1] := 1;

for i := 2 to datapoi-1 do begin
```

```
a[i,i+1] := dx[i-1];
a[i,i-1] := dx[i];
end;
```

{The following part of the program solves the matrix for the ks values.}

```
for i := 1 to datapoi-1 do begin
a[i+1,datapoi+1] := a[i+1,datapoi+1]-a[i,datapoi+1]*a[i+1,i]/a[i,i];
a[i+1,i+1] := a[i+1,i+1]-a[i,i+1]*a[i+1,i]/a[i,i];
end;
```

```
js := datapoi+1;
repeat
js := js-1;
ks[js-1] := (a[js,datapoi+1]-a[js,js+1]*ks[js])/a[js,js];
until js = 1;
```

{The next part of this program determines the applicable value for each value of inc[i] chosen, the program calculates a t value.}

```
totfrac := 0;
```

```
for q := 1 to incno do begin
I := -1;
repeat
I := i +1;
until inc[q] <= dps[i+1];
t[q] := (inc[q]-dps[i])/dx[i+1];
```

{This part of the program determines the corresponding vols value for dps.}

```
s[q] := t[q]*vols[i+1]+(1-t[q])*vols[i]+dx[i+1]*
((ks[i]-dz[i+1])*t[q]*(1-t[q])*(1-t[q])-(ks[i+1]-
Dz[i+1])*(t[q])*(t[q])*(1-t[q]));
totfrac := totfrac + s[q];
end;

for q := 1 to incno do begin
s[q] := s[q]/totfrac;
end;
```

{At this point the psd data has been splined, and has been sorted out into 500 bits of data, the resin diameters are constituted as "inc" array, and the proportion of each size is stored as an array "s".}

{————————————————————————————————}

{The next part of the program will retrieve the expansion data.}

```
writeln('What is the name of the expansion vs flow file?');
writeln('(only the name is important)');
readln(qexp);
ClrScr;
prefix := 'exp';
qexp := (prefix) + (qexp) + (suffix);
Assign(exf, qexp);
reset(exf);
readln(exf, expansions);
readln(exf, temp);
readln(exf, diameter);
readln(exf, fwsh);

        for i := 0 to expansions - 1 do begin
```

```
readln(exf, velflow[i], expans[i]);
end;
```

{The expansion data has been stored as a few data points called velflow and expans, other parameters are the column diameter, temp, fwsh.}

{————————————————————————————}

{At this point the search algorithm starts}

{In the following section we define the boundaries of the parameters which are to be searched for.}

```
xmin[1] := 0.1040;
xmax[1] := 0.1300;
xmin[2] := 1.0000;
xmax[2] := 4.5000;
```

{This next section determines starting parameter values for the algorithm.}

```
X[1] := 0.1300;
X[2] := 5.0;
    for i := 1 to par do begin
    y[i] := x[i];
    p[i] := x[i];
    b[i] := x[i];
    end;
```

{"H" is the starting approach increment which will diminish with iteration.}

{The programming style that follows from here on is not strictly similar to what has gone before. This is because it is an adaption from a Turbo basic module}

```
H := 0.001;
```

```
k := h;
fe := 0;

detsumsqu;

zfi := zz;
flag := 1;
j := 1;
zfb := zfi;

200: x[j] := y[j] + k;

eatheror;

detsumsqu;

if zz < zfi then goto 280;

x[j] := y[j] - k;

eatheror;

detsumsqu;

if zz < zfi then goto 280;

x[j] := y[j];
goto 290;

280: y[j] := x[j];

display;
```

```
290: detsumsqu;

zfi := zz;

if j = par then goto 360;
j := j + 1;
goto 200;

360: if zfi < (zfb - 9.999999999999999e-30) then goto 540;
if flag = 0 then goto 420;
goto 490;

        420: for j := 1 to par do begin
        p[j] := b[j];
        y[j] := b[j];
        x[j] := b[j];

        eatheror;

        end;

detsumsqu;

flag := 1;
zfi := zz;
zfb := zz;
j := 1;
goto 200;

490: k := k / 2.5;
```

```
if k < 9.999999999999999e-38 then goto 700;
j := 1;
goto 200;

        540: for j := 1 to par do begin
        p[j] := 2 * y[j] - b[j];
        b[j] := y[j];
        x[j] := p[j];

        eatheror;

        y[j] := x[j]
        end;

detsumsqu;

zfb := zfi;
flag := 0;
zfi := zz;
j := 1;
goto 200;
```

{End of adapted module.}

{At this point the final values obtained are printed.}

```
700: ClrScr;
writeln('results');
        for I := 1 to par do
        writeln('xopt  ',i ,'=', p[i]:0:4);
        writeln('function optimum  : Qopt = ',zfb:0:14);
        writeln('number of iterations: iter = ', fe);
```

```
        writeln('end program now');
        readln;
end.
```

APPENDIX E

The following is a mathematical description of the various algorithms used in this thesis.

SPLINE ROUTINE

This algorithm was used to develop a continuous relationship between resin bead diameter and the volume fraction to the whole resin bed, at such resin bead diameter. Such a continuous relationship was necessary for the purposes of performing the product integration in the resin bead "diameter" domain with respect to bead terminal velocity and diameter volume fraction to the whole fluidized bed.

The ordinates of y_i are given at $x_i (i = 1,....,n)$, respectively.
Where x denotes resin bead diameter and y denotes volume fraction to the whole resin bed.

Let

$$h_i = x_{i+1} - x_i$$

denote the mesh point spacing.

Let y(x) be an interpolation curve through these points and define y'_i and y''_i as the first and second derivatives, respectively, of

$$y(x) \text{ at } x = x_i$$

Let y(x) be expressed in piece-wise fashion as

$$y(x) = f_i(x) \text{ for } x_i \leq x < x_{i+1}; \quad i = 1,....,n - 2$$
$$y(x) = f_i(x) \text{ for } x_{n-1} \leq x \leq x_n; \quad i = n - 1$$

with the following conditions on function value and first and second derivatives:

$$f_i(x_i) = y_i; \quad \textit{condition 1} \quad i = 1,\ldots,n-1$$
$$f_{i-1}(x_i) = y_i; \quad \textit{condition 2} \quad i = 2,\ldots,n$$
$$f_{i'-1}(x_i) = f_{i'}(x_i); \quad \textit{condition 3} \quad i = 2,\ldots,n-1$$
$$f_{i''-1}(x_i) = f_{i''}(x_i); \quad \textit{condition 4} \quad i = 2,\ldots,n-1$$

The individual cubic polynomial $f_i(x)$ can be expressed using the interval values y_i, y_{i+1} and either y'_i, y'_{i+1}, or y''_i, y''_{i+1} to represent the cubic coefficients.
Assuming $y''(x)$ = constant each interval means that $y''(x)$ is linear, we get

$$f_{i''} = y_{i''}\left(\frac{x_{i+1} - x}{h_i}\right) + y_{i''+1}\left(\frac{x - x_i}{h_i}\right)$$

Integrating twice more and selecting the constant of integration such that the conditions 1 and 2 are satisfied yields:

$$f_i(x) = y_i\left(\frac{x_{i+1} - x}{h_i}\right) + y_{i+1}\left(\frac{x - x_i}{h_i}\right)$$
$$- \frac{h_i^2}{6} y_{i''}\left[\frac{x_{i+1} - x}{h_i} - \left(\frac{x_{i+1} - x}{h_i}\right)^3\right]$$
$$- \frac{h_i^2}{6} y_{i''+1}\left[\frac{x - x_i}{h_i} - \left(\frac{x - x_i}{h_i}\right)^3\right]$$

which identically satisfies the continuity condition on the second derivative(condition 4).
Expanding the LHS and the RHS of the third condition equation by differentiating the above equation and evaluating yields, respectively,

$$f_{i'}(x_i) = \frac{y_{i+1} - y_i}{h_i} - \frac{h_i}{6}(2y_{i''} + y_{i+1})$$
$$f_{i'-1}(x_i) = \frac{y_i - y_{i-1}}{h_{i-1}} + \frac{h_{i-1}}{6}(y_{i''-1} + 2y_{i''})$$

which, when equated, produce the condition;

$$h_{i-1}\,y_{i-1} + 2(h_{i-1})\,y_i + h_i\,y_{i+1} = 6\left(\frac{y_{i+1} - y_i}{h_i} - \frac{y_i - y_{i-1}}{h_{i-1}}\right)$$
$$i = 2,\ldots,n-1$$

which must be satisfied at n - 2 points by the n unknown quantities y''_i. Two more conditions are required on the y''_i, and these are obtained by specifying one end condition at each end.

Specifying the end second derivatives y_1'' and y_n'' leaves n - 2 unknowns, which can be obtained by solving the n - 2 equation of the above equation. The coefficient matrix is tri-diagonal, with the diagonal term being dominant.

The spline is described as a global curve, i.e. altering a single y_i or end condition affects the spline throughout $[x_1, _n]$, the dominant diagonal term causes such effects to become small rapidly as the distance from the altered point increases, virtually eliminating round-off problems.

NEWTON'S METHOD
A DIFFERENTIAL SEARCH TECHNIQUE

This routine was used to solve for terminal velocity in the Shiller Nauman empirical model. The terminal velocity variable is incorporated in the Reynolds Number. which appears twice in the equation. As each Reynolds Number. is raised to a different indices an iterative search method such as "Newton's method" has to be used to locate the terminal velocity given all other variables.

Newton's method of iteration uses extrapolation based on a line that is a tangent to the curve at a point. In essence the method is an analytical substitution of the local tangent line for the function and then the use of the zero of this line as the next approximation to the zero of the function.

The method is developed from a Taylor's expansion of the form:

$$f(x_n + h) = f(x_n) + hf(x_n) + \frac{h^2}{x_n} f''(x_n) + \ldots$$

The h^2 and higher order terms are dropped, and $x_n + h = x_{x+1}$ is used. It is assumed that the step from x_n to x_{n+1} moves the function valve close to a root so that $f(x_n + h) = 0$. Then:

$$x_{n+1} = x_n - \frac{f(x_n)}{f'(x_n)}$$

The value x_{n+1} is equivalent to the point where the curve tangent at x_n passes through the x-axis. Since the curve f(x) is likely not a straight line, the functional value $f(x_{n-1})$ is likely not to be exactly zero. For this reason the process is repeated using $x_n = x_{n+1}$ as a new base point. When the value of $f(x_{n+1})$ is sufficiently small, the process is terminated.

HOOK & JEEVES OPTIMIZATION, (THE METHOD OF)

To locate the free wet settled voidage of the resin bed and the apparent density of the resin, an iterative optimization locative algorithm is required. As the search domain in this particular application is characterised by extreme peaks, large gradients and localized minima. It was decided to use a stable, relatively simple technique such as the Hook & Jeeves optimization algorithm.

The method is based on the assumption of unimodality and is used to find the minimum of a multi-variable, unconstrained function of the form:

$$MERIT = F(x_1, x_2, \ldots, x_n).$$

The algorithm proceeds as follows. First, a base point in the feasible design space is chosen along the exploration step sizes. Next, an exploration is performed at given increment along each of the independent variable directions following the logic shown in Figure 21.

When ever a functional improvement is obtained, a new temporary base point is established. Once this exploration is complete, a new base point is established, and a "pattern move" takes place. This pattern move consists of an extrapolation along a line between the new base point and the previous base point.

The distance moved beyond the best base point is somewhat larger than the distance between the two base points. Mathematically, this extrapolation is:

$$x_{i,o}^{k+1} = x_i^{k+1} + \alpha\left[x_i^{k+1} - x_i^k \right]$$

where $x_{i,o}^{k+1}$ becomes a new temporary base point or "head". In this expression, "i" is the variable index, "k" is the stage index, and "alpha" is an acceleration factor that is greater than or equal to 1.0. Once the new temporary base point has been found, an exploration about this point is nstituted to see if a better base point can be found. This exploration also uses the logic of Fig.22. I If the temporary head or any of its neighbouring points are a better base, the pattern process repeats using successive pattern extrapolation becomes bolder and bolder until the process oversteps the peak or a ridge. At this point the previous "best base" is recalled, the local exploration step size is decreased, and the pattern-building process begins again. Once the step size is decreased below a predetermined value and still no substantial change in the merit value can be achieved, the procedure terminates.

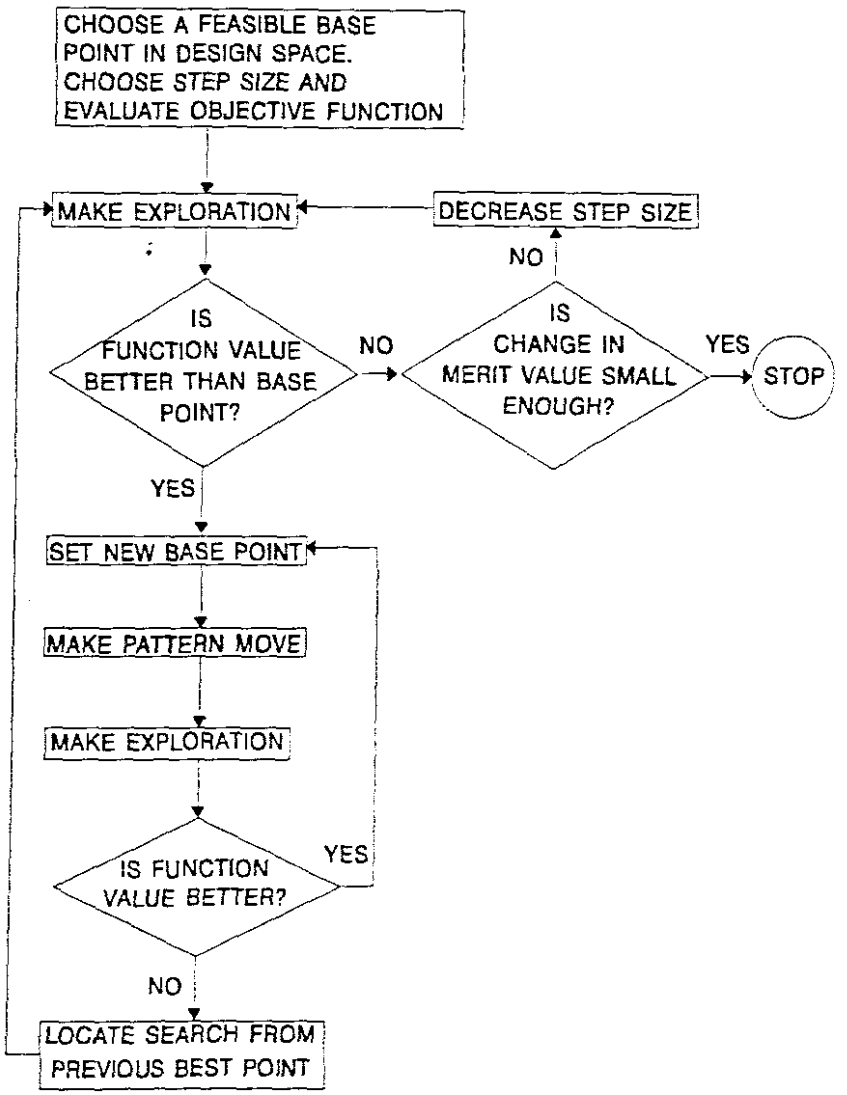

Figure 21. The Hook & Jevees pattern search algorithm

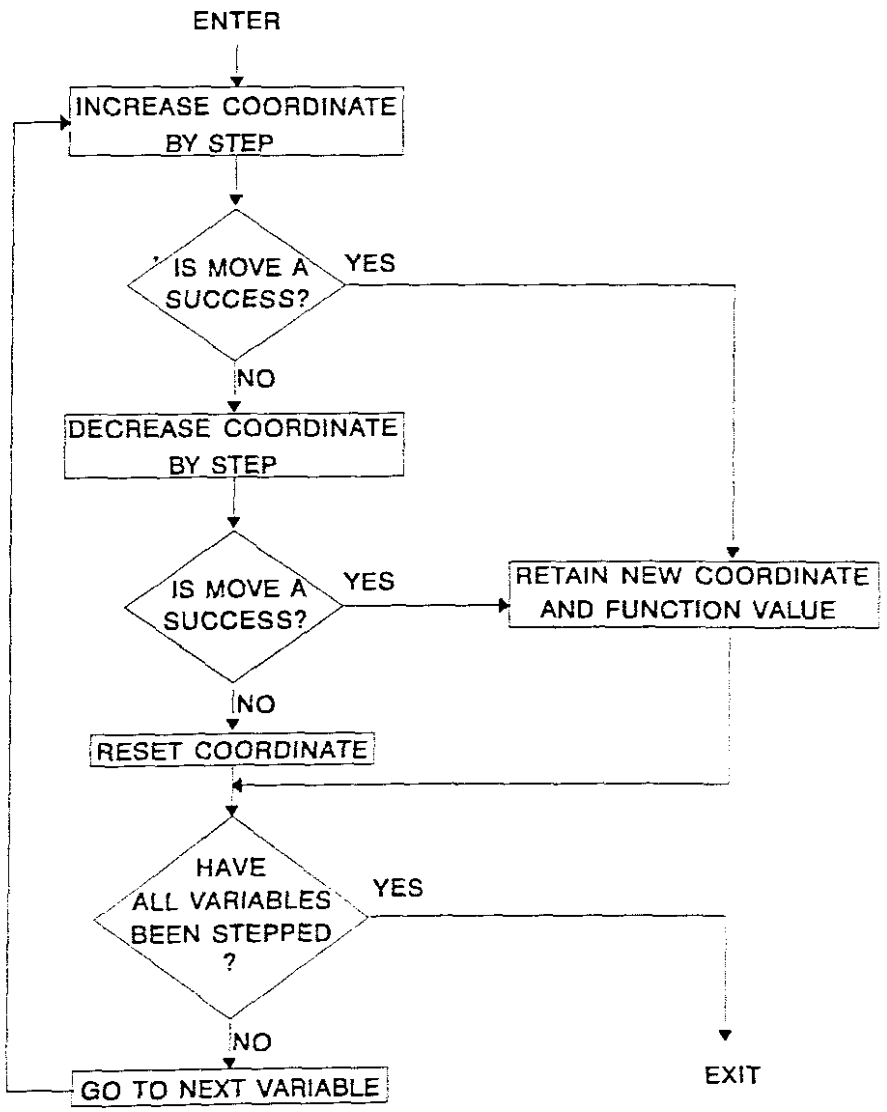

Figure 22. The exploration method used in the Hooke and Jeeves algorithm.

APPENDIX F

RAW DATA OF FLUIDIZATION TESTWORK

RESIN C26

A relatively dense, strong acid resin with a macroporous, styrene di-vinyl-benzene, co-polymer matrix and a sulphonic active site fluidized in the hydrogen form.

30mm diameter column

Particle size distribution

screen mesh sizing (microns)	volume in ml retained 12degC	15/18/21/25degC
300	0.6	1.9
355	4.4	0.6
425	5.0	4.5
500	25.5	5.0
600	6.0	25.5
710	2.8	6.0
850	3.2	2.8
1000	1.9	3.2
1180	1.2	1.6

30mm column diameter

Expansions

12degC		15degC		18degC	
ml/min	%	ml/min	%	ml/min	%
36.5	11.9	30.5	10.4	30.0	14.9
57.5	29.9	62.5	32.8	62.5	32.8
88.5	52.2	95.7	53.7	94.5	56.7
112.7	82.1	132.9	77.6	126.6	80.6
145.6	132.8	175.1	113.4	161.9	110.4
	202.8	131.1	193.0	141.8	
density 1109		density 1153		density 1124	

voidage 0.45	voidage 0.377	voidage 0.388
SS 156.96	SS 23.66	SS 17.39

21degC		25degC	
ml/min	%	ml/min	%
30.5	14.9	38.5	16.4
64.2	34.3	81.8	35.8
109.9	58.2	122.1	59.7
149.9	80.6	160.9	85.1
192.6	109.0	191.3	11.9
226.8	135.8	226.0	132.8
density 1161		density 1135	
voidage	0.339	voidage	0.375
SS	11.69	SS	55.88

40mm column diameter

Particle size distribution

screen mesh sizing sizing (microns)	volume in ml retained 12/15/18/21/25degC
300	2.1
355	10.6
425	13.0
500	65.7
600	28.4
710	7.3
850	8.9
1000	5.0
1180	4.1

Expansions

12degC		15degC		18degC	
ml/min	%	ml/min	%	ml/min	%
60.0	19.9	63.0	20.2	67.5	21.1
118.8	45.6	122.5	44.7	132.6	45.6
170.6	68.1	190.6	70.2	199.9	71.1
256.3	109.3	258.5	106.1	281.2	105.3
284.9	125.0	299.1	24.6	312.7	124.6
314.2	142.8	331.1	147.4	343.8	146.5
density 1158		density 1151		density 1147	
voidage	0.378	voidage	0.381	voidage	0.382
SS	57.0	SS	17.76	SS	31.97

21degC		25degC	
ml/min	%	ml/min	%
69.6	21.1	73.2	20.2
137.9	46.5	145.7	44.7
211.4	71.1	223.9	70.2
295.9	106.1	308.4	106.1
339.6	124.6	259.3	122.8
362.2	147.4	381.9	145.6
density 1151		density 1148	
voidage	0.367	voidage	0.365
SS	72.6	SS	73.69

<u>50mm column diameter</u>

Particle size distributions

screen mesh sizing	volume in ml retained
sizing (microns)	12/15/18/21/25degC
300	7.8
355	13.7
425	16.9

500	80.8
600	45.6
710	10.4
850	10.5
1000	7.8
1180	5.3

Expansions

12degC		15degC		18degC	
ml/min	%	ml/min	%	ml/min	%
87.5	19.82	88.5	21.6	88.2	19.8
184.9	48.65	187.5	49.6	209.9	51.4
266.1	73.87	282.6	75.7	297.5	73.9
332.2	100.90	366.1	103.6	385.1	101.8
396.0	120.72	418.4	122.5	452.2	120.7
446.1	145.05	455.0	146.0	488.5	144.1
density 1140		density 1135		density 1147	
voidage	0.381	voidage	0.376	voidage	0.382
SS	15.93	SS	44.42	SS	31.97

21degC		25degC	
ml/min	%	ml/min	%
91.5	20.7	100.6	21.6
210.9	50.5	221.3	48.7
309.2	75.7	332.7	76.6
396.0	101.8	424.8	101.8
447.3	121.6	518.9	122.5
518.9	142.3	537.2	142.3
density 1142		density 1143	
voidage	0.342	voidage	0.337

SS	17.36	SS	98.78

60mm column diameter

Particle size distributions

screen mesh sizing sizing (microns)	volume in ml retained 12/15/18/21/25degC
300	7.8
355	13.7
425	16.9
500	80.8
600	45.6
710	10.4
850	10.5
1000	7.8
1180	5.3

Expansions

12degC		15degC		18degC	
ml/min	%	ml/min	%	ml/min	%
138.7	20.5	149.6	20.5	164.4	20.5
279.7	47.4	284.5	43.6	291.9	43.6
424.6	76.9	449.7	74.4	477.8	75.6
566.7	111.5	545.5	101.3	627.3	101.3
651.5	132.1	651.9	123.1	713.1	123.1
722.9	150.0	727.8	148.7	795.1	146.2
density 1158		density 1142		density 1153	
voidage	0.366	voidage	0.389	voidage	0.372
SS	13.43	SS	26.34	SS	13.99

21degC		25degC	
ml/min	%	ml/min	%
174.5	21.8	198.0	21.8
333.0	47.4	332.3	43.6
496.0	73.1	532.6	73.1
633.7	100.0	658.8	100.0
731.4	123.1	815.2	125.6
831.1	147.4	914.9	146.2
density 1148		density 1154	
voidage	0.369	voidage	0.352
SS	6.80	SS	31.68

Summary of density

temp → column↓	12degC	15degC	18degC	21degC	25degC
30mm	1109*	1153	1124	1161	1135*
40mm	1158*	1151	1147	1151*	1148*
50mm	1140	1135	1140*	1142	1143*
60mm	1158	1142	1153	1148	1154

* denotes poor fits ("Sum of Squares" in excess of 50)

average = 1147,

standard deviation = 9.712

Summary of voidage

temp → column↓	12degC	15degC	18degC	21degC	25degC
30mm	0.45*	0.377	0.388	0.339	0.375*
40mm	0.378*	0.381	0.382	0.367*	0.365*
50mm	0.381	0.376	0.363*	0.327	0.325*
60mm	0.366	0.389	0.372	0.369	0.352

* denotes poor fits ("Sum of Squares" in excess of 50)

average = 0.369,

standard deviation = 0.0182

IRA958

A relatively low density strong base resin with a macroporous crosslinked acrylic di-vinyl-benzene, copolymer matrix structure and an active site consisting of tri-methyl ammonium groups. Fluidized mainly in the chlorine form.

30mm diameter column

Particle size distribution

screen mesh sizing (microns)	volume in mls retained 12/15/18/21/25degC
300	0
355	0
425	1.2
500	2.0
600	4.5
710	19.5
850	15.2
1000	5.0
1180	1.7

Expansions

12degC		15degC		18degC	
ml/min	%	ml/min	%	ml/min	%
22.0	17.9	25.6	81.0	25.9	19.4
54.4	40.3	56.9	96.0	56.8	41.8
96.5	76.1	99.4	115.0	102.3	73.1
129.9	102.9	131.8	135.0	138.5	101.5
148.6	123.9	160.3	151.0	166.2	123.9
177.1	144.8	180.3	163.0	184.5	146.3
density 1092		density 1089		density 1084	

voidage	0.335	voidage	0.333	voidage	0.335
SS	39.23	SS	22.66	SS	25.77

21degC		25degC	
ml/min	%	ml/min	%
27.0	19.4	27.4	19.4
56.9	41.8	59.6	40.3
111.5	71.6	112.4	68.7
146.5	100.0	150.1	101.5
179.9	125.4	184.3	123.9
192.3	144.8	197.4	140.3
density 1085		density 1081	
voidage	0.330	voidage	0.327
SS	83.80	SS	59.36

40mm column diameter

Particle size distribution

screen mesh sizing sizing (microns)	volume in ml retained 12/15/18/21/25degC
300	0.3
355	0.5
425	2.3
500	2.9
600	10.7
710	54.5
850	33.0
1000	19.9
1180	4.1

Expansions

12degC		15degC		18degC	
ml/min	%	ml/min	%	ml/min	%
49.5	19.0	53.2	20.0	57.2	18.0
98.0	42.0	105.2	43.0	108.1	44.0
164.6	76.1	166.5	74.0	166.2	71.0
217.7	104.0	220.9	108.0	224.2	101.0
257.4	123.0	261.2	125.0	265.1	123.0
279.3	146.0	284.3	146.0	292.5	145.0
density 1090		density 1084		density 1080	
voidage	0.321	voidage	0.317	voidage	0.323
SS	40.65	SS	104.3	SS	71.82

21degC		25degC	
ml/min	%	ml/min	%
59.8	20.0	61.2	18.0
112.9	45.0	111.3	41.0
172.4	72.0	193.5	74.0
231.6	105.0	239.3	103.0
275.2	124.0	280.4	123.0
293.1	143.0	310.2	145.0
density 1074		density 1071	
voidage	0.328	voidage	0.325
SS	51.64	SS	100.45

50mm column diameter

Particle size distribution

screen mesh sizing sizing (microns)	volume in ml retained 12/15/18/21/25degC
300	0.9
355	2.2
425	5.5
500	10.9
600	20.8
710	70.2
850	39.3
1000	11.3
1180	4.9

Expansions

12degC		15degC		18degC	
ml/min	%	ml/min	%	ml/min	%
69.5	20.3	69.8	18.4	70.8	17.5
121.4	40.7	128.9	45.6	136.1	45.6
211.3	72.8	229.8	73.8	229.8	73.8
282.5	101.9	298.5	100.0	310.3	100.0
325.2	124.3	331.2	121.4	352.9	122.3
396.0	147.6	428.9	144.7	465.8	144.7
density 1088		density 1092		density 1098	
voidage	0.308	voidage	0.283	voidage	0.258
SS	120.0	SS	221.7	SS	278.2

21degC		25degC	
ml/min	%	ml/min	%
75.7	18.4	78.3	19.4
148.2	45.6	153.5	44.7

232.8	70.9	255.8	71.8
332.9	101.0	346.8	99.0
389.6	121.4	413.7	124.3
471.9	141.7	487.8	142.7
density 1074		density 1084	
voidage	0.328	voidage	0.286
SS	51.64	SS	100.45

60mm column diameter

Particle size distribution

screen mesh sizing sizing (microns)	volume in ml retained 12/15/18/21/25degC
300	3.2
355	5.2
425	8.3
500	18.8
600	31.0
710	83.5
850	47.9
1000	18.2
1180	6.7

Expansions

12degC		15degC		18degC	
ml/min	%	ml/min	%	ml/min	%
98.8	21.1	109.5	18.9	115.7	22.2
182.5	43.3	191.9	42.2	199.2	41.1
280.9	72.2	312.7	73.3	330.1	73.3
372.4	100.0	397.6	102.2	423.5	100.0
451.6	122.2	487.8	120.0	499.8	121.1

528.5	147.8	565.1	146.7	602.0	148.9
density 1086		density 1085		density 1084	
voidage	0.316	voidage	0.319	voidage	0.310
SS	59.8	SS	114.6	SS	71.2

21degC		25degC	
ml/min	%	ml/min	%
120.4	21.1	128.3	22.2
212.8	41.1	226.2	42.2
348.7	73.3	369.6	74.4
456.9	101.1	487.1	102.2
528.2	122.2	554.5	123.3
638.2	147.8	666.7	144.4
density 1083		density 1082	
voidage	0.307	voidage	0.295
SS	93.55	SS	112.0

Summary of density

temp → column↓	12degC	15degC	18degC	21degC	25degC
30mm	1092	1089	1084	1085*	1081
40mm	1090	1084*	1080	1074	1071*
50mm	1088*	1092*	1098*	1091*	1084
60mm	1086	1085*	1084	1083*	1082*

* denotes poor fits ("Sum of Squares" in excess of 80)

average = 1085,

standard deviation = 6.036

Summary of voidage

temp → column↓	12degC	15degC	18degC	21degC	25degC
30mm	0.335	0.334	0.335	0.330*	0.327
40mm	0.321	0.317*	0.323	0.328	0.325*
50mm	0.308	0.283	0.256	0.277	0.286
60mm	0.316	0.319	0.310	0.307	0.295

* Denotes poor fits ("Sum of Squares" in excess of 80)

average = 0.313,

standard deviation = 0.0227

APPENDIX G

APPENDIX G

:covery of metal cyanides using a fluidized bed of resin

J.Nesbitt
:ersity of Stellenbosch, Cape Town, South Africa

T.Petersen
:e Technikon, Cape Town, South Africa

STRACT: This study focuses into the feasibility of the recovery of metal cyanide complexes from the fluent of metallurgical processing plants, by using a strong-base ion exchange resin, IRA-958, in a idized bed application. The use of a novel technique for examining the expansion of a fluidized bed of in with particular application to ion exchange, is applied, which suggests that the fluidization teristics of IRA-958 are readily predictable. A single stage cyanide recovery plant, which recovers tal cyanide complexes by ion exchange in a fluidized bed application, is proposed.

NTRODUCTION

e high cost of cyanide consumption in the mining ustry together with increasingly stricter ulation on effluent cyanide concentrations has ce research into the recovery of cyanide, a essity. Natural attenuation in slimes dams or ing ponds continues to be the accepted method of anide destruction, despite the fact that more ent studies have indicated that certain of the re stable metal cyanide complexes can exist in e environment for up to ten years. It is also ificant that most published (patented) processes r the destruction or recovery of cyanide, are practical for the purposes of recovery from non-ified tailings of large mineral processing plants. ere the effluent flowrates are almost always siderable. In most of the patented ion exchange ocesses a strong-base resin, IRA-400 (now A420) is advocated, despite clearly documented ficulties in the removal of the adsorbed metal anide complexes. Furthermore, regeneration can achieved only, by the use of highly toxic idizing agents[1].

RA-958 is strong-base, macroporous resin which s a crosslinked acrylic copolymer matrix (very ge pore sizes "macroreticular"). Currently, it es application in sugar refining plants, where its ief function is the adsorption of large organic olecules, similar in size and nature to metal anide complexes.

Advantages of the fluidized bed route are the efficient use of resin holdup, and the typically low pressure drop obtained when compared to that of a fixed bed of equivalent ion exchange duty.

In this paper the performance of an "Amberlite" resin IRA-958, in the adsorption and desorption of some of the more abundant metal cyanide complexes, e.g. iron and copper were investigated. Furthermore, the competitive adsorption between sulphate and metal cyanide complexes in solution, was examined.

One of the difficulties encountered in bed expansion test work, is the determination of the free wet-settled voidage of the resin bed, and the apparent density of the resin. As both of these values are a requirement for the application of any bed expansion prediction model, a novel technique of applying the *Serial model*[2] to expansion vs liquid velocity data, was developed.

2 BACKGROUND

There is evidence that by varying the functional group of the adsorbent resin, selectivity can be achieved on the basis of molecular valency. Resins with tri-ethyl ammonium groups have been shown to be more selective towards the mono- and bi-valent metal cyanides[3], e.g. $Au(CN)_2^-$, and $Ni(CN)_4^{-2}$,

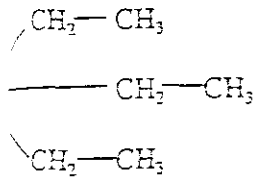

ethyl ammonium group

the tri-methyl ammonia functional group to attract the multi-valent metal cyanide plexes. e.g. $Fe(CN)_6^{-3}$, $Cu(CN)_4^{-3}$.

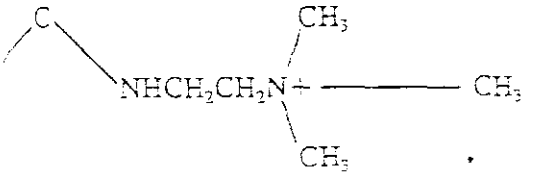

methyl ammonium group
ctional group of IRA-958)

hoosing a resin for the recovery of metal ides it is essential that this selectivity tendency aken into consideration. The more commonly ed metal cyanides of chromium, iron, and lt, all result in multivalent complexes due to the e number of CN^- groups which complex with e elements. Copper readily forms three ferent complexes, but it is generally accepted that e presence of an excess of free cyanide, the ent complex will form. Other common sition metals such as nickel, and zinc are known form di-valent complexes.

hree transition metals, readily identified in en and seepage solutions in mining operations e recognized in view of their great abundance innate tendency to form metal cyanides. ording to Smith and Mudder[4], the most dant metals found in mineral slurries, are iron. per, and nickel (Table 1). Cobalt, although not undant, is also of particular interest, in view of ability for certain cobaltic cyanide species to ion strong-base resins by polymerization within resin matrix[5].

ble 1

ment	average concentration range in barren, decant, and seepage solutions (ppm)
n	0.5 - 40.0
pper	0.1 - 400.0
kel	0.02 - 10.0
balt	unpublished

The tri-methyl ammonium group of IRA-958 combined with the macroporous matrix structure of the resin should result in excellent adsorption characteristics towards multivalent metal cyanides i.e. iron, copper, and cobalt. The nickel cyanide complex is divalent and hence would be less favoured by the resin's functional group. However, it is assumed that there would nevertheless be some adsorption thereof, albeit of a limited nature. As in the case of the large organic molecules adsorbed in the sugar industry, the macroreticular pore structure of IRA-958 should make the removal of large metal cyanides relatively uncomplicated. The recommended regeneration agent is a NaCl solution, a far cheaper and less toxic chemical than those traditionally used to regenerate the IRA-400 strong-base resin.

3 ION EXCHANGE TESTWORK

A matrix of tests were conducted in which an IRA-958 strong-base resin was tested in its ability to adsorb and desorb metal cyanides when the four metals listed in Table 1 are in solution, concurrent with an excess of free cyanide. Furthermore, it was attempted to determine if the presence of high concentrations of sulphate, a regular phenomenon in mineral slurries, affects the adsorption kinetics or equilibrium values with respect to IRA-958.

The four types of metal cyanide complexes known to form in solution in the presence of an excess of free cyanide, are $Fe(III)(CN)_6^{-3}$, $Cu(CN)_4^{-3}$, $Ni(CN)_4^{-2}$ and $Co(CN)_6^{-3}$.

For the purposes of adsorption and desorption test work, separate solutions containing each of these metal complexes, at concentrations similar to that found in industry, were synthesised in the laboratory. The ferric and nickel cyanide complexes were fabricated by the dissolution of their potassium salts, i.e. $K_3Fe(III)(CN)_6$, and $K_2Ni(CN)_4$. The copper complex was prepared by dissolving $Cu_2(CN)_2$ into an aqueous solution containing an amount of KCN in excess of the stoichiometric quantity required for the formation of $Cu(CN)_4^{-3}$. This complex has the highest number of cyanide groups possible for the cuprous ion (tetra), and it is assumed that this copper complex will readily form in mining effluent, as there will always be an excess of free cyanide. The cobalt complex was prepared by dissolving $CoSO_4$ and KCN in aqueous solution in the stoichiometric quantities required to form the $Co(CN)_6^{-3}$ complex.

Adsorption tests

four synthesised metal cyanide solutions scribed above, were used in separate batch sorption tests carried out in 1,5 litre baffled kers, each agitated by a magnetic stirrer. As the etics of adsorption for each of these complexes compared, special attention was given to suring that the geometric configuration, and gation power input per unit volume, for each ker were identical.

The adsorption test was started by adding a antity of resin in the chlorine form to each ker, which was calculated to adsorb two thirds the metal cyanide present in solution at uration. Eight samples were then taken at reasing time intervals, while a nineth sample racted at twenty four hours gave an equilibrium lue. All tests were then repeated under identical nditions with the addition of 2.22g Na_2SO_4, so as attain a concentration of 1000 ppm sulphate in lution.

The results of the first set of adsorption tests Figure 1), where no competing anions were esent, indicated that all of the cyanide complexes sted, are readily and rapidly adsorbed onto RA-958. The second set of adsorption tests Figure 2) demonstrated that even in the presence of large excess of sulphate (1000ppm), all four metal yanides were still found to be preferentially dsorbed. In both sets of tests rapid kinetics were bserved while the equilibrium value of $Ni(CN)_4^{-2}$ ppeared to be marginally affected by the presence f sulphate. This situation could be attributed to the ivalent state of the nickel cyanide complex, which s not favoured by the tri-methyl ammonium group. t is interesting to note that almost 90% of quilibrium value is attained with in one hour of the ommencement of adsorption.

3.2 Desorption tests

A further matrix of tests were conducted in which nalytical grade NaCl and brine solution were eparately tested as regeneration agents. These tests were carried out in batch reactors of the same dimensions as those used in the adsorption tests. Standard solutions of NaCl were contacted with four separate quantities of resin, each saturated with one of the four metal cyanides. These tests were conducted in the same manner as those of the adsorption tests, with samples being extracted from the batch reactor at increasing time intervals, and an equilibrium value being taken at twenty four hours. The results of this batch of tests are shown in Figure 3.

The regeneration tests were repeated with brine solution of approximately the same ionic strength and the results thereof are given in Figure 4.

It is reasonable to assert that the results in Figures 3 and 4 are good, if one considers that they were achieved after only a single "batch" contact with the regenerant. The tendency for the nickel cyanide complex to be easily dislodged from the resin, can be explained by the theory of lower affinity for which the tri-methyl ammonium functional group has for this bivalent complex. As in the adsorption tests, the kinetics of resin regeneration are discerned to be rapid, with ninety percent of the equilibrium values being reached within one hour.

From Figure 4 it can be deduced that the quality of regeneration in brine solution is on a parity with that of analytical grade NaCl solution, with marginal improvements being observed in the removal of the iron and nickel cyanide complexes.

4 FLUIDIZATION CHARACTERISTICS

The second part of this study constituted the development of a technique for the better understanding of the fluidization characteristics of a bed of IRA-958 undergoing ion exchange. The design of a receptacle in which adsorption might occur in this manner, could only be attempted if there is a thorough knowledge of the expansion of the resin bed during the loading or regeneration operation. It is also reasonable to assume that expansion coefficients are likely to change during the ion exchange process, in view of the expected increase or decrease in resin particle size and density. In the case of the former only a moderate change is envisaged, as IRA-958 is a macroporous resin with a macroreticular structure, which displays only a slight change in resin bead diameter during loading or regeneration. In the instance of resin density a large change is expected as the adsorption and desorption cycle entails the active sites exchanging Cl^- ions for metal cyanide ions, which have a relatively higher mass number per equivalent.

The Levenspiel criterion[6], for determining fluidization stability suggests that resin beads fluidized by an aqueous medium will tend to exhibit particulate or smooth fluidization. Therefore, by definition it could be expected that the resin bed

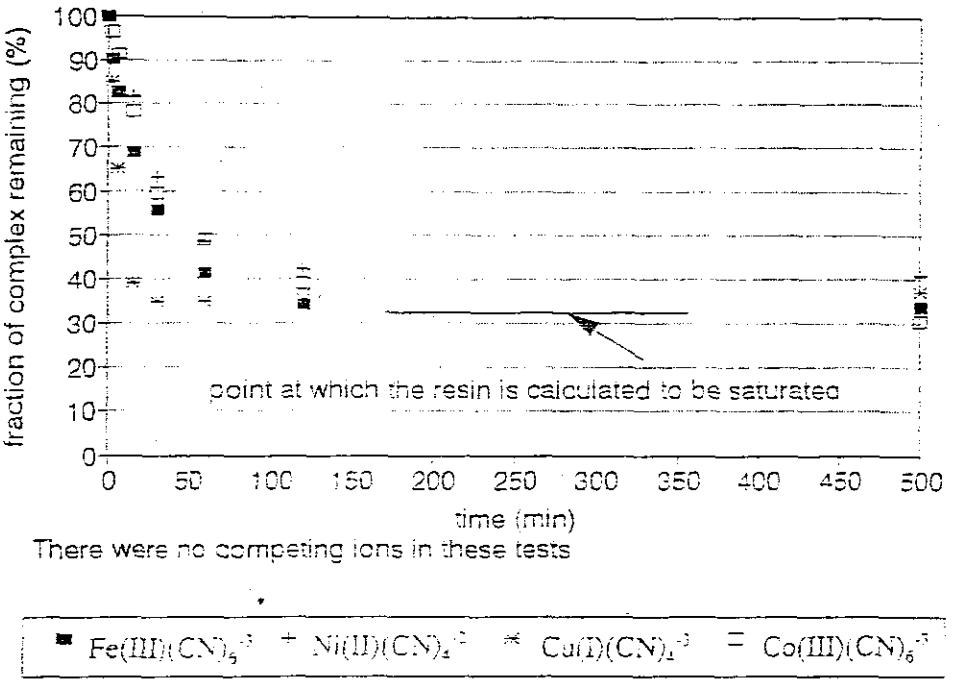

FIG.1 ADSORPTION OF FOUR METAL CYANIDES ONTO IRA958 STRONG BASE RESIN

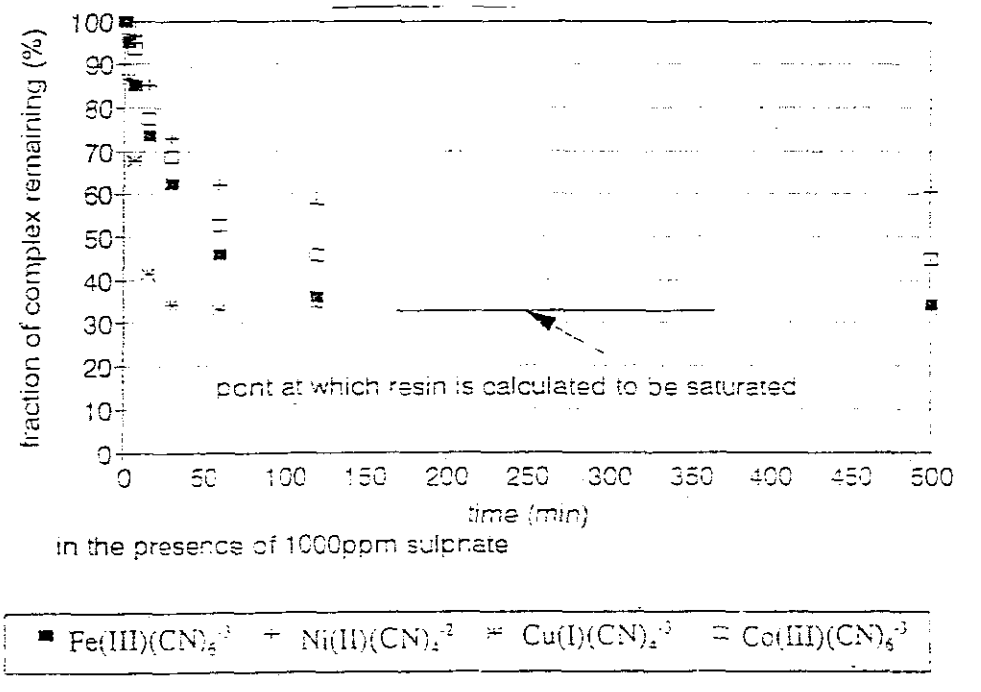

FIG.2 ADSORPTION OF FOUR METAL CYANIDES ONTO IRA958 STRONG BASE RESIN

will expand progressively with increasing liquid velocity, while maintaining its uniform character. The agitation of individual resin beads could also be expected to increase with increasing liquid velocity, which in turn could enhance mass transfer and ultimately result in improved kinetics of adsorption.

The design and construction of a fluidized bed reactor would require optimization, or at least, determination of the constraints of the linear fluidization velocity. A flow would have to be established at a velocity not exceeding the terminal velocity of the smallest resin bead in the least dense state, and not less than the minimum fluidization velocity of the largest bead.

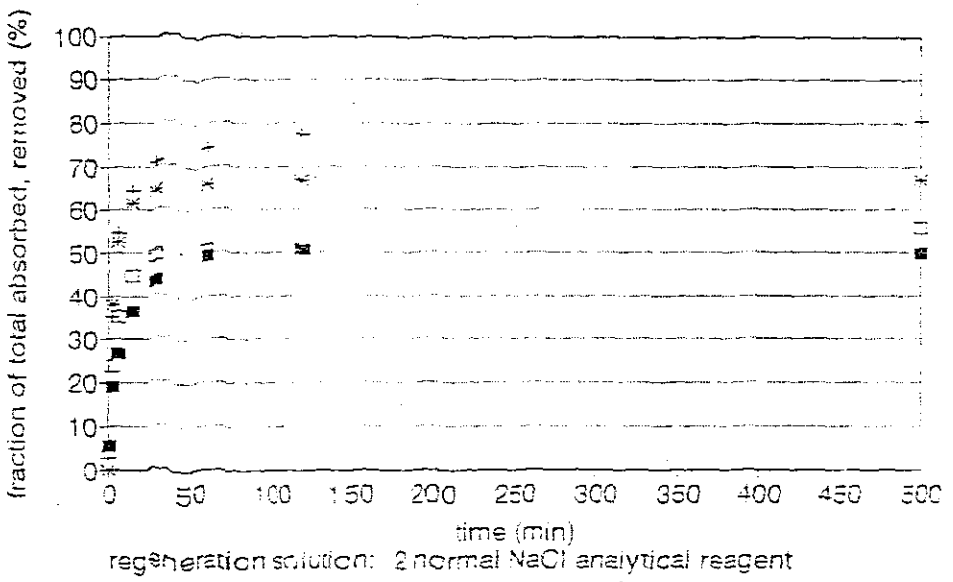

FIG.3 DESORPTION OF FOUR METAL CYANIDES FROM IRA958 STRONG BASE RESIN

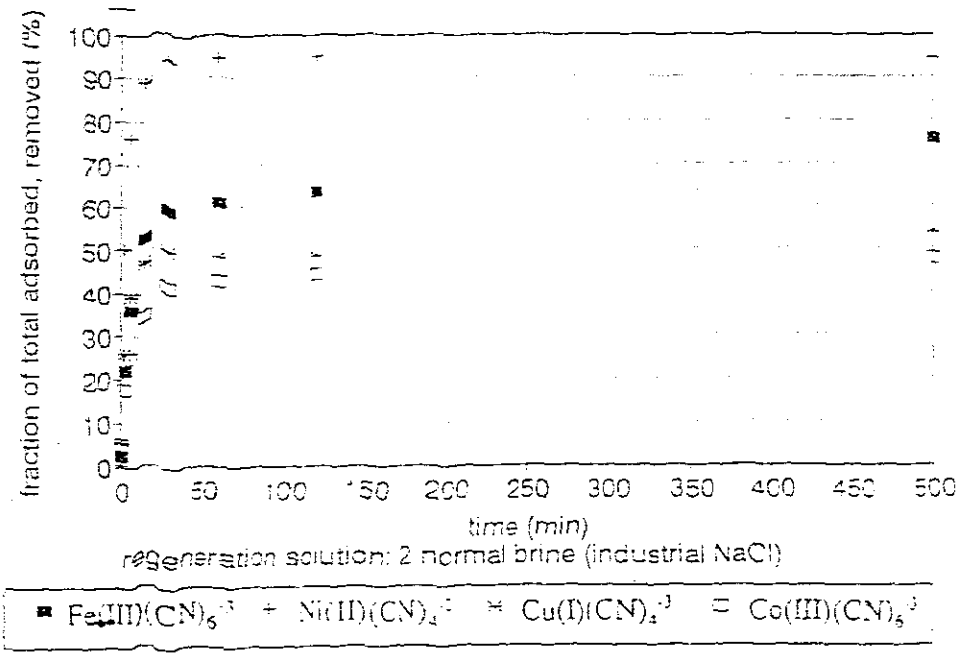

FIG.4 DESORPTION OF FOUR METAL CYANIDES FROM IRA958 STRONG BASE RESIN

3.1 The Serial model

The *Serial model* describes the relationship between the expansion of a multi species fluidized bed, and the linear liquid velocity, given the physical properties of the solid particles and the fluidization medium. It assumes that the overall expansion of a heterogenous particulately fluidized bed of particles is simply the sum of the individual expansions that each species would display, if fluidized separately, by the same parameters.

The *Serial model* is based on the Richardson and Zaki[7] equation (1) which describes the expansion characteristics of a mono-species, homogeneously fluidized bed, and from which the expansion component, for a given linear liquid velocity, may be calculated using equation (2).

$$\frac{u}{u_t} = e^n \qquad (1)$$

where:

u	=	empty tube linear fluid velocity(e=1)	[m/s]
u_t	=	particle terminal velocity	[m/s]
e	=	voidage	

n = an empirical parameter which is function of particle Galileo No.

$$EF = \frac{1-e}{1-e_{fws}} \quad (2)$$

where:

EF = expansion component (1 = no expansion) (2 = 100% expansion)
e_{fws} = free wet settled voidage

If the theory on which the serial model is based is applied to resin, the overall bed expansion component should be equal to the sum of the individual expansion component's advanced by the various resin size fractions. Thus:

$$EF_t = [\sum_{i=dp_s}^{i=dp_l} V_i.(EF_i-1)] + 1 \quad . \quad (3)$$

where:

V_i = the volume fraction of the ith particle size,
dp_l = the largest particle size, [m]
dp_s = the smallest particle size, [m]
EF_t = total bed expansion,
EF_i = the expansion component of the ith resin size.

The terminal velocity and n value for the individual resin sizes, both of which are required by equation (1), can be calculated from the following published empirical relationships:

$$Ga = 18.Re_t + 2,7.Re_t^{1.687} \quad (3.6<Ga<10^5) \quad (4)^{[8]}$$

$$n = [5,5+23\frac{d}{d_t}]Ga^{-0.075} \quad (21<Ga<2.4E4) \quad (5)^{[8]}$$

where:

$$Ga = \frac{d^3 g(\rho_s-\rho)\rho}{\mu^2}$$

$$Re_t = \frac{\rho d v_t}{\mu}$$

Re_t = particle Reynolds No. at terminal velocity
ρ_s = apparent density of resin [$kg.m^{-3}$]
ρ = density of fluidizing fluid [$kg.m^{-3}$]
d = diameter of bead [m]
d_t = diameter of containing vessel[m]
μ = viscosity of fluidizing fluid [$kg.m^{-1}s^{-1}$]
v_t = terminal velocity of bead [$m.s^{-1}$]
g = gravitational acceleration [$m.s^{-2}$]

With the exception of resin density and free wet-settled voidage, all of the parameters listed are easily measurable. As the resin has a macroreticular structure (sponge), where the liquid phase is continuous throughout the pores of the individual beads, it is impossible to use a gravimetric approach to determine the true wet-settled density of the resin or the voidage of the bed. However, to over come this problem, a technique was used, which comprised of fitting the *Serial model* to *expansion vs linear velocity data*, by searching for free wet settled voidage and apparent resin density, for an optimal sum of squares. The method of Hook and Jeeves was used to locate the best fit parameters.

Other data required by the serial model are the particle size distribution, measured by multiple screen analysis, while the density and viscosity of the fluidizing medium can be calculated from liquid temperature. Figure 5 is the logic diagram of that section of the algorithm which covers the iterative check utilized by the Hook Jeeves routine to determine best direction for parameter improvement.

4.2 Fluidization testwork

The apparatus used for the fluidization testwork consisted of a 40 mm diameter glass tube of about 1 metre in length, closed off at the bottom by a sintered glass distributer with an average pore size of about 17 - 40 microns. For loading purposes, metal cyanide solution containing the required number of equivalents was pumped by a peristaltic pump, from a one litre container to the bottom of the column, and then returned from the top of the column back to the container in a closed circuit. To acquire raw, expansion vs specific liquid velocity data, distilled water was fed at various different flow rates into the bottom of the column from a header tank, so as to preclude any vibration.

The $Fe(III)(CN)_6^{-3}$ metal cyanide ion was chosen as the loading ion, primarily because of its abundance in effluents, and secondly because of the ease with which its presence can be determined on the basis of solution colour. Furthermore, it has a

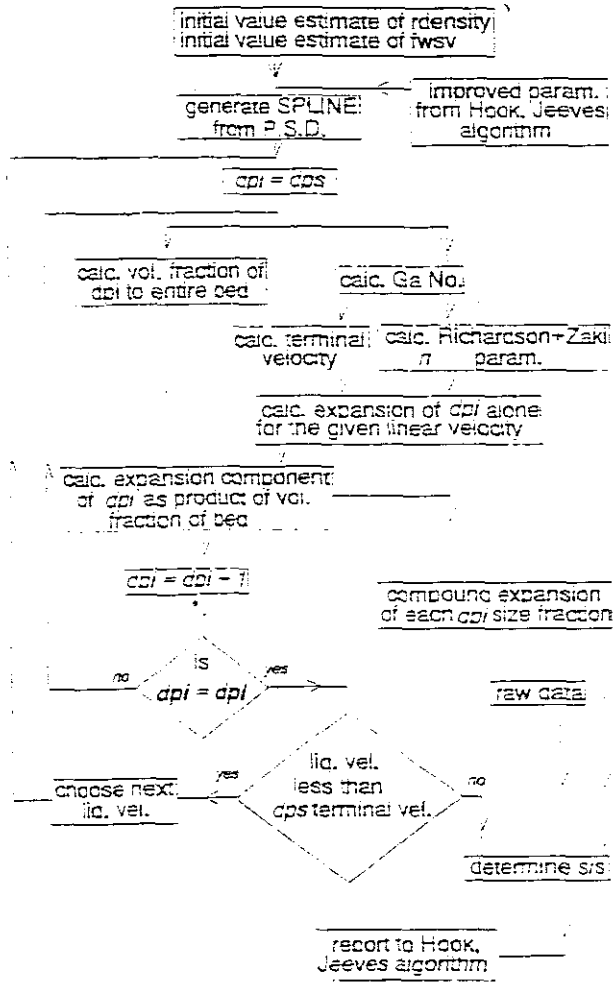

FIG.5 LOGIC DIAGRAM

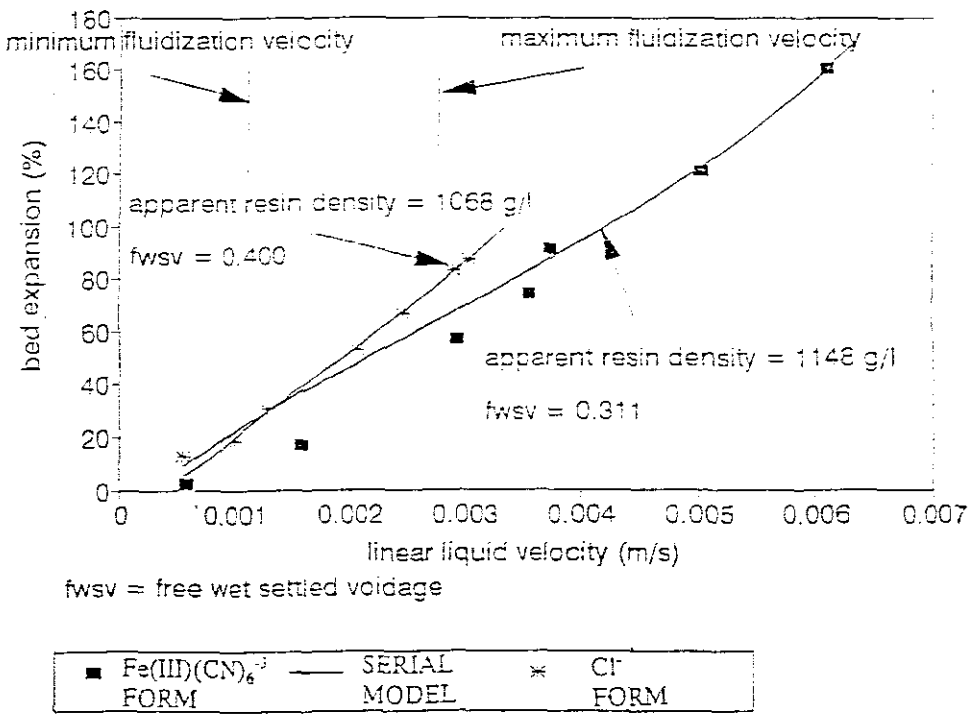

fwsv = free wet settled voidage

■ $Fe(III)(CN)_6^{-3}$ FORM — SERIAL MODEL * Cl^- FORM

FIG.6 EXPANSION VS LIQUID VELOCITY

higher mass per equivalent than $Cu(CN)_4^{-3}$, the other most abundant metal cyanide, which means that during loading the expected larger density change would result in greater variations to the fluidization characteristics of the resin.

Figure 6 presents the results of the expansion behaviour of IRA-958 in the Cl^- and $Fe(III)(CN)_6^{-3}$ forms, including the fitted *Serial model*. As can be predicted, there is a large difference in the curves mainly as a result of altered density and free wet-settled voidage.

5 CONCLUSION

It is clear from the study presented in this paper, that if the ion exchange route for the removal and/or recovery of metal cyanide ions is to be pursued, the use of "Amberlite" IRA-958 resin may well be a feasible alternative. It is envisaged that a mineral plant effluent, preceded by semi-clarification (e.g. bank of hydrocyclones), might then be contacted with IRA-958 resin in a semi-continuous fluidized bed application (Cloete, Streat column)[9], before disposal on the slimes dam, or tailing pond.

REFERENCES

1. Wittect Development Inc. 1986. Recovery of cyanide from waste waters by an ion exchange process. S.A. patent ZA8607235
2. Epstein, N. ,Leclair, B.P. & Pruden, B.B. 1981 Liquid fluidization of binary particle mixtures-I, *Chem. Engng. Sci.*
3. Reveros, P.A., Molnar, R.E., & McNamara, V.M. 1993. Alternative tecnology to decrease the enviromental impact of gold milling. *C.I.M.*
4. Smith, A. & Mudder, T. 1991. The chemistry and cyanidation wastes, *Mining journal books limited*:London
5. Fleming, C.A. & Hancock, R.D. 1979. The mechanism in the poisoning of anion-exchange resins by cobalt cyanide. *S.A.I.M.M.*
6. Levenspiel, O. & Kunii, D. 1969. *Fluidization engineering*. John Wiley and Sons Inc: London.
7. Wilhelm, R.H. & Kwauk, M. 1948. Fluidization of solids particles. *Chem. Ing. Prog.*
8. Richardson, J.F. & Zaki, W.N. 1954. Sedimentation of fluidization: 1. *Trans. Instn. Chem. Engrs.* 32: 35-52.
9. Mak, A.N.S., Kuiper, P.C., Hamersma, P.J. & Fortuin, J.M:H. 1993. Contitinuous ion exchange in a pulsed packed column contained structured packing: Mass-Transfer-controlled-Kinetics. *Chem. Engng. Sci.*

APPENDIX H

SEPARATION SCIENCE AND TECHNOLOGY, 30(15), pp. 2979–2988, 1995

Feasibility of Recovering High Valency Metal Cyanide Complexes with a Fluidized Bed of Resin

A. B. NESBITT
DEPARTMENT OF CHEMICAL ENGINEERING
UNIVERSITY OF STELLENBOSCH
PRIVATE BAG X5018, STELLENBOSCH 7599, SOUTH AFRICA

F. W. PETERSEN
SCHOOL OF PHYSICAL SCIENCES: CHEMICAL ENGINEERING
CAPE TECHNIKON
PO BOX 652, CAPE TOWN 8000, SOUTH AFRICA

ABSTRACT

A commercially available strong base ion-exchange resin IRA 958 was used to recover polyvalent metal cyanide complexes in a fluidized-bed application. A method for modeling the expansion of a fluidized bed of resin is proposed. The method takes into account the difficulties associated with the hydrodynamic characteristics of a macroporous resin of this nature.

INTRODUCTION

The recovery of metal cyanides from the effluent of mineral processing plants has been of interest to engineers for many years. Cyanide, which has been used for the leaching of gold for most of this century, has the preference to combine with many transition metals, forming mono-, di-, and polyvalent metal cyanide complexes. Although cyanide is poisonous to all life forms, its natural attenuation in the environment is well understood and normally follows a predictable mechanism. Free cyanide is rapidly destroyed in the presence of ultraviolet light, while weak complexes, e.g., $Zn(CN)_4^{2-}$ and $Cd(CN)_3^-$, tend to destruct relatively quickly. Moderately strong to strong complexes, such as $Cu(CN)_2^{3-}$, $Co(CN)_6^{4-}$, $Ni(CN)_4^{2-}$, and $Fe(CN)_6^{4-}$, which form readily under suitable conditions and

are found in great abundance in the effluent of mineral processing plants, can exist in the environment for up to 5 years. Smith and Mudder (1) published the average concentrations of transition metals in the effluent of mineral processing plants throughout the world, and from their data it is clear that *copper* and *iron* are responsible for the holdup of free cyanide. This conclusion is reached when cyanide holdup is defined on the basis of the product of their (copper, iron) average global concentrations in the effluent, and the stoichiometric number of cyanide molecules which will attach when an excess of free cyanide is present.

As the pH of any cyanide-bearing mineral slurry has to be elevated to prevent the formation of HCN, only strong-base resins can be considered for the removal of metal cyanides. Research carried out in recent years (2) has shown that it is possible to selectively adsorb metal cyanides onto strong-base resins on the basis of polyatomic valency. The triethyl-ammonium functional group has a greater affinity for the mono- and divalent metal cyanides, while the trimethyl-ammonium functional group tends to adsorb the polyvalent metal cyanides more readily. As iron and copper form polyvalent metal cyanides in the presence of an excess of free cyanide, it is clear that only a resin with the trimethyl-ammonium functional group should be considered.

The poor desorption performance of metal cyanides from strong-base resins has been an obstacle to the commercial use of the ion-exchange route for cyanide retrieval. However, it was evident from initial tests that IRA958 strong-base resin, which has an acrylic matrix and a macroreticular pore structure, is able to adsorb and desorb these polyvalent metal cyanides fairly easily. IRA958 currently sees application in sugar refining plants, where its chief function is the adsorption of large organic molecules (de-ashing) similar in size and nature to metal cyanide complexes.

Attempting adsorption in a fluidized bed has the advantages of improved kinetics and a semicontinuous process operation (e.g., Streat–Cloete column) (3). Being able to predict the expansion of a fluidized bed of resin is essential for the purposes of designing a receptacle to hold the resin and for determining the ion-exchange duty that can be expected from such a fluidized bed. Despite a profusion of literature on the modeling of the expansion of a fluidized bed of particles, two characteristics of a fluidized bed of *resin* are not clearly addressed. The reticular nature of the resin bead would imply that the resin bead should primarily display an apparent density under fluidizing conditions, which would be impossible to measure using standard gravimetric means, and secondly would result in difficulty with the determination of the free wet-settled voidage. Both of these values are essential for the application of the *Serial model* (4) and for predict-

ing the bed expansion of any fluidized particles, which have the tendency to display particulate or smooth fluidization.

ADSORPTION

The cyanide complexes of nickel, iron, copper, and cobalt were adsorbed separately onto IRA958 in batch stirred tank reactors and in the presence of excess cyanide. The transition metal concentrations used were similar to the average concentrations found in the effluent of mineral processing plants throughout the world, and the amount of resin used was sufficient to adsorb approximately 66% of the metal cyanides present. The metal cyanides of iron and nickel were manufactured by the dissolution of their cyanide salts, while the solutions of cobalt and copper cyanide complexes were the result of the dissolution of their potassium salts in the presence of excess cyanide.

The adsorption process was repeated in the presence of 1000 ppm sulfate. Sulfate, like the metal cyanide complexes, is a polyatomic anion, and according to data published by Smith and Mudder (1), is present in high concentrations in mineral processing effluent. It is clear from Fig. 1 that all the polyvalent metal cyanides are readily and quickly adsorbed.

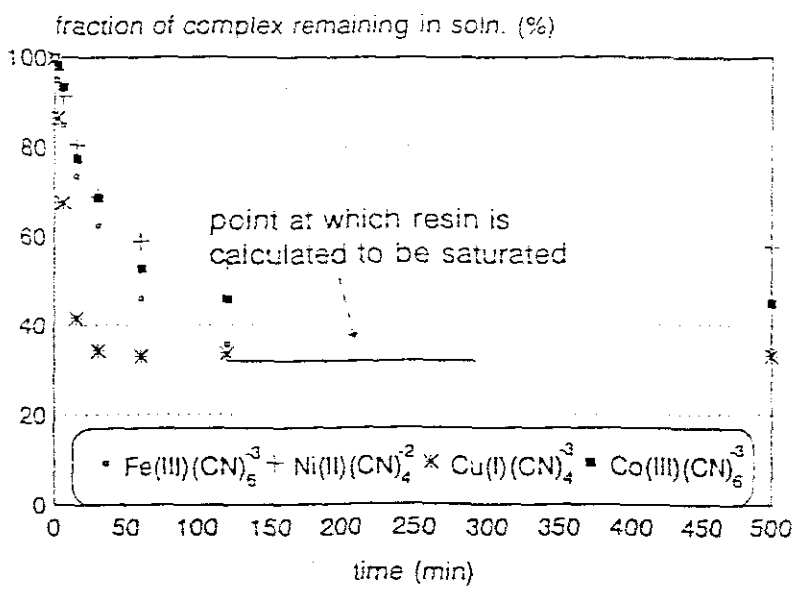

FIG. 1 Adsorption profiles of metal cyanides onto IRA 958. Initial concentration of Fe = 108.1 ppm, Ni = 91.52 ppm, Co = 138.4 ppm, Cu = 385.1 ppm; volume of wet-settled resin = 2 mL; volume of reactor = 1.5 L.

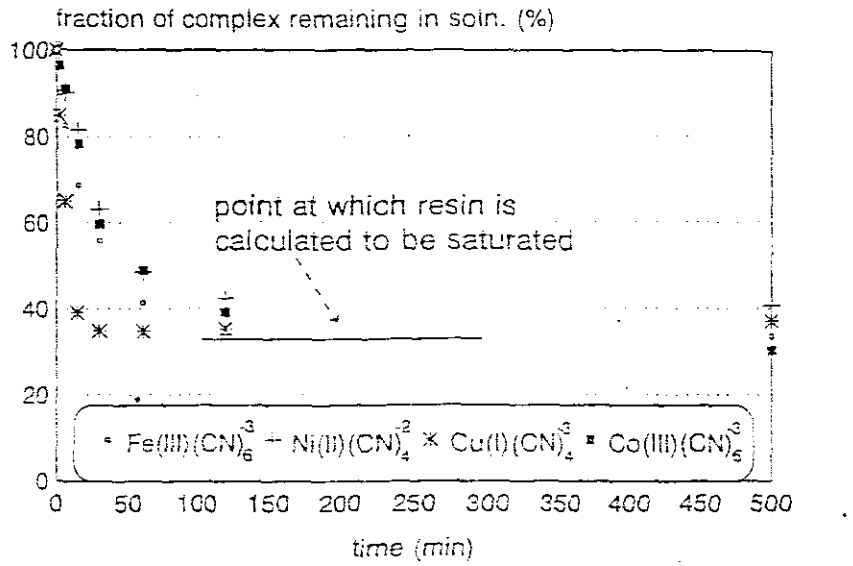

FIG. 2 Adsorption profiles of metal cyanides onto IRA 958 in the presence of 1000 ppm sulfate. Initial concentration of Fe = 105.8 ppm, Ni = 96.59 ppm, Co = 134.4 ppm, Cu = 375.6 ppm; volume of wet-settled resin = 2 mL; volume of reactor = 1.5 L.

The observation can also be made that the divalent nickel cyanide complex is not adsorbed quite as easily, which is in line with the previously stated affinity characteristics of the trimethyl-ammonium group. From Fig. 2 it is apparent that the addition of 1000 ppm sulfate only marginally affects the adsorption process, hence one may conclude that despite the presence of large amounts of sulfate in solution, IRA958 could still be used to adsorb metal cyanides.

DESORPTION

The loaded resins were regenerated separately in the same stirred tank reactors used for the adsorption process. Unlike other general purpose strong-base resins, i.e., IRA420, and IRA900, most of the metal cyanide complexes were readily and rapidly removed from IRA958. Figure 3 shows the desorption of the nickel, copper, cobalt, and iron cyanide complexes, with analytical grade 2 M sodium chloride solution used as an eluant. It is significant that this level of regeneration is achieved after only a single batch contact with the eluant. The regeneration exercise was repeated (Fig. 4). However, on this occasion a 2 M brine solution was used. Once again, most cyanide complexes were rapidly and readily removed, verifying that in normal industrial operation IRA958 could be safely and cheaply regenerated.

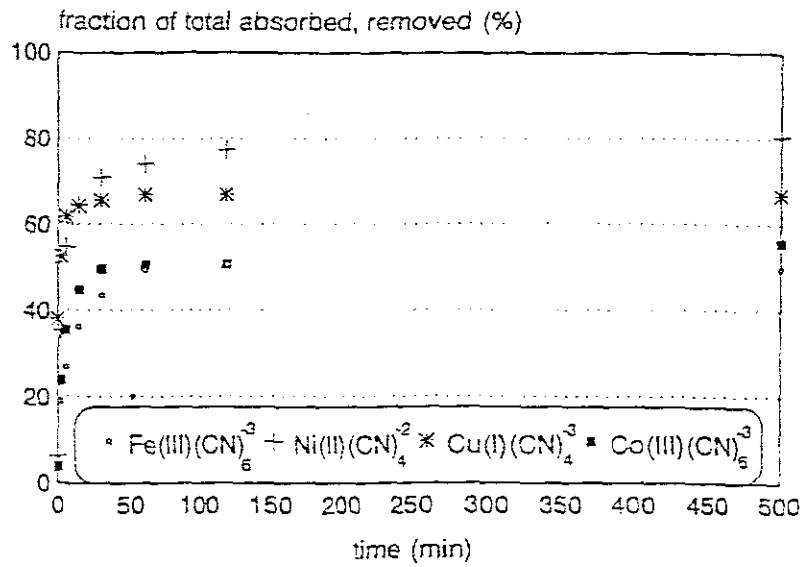

FIG. 3 Desorption profiles of metal cyanides from IRA 958 using NaCl (analytical grade). Loading of resin: Fe = 0.001 mole, Ni = 0.0008 mole, Co = 0.001 mole, Cu = 0.001 mole; volume of wet-settled resin = 5 mL; volume of reactor = 1.5 L.

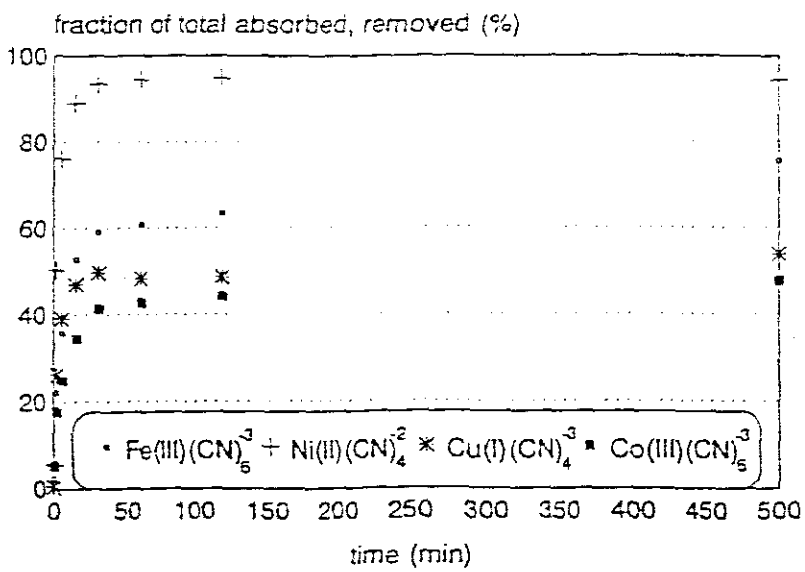

FIG. 4 Desorption profiles of metal cyanides from IRA 958 using brine. Loading of resin: Fe = 0.00128 mole, Ni = 0.0008 mole, Co = 0.0008 mole, Cu = 0.0009 mole; volume of wet-settled resin = 4.5 mL; volume of reactor = 1.5 L.

FLUIDIZATION CHARACTERISTICS

The Levenspiel criterion (5) for determining fluidization stability suggests that resin beads fluidized by an aqueous medium will tend to exhibit particulate or smooth fluidization. The design and construction of a fluidized-bed reactor would require optimization, or at least determination, of the constraints of the linear fluidization velocity. A flow would have to be established at a velocity not exceeding the terminal velocity of the smallest resin bead in the least dense state, and not less than the minimum fluidization velocity of the largest bead.

The *Serial Model*

The *Serial model* describes the relationship between the expansion of a multi-species fluidized-bed and the linear liquid velocity, given the physical properties of the solid particles and the fluidization medium. It assumes that the overall expansion of a heterogenous particulately fluidized-bed of particles is simply the sum of the individual expansions that each species would display, if fluidized separately, by the same parameters.

Equation (1) is based on Richardson and Zaki's approach (6) and describes the expansion characteristics of a mono-species, homogeneously fluidized-bed, and from which the expansion component for a given linear liquid velocity may be calculated by Eq. (2).

$$u/u_t = e^n \tag{1}$$

where u = empty tube linear fluid velocity ($e = 1$) [m/s]
u_t = particle terminal velocity [m/s]
e = voidage
n = an empirical parameter which is function of particle Galileo number

$$EF = \frac{1 - e}{1 - e_{fws}} \tag{2}$$

where EF = expansion component (1 = no expansion; 2 = 100% expansion)
e_{fws} = free wet settled voidage

If the theory on which the *Serial model* is based is applied to resin, the overall bed expansion component should be equal to the sum of the individual expansion components advanced by the various resin size fractions, thus:

$$EF_t = \left[\sum_{i=dp_s}^{i=dp_l} V_i(EF_i - 1)\right] + 1 \tag{3}$$

where V_i = the volume fraction of the ith particle size
dp_l = the largest particle size
dp_s = the smallest particle size
EF_t = total bed expansion
EF_i = the expansion component of the ith resin size

The terminal velocity and n value for the individual resin sizes, both of which are required by Eq. (1), can be calculated from the following published empirical relationships (6, 7):

$$\mathrm{Ga} = 18\mathrm{Re}_t + 2.7\mathrm{Re}_t^{1.687} \qquad (3.6 < \mathrm{Ga} < 10^5) \tag{4}$$

$$n = \left[5.5 + 23\frac{d}{d_t}\right]\mathrm{Ga}^{-0.075} \qquad (21 < \mathrm{Ga} < 2.4 \times 10^4) \tag{5}$$

$$\mathrm{Ga} = \frac{d^3 g(\rho_s - \rho)\rho}{\mu^2} \tag{6}$$

$$\mathrm{Re}_t = \frac{\rho d v_t}{\mu} \tag{7}$$

where Re_t = particle Reynolds number at terminal velocity
ρ_s = apparent density of resin [kg/m^3]
ρ = density of fluidizing fluid [kg/m^3]
d = diameter of bead [m]
d_t = diameter of containing vessel [m]
μ = viscosity of fluidizing fluid [kg/ms]
v_t = terminal velocity of bead [m/s]
g = gravitational acceleration [m/s^2]
Ga = Galileo number

With the exception of *resin density* and *free wet-settled voidage*, all of the parameters listed are easily measurable. As the resin has a macroreticular structure (sponge) where the liquid phase is continuous throughout the pores of the individual beads, it is impossible to use a gravimetric approach to determine the true wet density of the resin or the voidage of the settled bed. To overcome this problem, a technique was used which comprised of fitting the *Serial model* to expansion versus linear velocity data by searching for the free wet-settled voidage and apparent resin density for an optimal sum of squares. The method of Hook and Jeeves was used to locate the best fit parameters.

Other data required by the *Serial model* are the particle size distribution, measured by multiple screen analysis, while the density and viscosity of the fluidizing medium can be calculated from liquid temperature. Figure 5 is the logic diagram of that section of the algorithm which covers the iterative check utilized by the Hook Jeeves routine to determine best direction for parameter improvement.

Fluidization Testwork

IRA958 resin was fluidized in a 40-mm diameter column of about 1000 mm in length, the bottom of which was closed off by a sintered glass of about 17–40 μm in diameter. For loading and fluidizing purposes, a solution of $Fe(III)(CN)_6^{3-}$ was pumped by a peristaltic pump from a 1-L reservoir to the bottom of the column, and then returned from the top of the column back to the reservoir in a closed circuit. To acquire raw expansion versus flow-rate data at a specific loading, a measured amount of $Fe(III)(CN)_6^{3-}$ was added to the reservoir and the solution allowed to circulate through the resin bed for 20 hours to ensure that all the metal cyanide is adsorbed by the resin. With the liquid and solid phases in dynamic equilibrium, accurate expansion versus linear vertical liquid velocity data could be acquired.

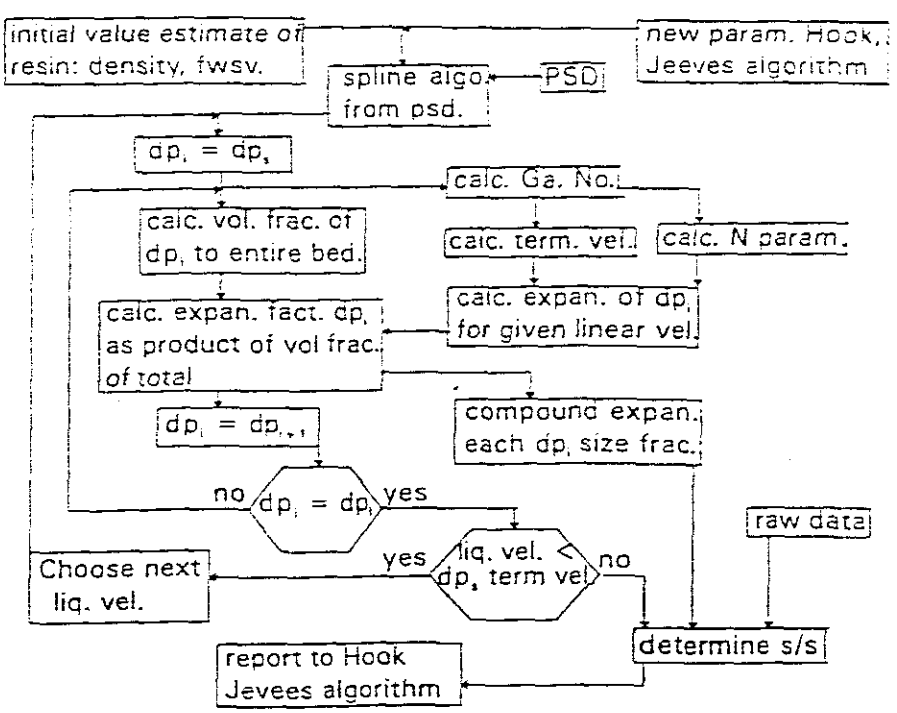

FIG. 5 Logic diagram.

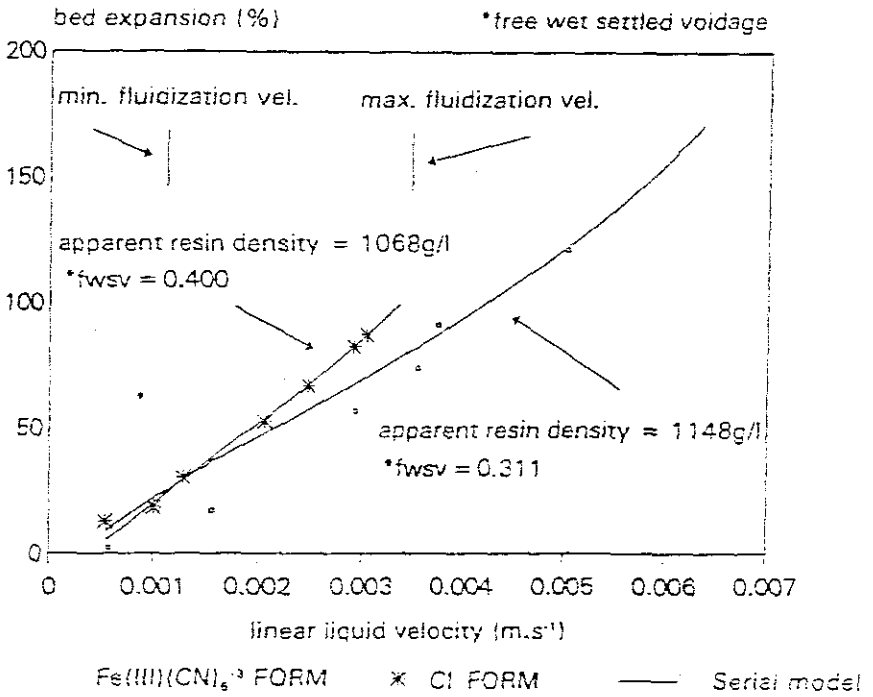

FIG. 6 Expansion versus liquid velocity.

The $Fe(III)(CN)_6^{3-}$ metal cyanide ion was chosen as the loading ion, primarily because of its abundance in the effluent and secondly because of the ease with which its presence can be determined on the basis of solution color. Furthermore, it has a higher mass per equivalent than $Cu(CN)_4^{3-}$, the other most abundant metal cyanide, which means that during loading the expected larger density change would result in greater variations to the fluidization characteristics of the resin. Figure 6 presents the results of the expansion behavior of IRA958 in the Cl^- and $Fe(III)(CN)_6^{3-}$ forms, including the fitted *Serial model*. As can be predicted, there is a large difference in the curves, mainly as a result of altered density and free wet-settled voidage.

CONCLUSION

It is clear from the study presented in this paper that if the ion-exchange route for the removal and/or recovery of metal cyanide ions is to be pursued, the use of Amberlite IRA-958 resin may well be a feasible alternative. It is envisaged that a mineral plant effluent, after undergoing semiclarification (e.g., bank of hydrocyclones), might be contacted with IRA-958 resin in a semicontinuous fluidized-bed application before disposal on the slimes dam or tailing pond.

REFERENCES

1. A. Smith and T. Mudder, *Min. J.* (1991).
2. P. Reveros, R. E. Molnar, and V. M. McNamara, *C.I.M.*, p. 48 (1981).
3. A. N. S. Mak, P. C. Kuiper, P. J. Hamersma, and J. M. H. Fortuin, *Chem. Eng. Sci.*, *23*, 153 (1993).
4. N. Epstein, B. P. Leclair, and B. B. Pruden, *Ibid.*, *30*, 247 (1981).
5. O. Levenspiel and D. Kumii, *Fluidization Engineering*, 1969.
6. J. F. Richardson and W. N. Zaki, *Trans. Inst. Chem. Eng.*, *32*, 35 (1954).
7. L. Schiller and D. Naumann, *Verh. Deut. Ing.*, p. 318 (1933).

Received by editor November 28, 1994
Revised February 3, 1995

APPENDIX I

A TECHNIQUE FOR PREDICTING THE FLUIDIZATION CHARACTERISTICS OF ION EXCHANGE RESINS

A B NESBITT* and F W PETERSEN+

*Department of Chemical Engineering
University of Stellenbosch,
Private Bag X5018, Stellenbosch, 7600, South Africa

+Department of Chemical Engineering
Cape Technikon,
PO Box 652, Cape Town, South Africa

Abstract

A novel method for quantifying the fluidization characteristics of ion exchange resin by using a simple integral - optimization technique based on the serial model, is proposed. This method is suitable for use in an algorithm for the optimization of a fluidized, ion exchange resin bed, receptacle design. The serial model theory is shown to represent the expansion of a poly-sized fluidized bed of resin satisfactorily.

Introduction

Since their development, semi-continuous fluidized bed ion exchange reactors such as the Cloete/Streat [1] and NIMCIX columns have been used in many industrial ion exchange applications. One of the difficulties encountered in designing fluidized bed ion exchange equipment is the optimization of resin compartment dimensions in either the loading or regeneration stages. These dimensions do not only affect the capital cost of construction, but also stricture the volume of resin in service at any one time, which ultimately dictates plant capacity and performance. Despite an abundance of information describing the particulate fluidization characteristics of particulate substances on the basis of their physical characteristics, the irregular nature of ion exchange resin as an aqueously fluidized solid, poses difficulties in this respect.

A typical resin bead is a spherical porous structure which undergoes a slight change in volume, and a more substantial change in skeletal density during the ion exchange process. Published mathematical correlations [2] for the prediction of expansion of a fluidized bed of particles require a particle density which, depending on its value, can have a great effect on the final expansion prediction. Being of a porous nature, it might be more correct to refer to a resin bead's 'apparent density' of fluidization, a property which will only be significant when the resin is in a turbulent suspension, with the continuous phase intruding into the porous resin. Therefore it is evident that the physical characteristics of the continuous phase will play a substantial role in dictating the apparent density of a resin bead, which is a

difficult constant to measure gravimetrically. Akapo *et al* [3] has advocated the reverse notion suggesting that particle density of porous aeratable powders could be measured by observing the expansion characteristics of the solid, while Nicollella *et al* [4] applies the theory through to liquid fluidized beds.

A further problem is the poly-sized nature of manufactured resin, which in itself, and in its alteration as a result of minor adjustments in the resin manufacturing process, plays a significant role in the fluidization behaviour of the resin. Only recently have certain resin manufacturers developed a process for manufacturing a mono-sized ion exchange resin, and this only for the most commonly consumed resins. Hartman *et al* [5] and Foscolo *et al* [6] both report that a wide range of particle size distribution, amongst other phenomena, has a substantial affect on fluidization behaviour. However, there is approximately a four fold difference in diameter from the smallest to the largest resin bead as supplied by most resin manufacturers, and the particle size distribution varies greatly from batch to batch.

Empirical relationships which describe the expansion of a fluidized bed always correlate voidage to fluid velocity, and hence require the free wet-settled voidage as a necessary base constant from which an expanded voidage, and hence a bed expansion, can be calculated. The free wet-settled voidage, just as the apparent density of fluidization, will also be a difficult quantity to measure when using a porous discontinuous phase such as ion exchange resin. Another observation is that this value is not necessarily constant and depends poignantly on the manner in which the bed is allowed to settle.

It is the objective of this study to establish whether existing fluidized bed technology, can be adapted and utilized for a bed of fluidized resin. Furthermore, it will be shown that given the particle size distribution, an adapted version of the *serial or integral* model can be fitted to measured expansion data by searching for resin apparent density and bed free wet-settled voidage.

Theory

The Mono-sized particle bed

The Levenspiel criterion [7] for determining fluidization stability suggests that resin beads fluidized in an aqueous medium will tend to exhibit particulate or smooth fluidization over a large range of fluidization velocities. Under these circumstances it will be expected that the well established Richardson and Zaki equation will describe the relationship between voidage and fluidization velocity for a mono-sized bed of fluidized resin satisfactorily.

$$U = U_t . e^{n} \qquad [1]$$

where:

$$n = [5.5 + 23\frac{d}{D}]\,Ga^{-0.075} \quad (21 < Ga < 2.4 \times 10^4)$$

$$Ga = \frac{d^3 g(\rho_s - \rho_f)\rho_f}{\mu^2}$$

To calculate the actual bed expansion, based on the change in voidage from the free wet-settled condition, the following relationship can be used:

$$E = \frac{1-e_{fws}}{1-e} \qquad [2]$$

The multi-sized particle bed

Two theories have been presented regarding the effective prediction of expansion of constant density poly-sized particulately fluidized beds. The *averaging* model [8-9], which assumes a single particle diameter to be representative of the entire bed, has been demonstrated by Epstein *et al* [10] to be inadequate at high voidages where the expansion contribution of the smaller sized particles tend to dominate. The averaging approach has also been proposed by Wen *et al* [9] for beds with a largest to smallest particle size ratio of not greater that 1.3. The shortcomings of the averaging model seem to outweigh the advantageous lack of computational calisthenics, especially when one considers what vast computative powers are readily available.

The *serial* or *incremental* model is proposed by a number of authors [2, 11] and assumes that the overall expansion of a particulately fluidized bed of particles is simply the sum of the individual expansions that each species would display, if fluidized separately by the same parameters. The classification of particles in the axial dimension, a phenomenon which has been measured by Garside *et al* [12] has shown that the variation of local voidage can be predicted by assuming the bed to be totally classified even in the regions where classification is absent. This loans credence to the *serial model* as a semi-fundamental representation of the real condition, which may be described as one in which each particle contains a certain voidage envelop around itself dictated by its physical characteristics and that of the continuous phase.

If the serial model is applied to a poly-sized fluidized bed, the overall bed expansion component should be equal to the sum of the individual expansion components advanced by the various size fractions. Thus:

$$E_t = [\sum_{d_s}^{d_l} V_i (E_i - 1)] + 1 \qquad [3]$$

If one accepts the volume fraction (V_f), and terminal velocity (u_t), to be a function of particle size (d) thus,

$$V_f = G(d) \qquad [4]$$

$$U_t = f(d) \qquad [5]$$

an integrated combination of Equations 1, 2, 4 and 5, for the entire bed, results in the following:

$$E = 1 + \int_{d=0}^{d=\infty} G(d) \cdot \left[\frac{1-\varepsilon_{fMS}}{1-(u/f(d))^{1/N}} - 1 \right] d\,d \qquad [6]$$

If the *serial model* is valid, Equation 6 should effectively predict the expansion factor of a liquid fluidized bed of constant density poly-sized particles, such as resins.

Particle size distribution

It is clear that the relationship symbolised by Equation 4 could take on any form, the only prerequisite being that each particle size have a singular volume fraction value. It is also reasonable to assume that in most applications the particle size distribution of resin will not be a function of discontinuous nature, and therefore for the purposes of this study a spline routine was use to develop a continuous functional relationship. All sets of raw distribution data were normalized, before the spline routine was applied.

If X_i is the volume fraction of the resin in the *i*th of the total N inter screen intervals, and L_i is the extent of this interval in particle diameters, then the size fraction (S_i) is given by:

$$S_i = \frac{X_i / L_i}{\sum_{q=1}^{N} X_q / L_q} \qquad [7]$$

The arithmetic mean of the screen fraction limits of the ith fraction was then paired with the calculated normalized volume fraction of the ith interval, before being splined for development into an algorithm based continuous function.

Terminal velocity

There are a number of published models (Equation 5) for terminal velocity of spherical particles, and as ion exchange resin beads can be assumed to have a near perfect spherical shape, the correspondence of these models could easily be tested.

The terminal velocities of different diameter beads of the same resin in an identical chemical matrix solution were measured in the laboratory. A middle sized bead of 696 microns was then used in the Hartman model [Equation 9], and the particle density input slowly increased above that of water until the measured terminal velocity was predicted. The obtained density was then used to predict the terminal velocities of the entire range of particle sizes by both the Hartman and the Shiller models [Equation 8]. The Ladenburg correction factor[15] was used to correct the model predictions for a finite medium.

Model of Shiller *et al* [13]

$$Ga = 18.Re_t + 2,7.Re_t^{1,687} \qquad [8]$$

with:

$$Re_t = \frac{\rho_s.dp.V_t}{\mu}$$

Model of Hartman *et al* [14]

$$\log_{10}Re_t = P(A) + \log_{10}R(A) \qquad [9]$$

with:

$$P(A) = [(0,0017795.A - 0,0573).A + 1,0315].A - 1,26222$$

$$R(A) = 0,99947 + 0,01853.\sin(1,848.A - 3,14)$$

$$A = \log_{10}Ga$$

The Ladenburg correction factor

$$Correction\ Factor = [1 + 2.4(dp/dt)] \qquad [10]$$

From Figure 1 it can be deduced that in the field of interest the models vary only marginally in their predictions. In view of the above, and the fact that the model of Shiller *et al* [13] requires an iterative search when solving for terminal velocity, it was decided to use the model of Hartman *et al* [14] in all calculations.

Test work

Terminal velocities

All terminal velocity tests were carried out in a two meter high glass tube with an internal diameter of about 40 mm. The diameter of the resin beads were measured by micrometer. The fall speed was calculated by measuring the time taken for the bead to cover a predetermined vertical distance. To ensure accuracy, only the terminal velocity of beads which maintained a preset distance from the side of the tube were recorded.

Expansion data

The apparatus used for the resin expansion testwork consisted of a 40 mm diameter glass tube of about 1 meter in length, closed off at the bottom by a sintered glass fluid distributer with an average pore size of about 17 - 40 microns. Varying quantities of different types of resin were placed into this glass tube and their fluidization characteristics observed.

To acquire raw expansion versus specific liquid velocity data, distilled water was fed via a controlling gate valve to the bottom of the column from a header tank so as to preclude any vibration. Deionized water leaving the top of the column ran into a reservoir from where it was pumped back to the header tank by a peristaltic pump in a closed loop. The temperature in both the header tank and the reservoir were maintained at constant temperature by a system of temperature controllers. The level of the deionized water in the header tank was kept constant by a feed back controller which controlled the pumping rate of the peristaltic pump. A vacuum breaker was installed at the fluid outlet of the column so as to prevent siphoning action from causing a variation in the vertical pressure drop across the bed. Figure 2 presents the expansion test apparatus.

Three types of resin were tested i.e., a gel type strong acid resin, a macroporous strong acid resin, and a macroreticular strong base resin. Each were fluidized at various flowrates spanning from the estimated minimum fluidization velocity up to near elutriation of the smallest beads. Wet sieve analysis was used to measure the particle size distributions. The viscosity and density of the deionized water was calculated from the temperature.

Results and discussion

The normalized particle size distributions of the macroporous strong acid resin was found to be discontinuous, and hence the spline fitting algorithm had to be adapted. These particle size distributions are depicted in Figure 3.

Fitting the model

Despite most of the parameters of Equation 6 being easily measurable, as formally explained, the free wet settled voidage and apparent density still remain an effective obstacle in the application of this equation. However, to overcome this problem a technique was used which comprised of fitting the *serial model* to expansion versus linear velocity data, by searching for free wet settled voidage and apparent resin density for an optimal sum of squares. These results are presented in Figure 4 (gel resin), Figure 5 (macroporous resin) and Figure 6 (macroreticular resin).

An early observation was that a proportional change, based on preset boundaries of free wet-settled voidage resulted in a far greater change in the sum of square errors than an apparent density change of a similar proportion. It was therefore assumed that the problem may be of a highly nonlinear nature. However, before general search algorithm was selected the topography of a few search areas were evaluated, and found to take on a general form for all of the resins tested.

The most striking feature of the optimization topography is clearly the narrow trough running diagonally across the search area as illustrated in Figure 7. Furthermore, it was observed that the use of smaller increments in the integrating process did not dramatically improve accuracy. A study of the optimization topography showed that the larger the integrating increment, the more jagged the optimization contour lines, which could lead to unnecessary digression by the search algorithm. Examination of the residuals showed a poorer fit at lower expansions, a phenomenon which could possibly be attributed to distributer characteristics. Intense mixing was observed in the area directly above the sintered glass distributer.

Conclusion

The algorithm presented in this paper can be used effectively to model the expansion of a fluidized bed of ion exchange resin, and therefore could be used to optimize the dimensions of an accommodating receptacle. From the observations made in this paper, it would seem that the *serial model* is able to effectively portray the fluidization expansion of fluidized resin.

List of symbols

e voidage
e_{fws} free wet settled voidage
d resin bead diameter (m).

d_l largest resin bead diameter (m).
d_s smallest resin bead diameter (m).
dt diameter of fluidization vessel (m).
E expansion component (1 = no expansion)
(2 = 100% expansion)
E_i expansion component of the ith resin fraction.
E_t total bed expansion factor
Ga Galileo No.
g gravitational acceleration constant ($m.s^{-2}$).
L_i size, in particle diameters of ith interval.(m).
n empirical parameter of the Zaki equation
Re_t particle Reynolds No. at terminal velocity
S_i normalized volume fraction of the ith screen fraction
U empty tube linear fluid velocity(e = 1) ($m.s^{-1}$).
U_t particle terminal velocity ($m.s^{-1}$).
V_i bed volume fraction of the ith particle size
X_i non normalized volume fraction of the ith size fraction

Greek letters

ρ_s apparent particle density ($kg.m^{-3}$).
ρ_l liquid density ($kg.m^{-3}$).
μ liquid viscosity (Pa.s)

References

[1] M. Streat, J. Separ. Proc. Technol. 1 (1980), 10.

[2] J.F. Richardson, W.N. Zaki, Trans. Instn. Chem. Engrs, 32 (1954) 35.

[3] S. Akapo, T.M. Khong, C.P. Simpson, B. Toussaint, J.G. Yates, PowderTechnol,58(1989)237.

[4] C. Nicollella, A. Converti, R. Di Felice, M. Rovatti, Chem. Eng. Sci.,50 (1994) 1059.

[5] M. Hartman, V. Havlin, K. Svaboda, Chem. Eng. Sci., 44 (1989) 2770.

[6] P.U. Foscolo, R. Di Felice, L.G. Gibilaro, Chem. Engng Process 22 (1987) 69.

[7] O. Levenspiel, K. Kunii, Fluidization engineering. John Wiley and Sons Inc London (1969)

[8] A. Amirtharajah, J.L. Cleasby, J. Am. Water Works Assoc. 64 (1972) 52.

[9] C.Y. Wen, Y.H. Yu, Chem. Engng Progr. Symp. Series Chem. 62 (1966) 100.

[10] N. Epstein, B.P. Leclair, B.B. Pruden, Chem. Eng. Sci., 36 (1981) 1803.

[11] E.W. Lewis, E.W. Bowerman, Chem. Engng Progr. 48 (1952) 603

[12] M.R. Al-Dibouni, J. Garside, Trans IChemE., 57 (1979) 94

[13] L. Shiller, A. Naumann, Ver. Deut. Ing. 77 (1933) 318.

[14] M. Hartman, V. Havlin, O. Trnka, M. Casky, Chem. Engng, Sci. 44 (1989) 1743

[15] R.A. Ladenburg, Phys. 23 (1907) 447.

FIG. 1

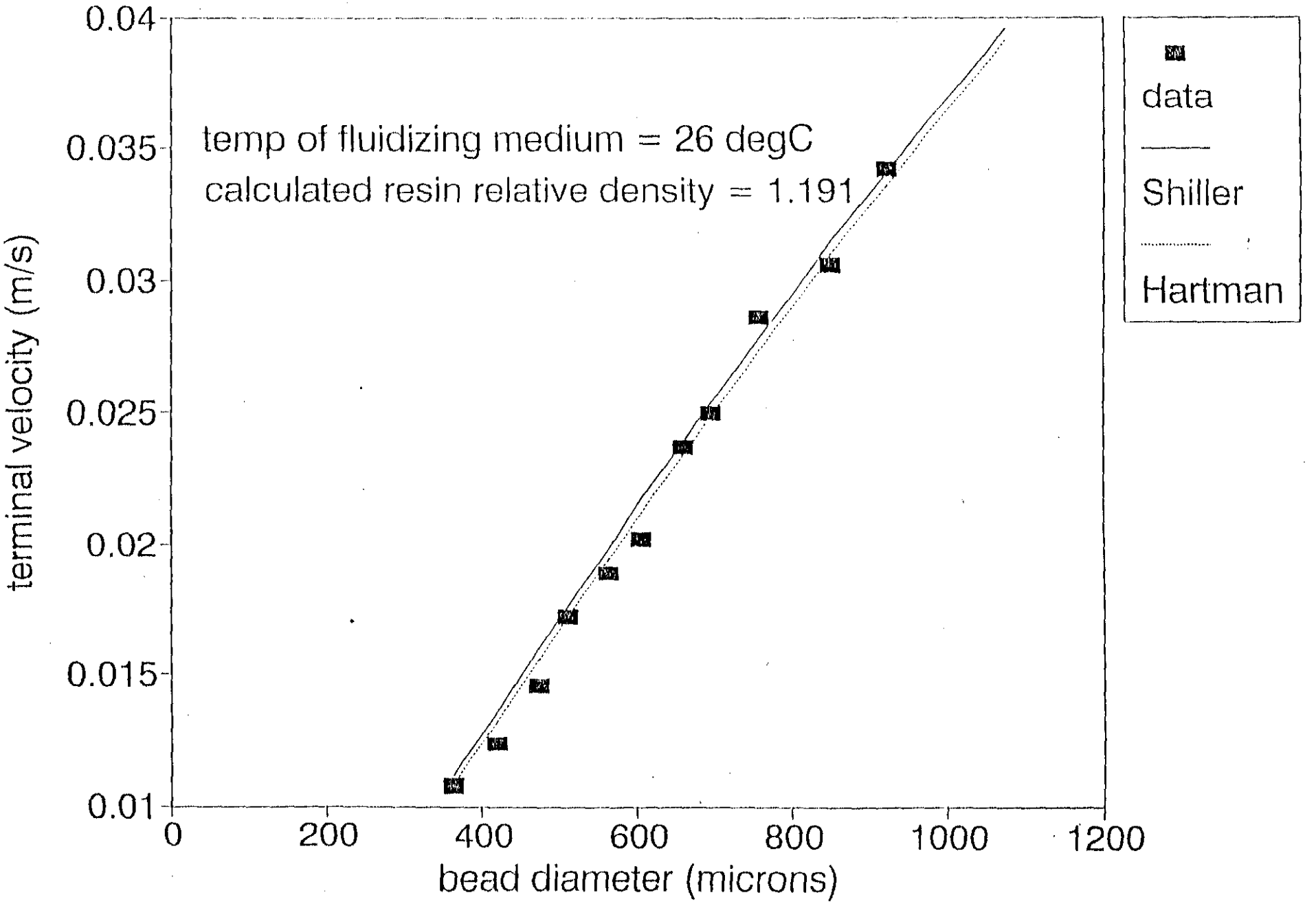
0.04
0.035
0.03
0.025
0.02
0.015
0.01
terminal velocity (m/s)
temp of fluidizing medium = 26 degC
calculated resin relative density = 1.191
data
Shiller
Hartman
0
200
400
600
800
1000
1200
bead diameter (microns)

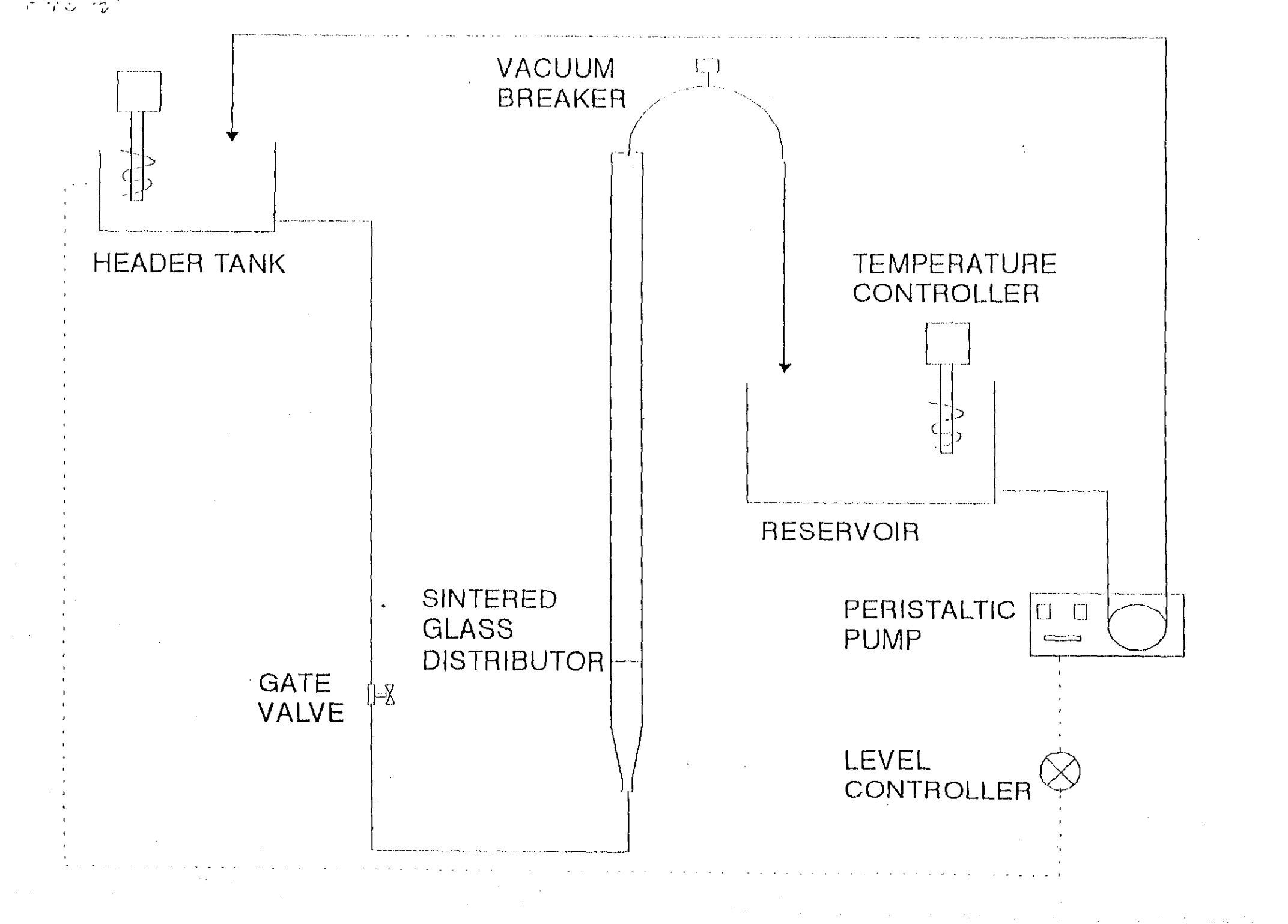
VACUUM
BREAKER
HEADER TANK
TEMPERATURE
CONTROLLER
RESERVOIR
SINTERED
GLASS
DISTRIBUTOR
PERISTALTIC
PUMP
GATE
VALVE
LEVEL
CONTROLLER

FIG. 3

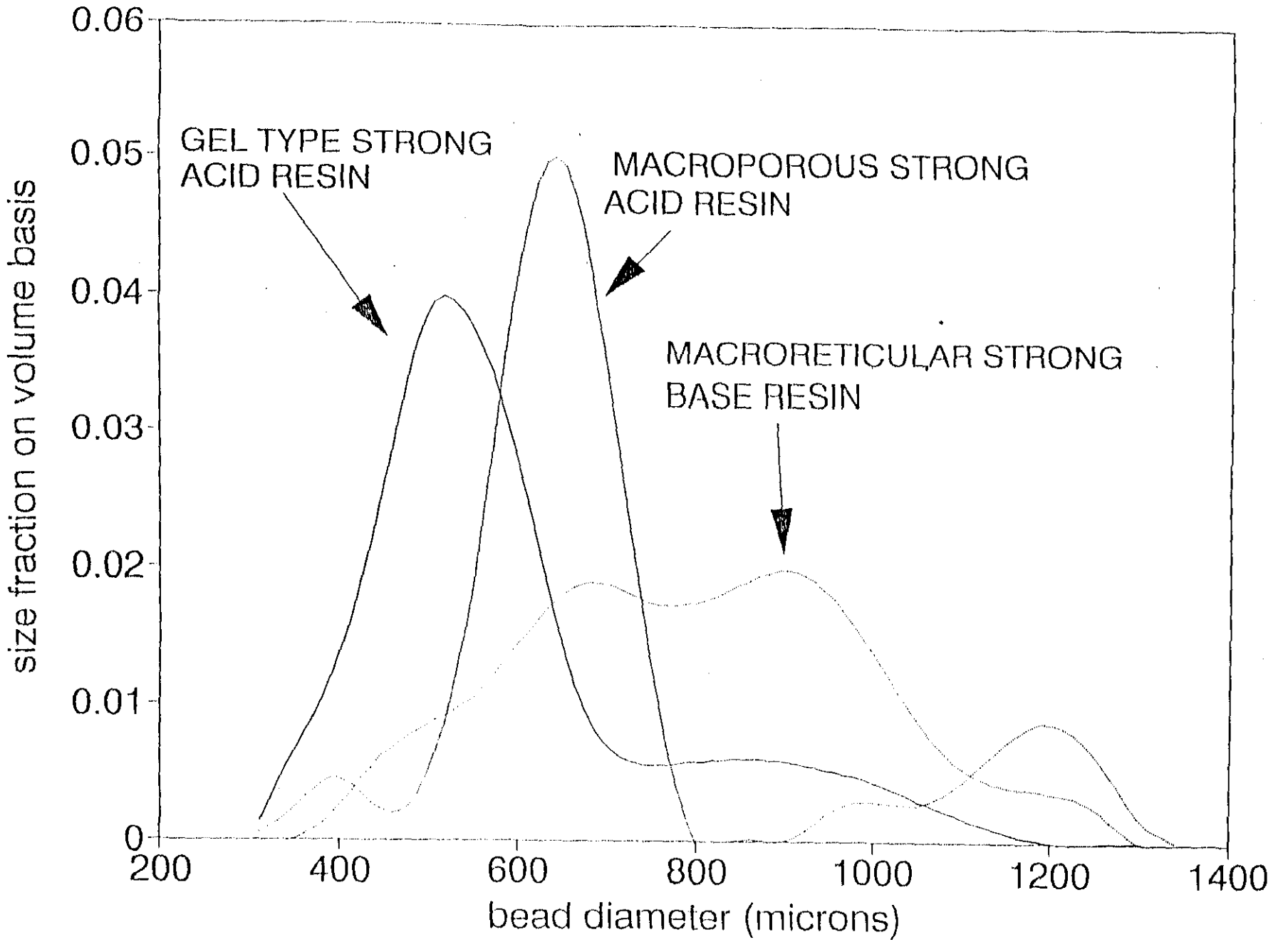
0.06
0.05
0.04
0.03
0.02
0.01
0
size fraction on volume basis
GEL TYPE STRONG ACID RESIN
MACROPOROUS STRONG ACID RESIN
MACRORETICULAR STRONG BASE RESIN
200
400
600
800
1000
1200
1400
bead diameter (microns)

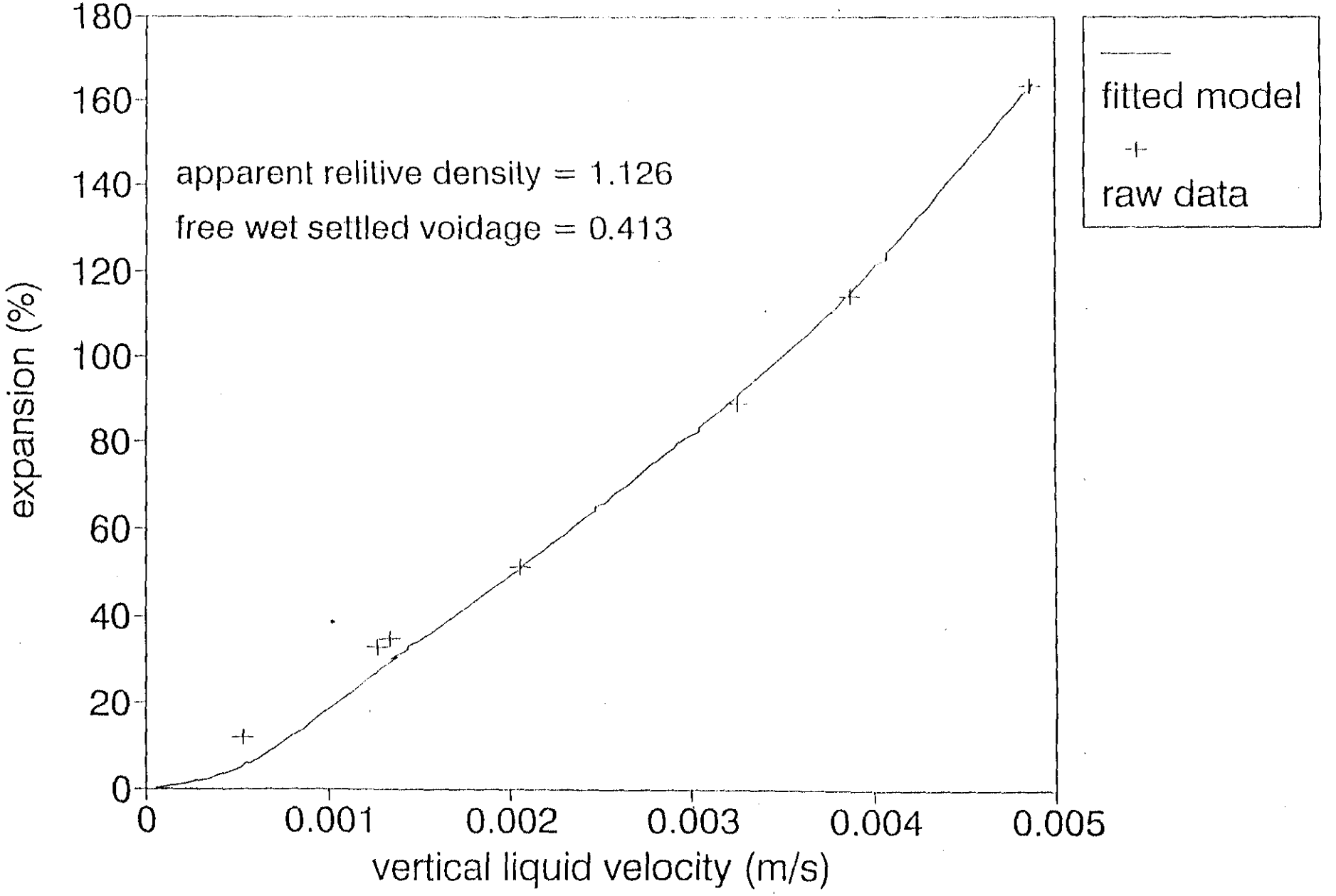
GEL TYPE STRONG ACID RESIN
apparent relitive density = 1.126
free wet settled voidage = 0.413
fitted model
raw data
expansion (%)
180
160
140
120
100
80
60
40
20
0
0
0.001
0.002
0.003
0.004
0.005
vertical liquid velocity (m/s)

-16,5

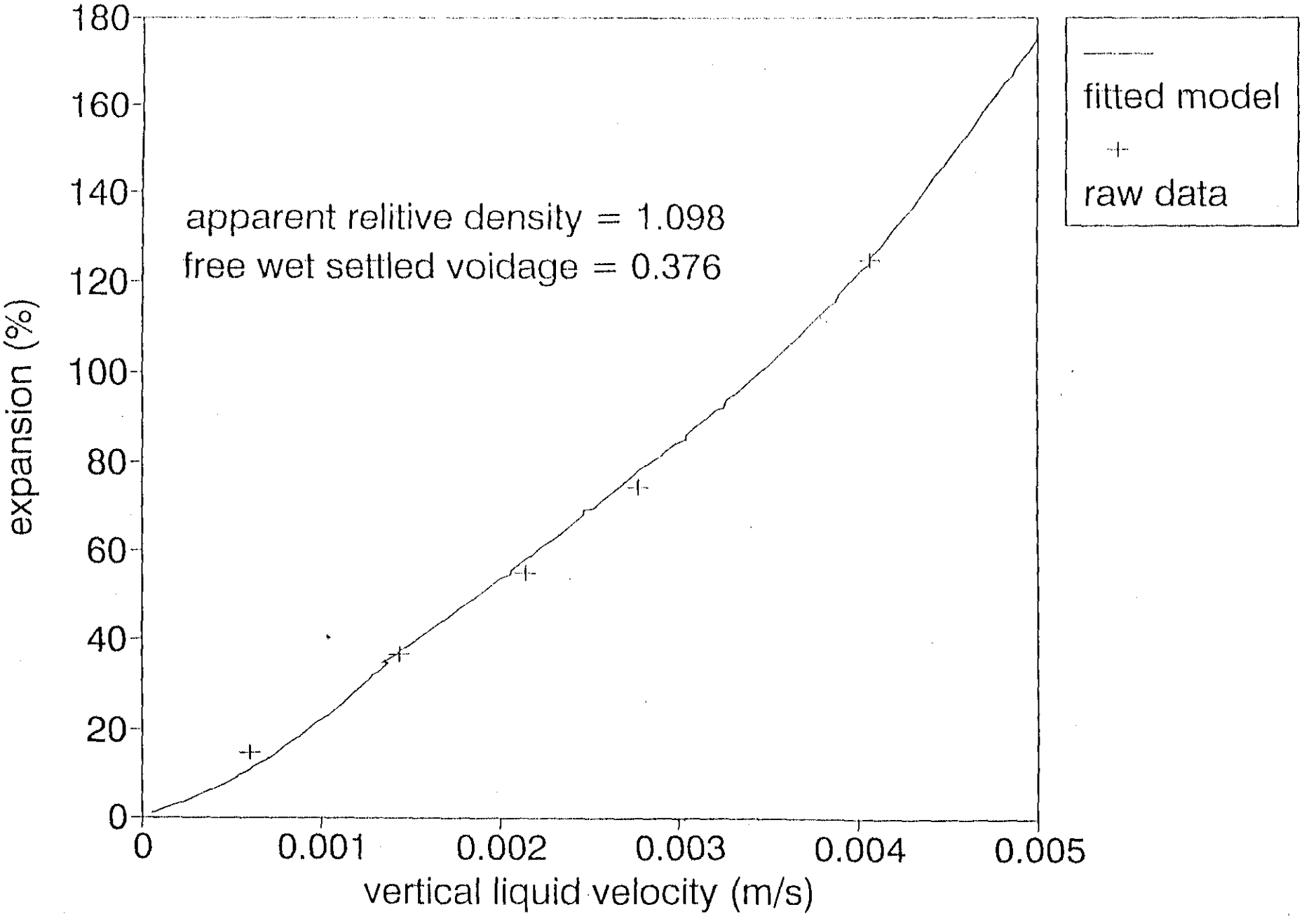
180
160
140
120
100
80
60
40
20
0
expansion (%)
apparent relitive density = 1.098
free wet settled voidage = 0.376
fitted model
raw data
0
0.001
0.002
0.003
0.004
0.005
vertical liquid velocity (m/s)

Fig. 6

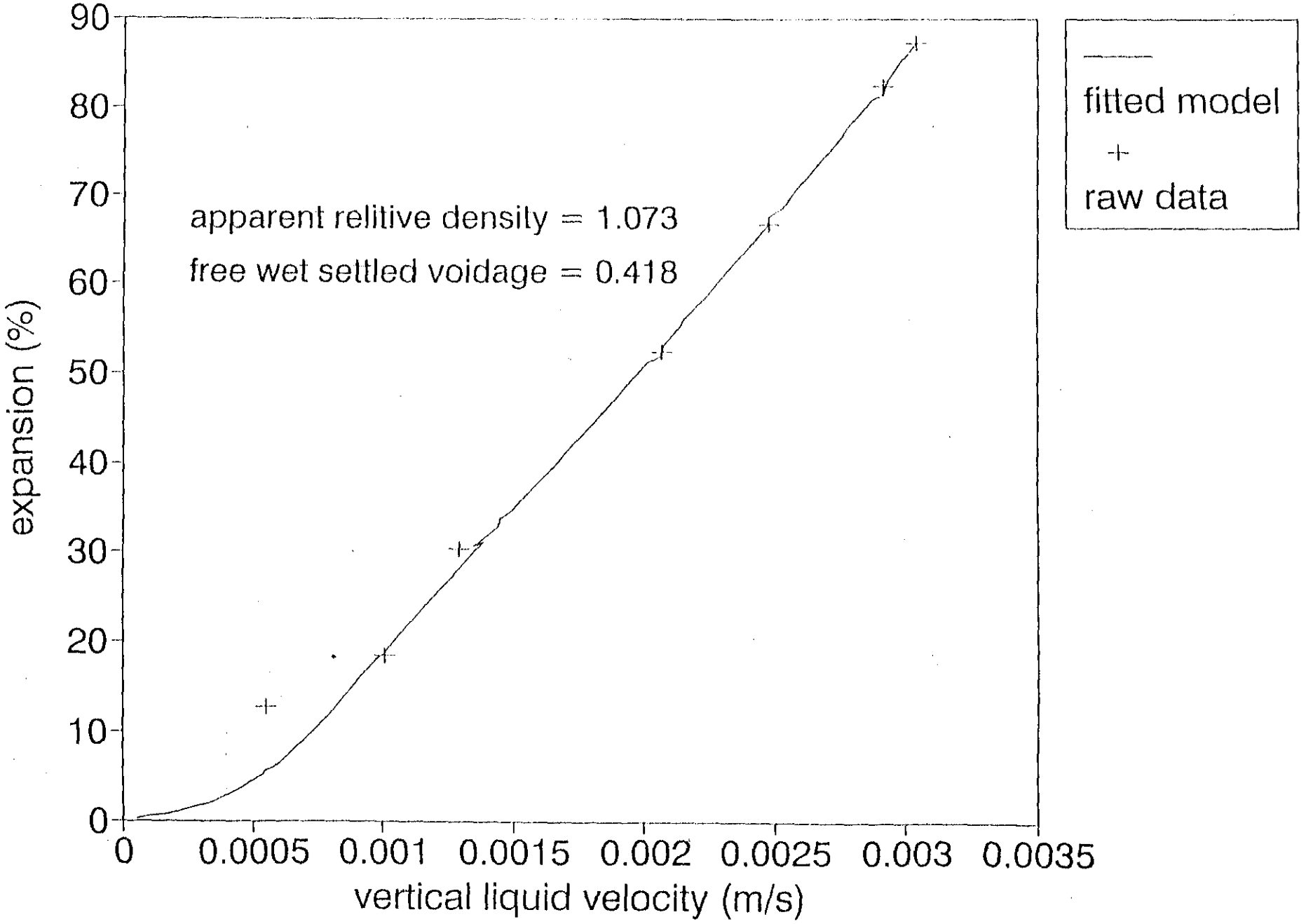
90
80
70
60
50
40
30
20
10
0
expansion (%)
apparent relitive density = 1.073
free wet settled voidage = 0.418
fitted model
raw data
0
0.0005
0.001
0.0015
0.002
0.0025
0.003
0.0035
vertical liquid velocity (m/s)

FIG. 2

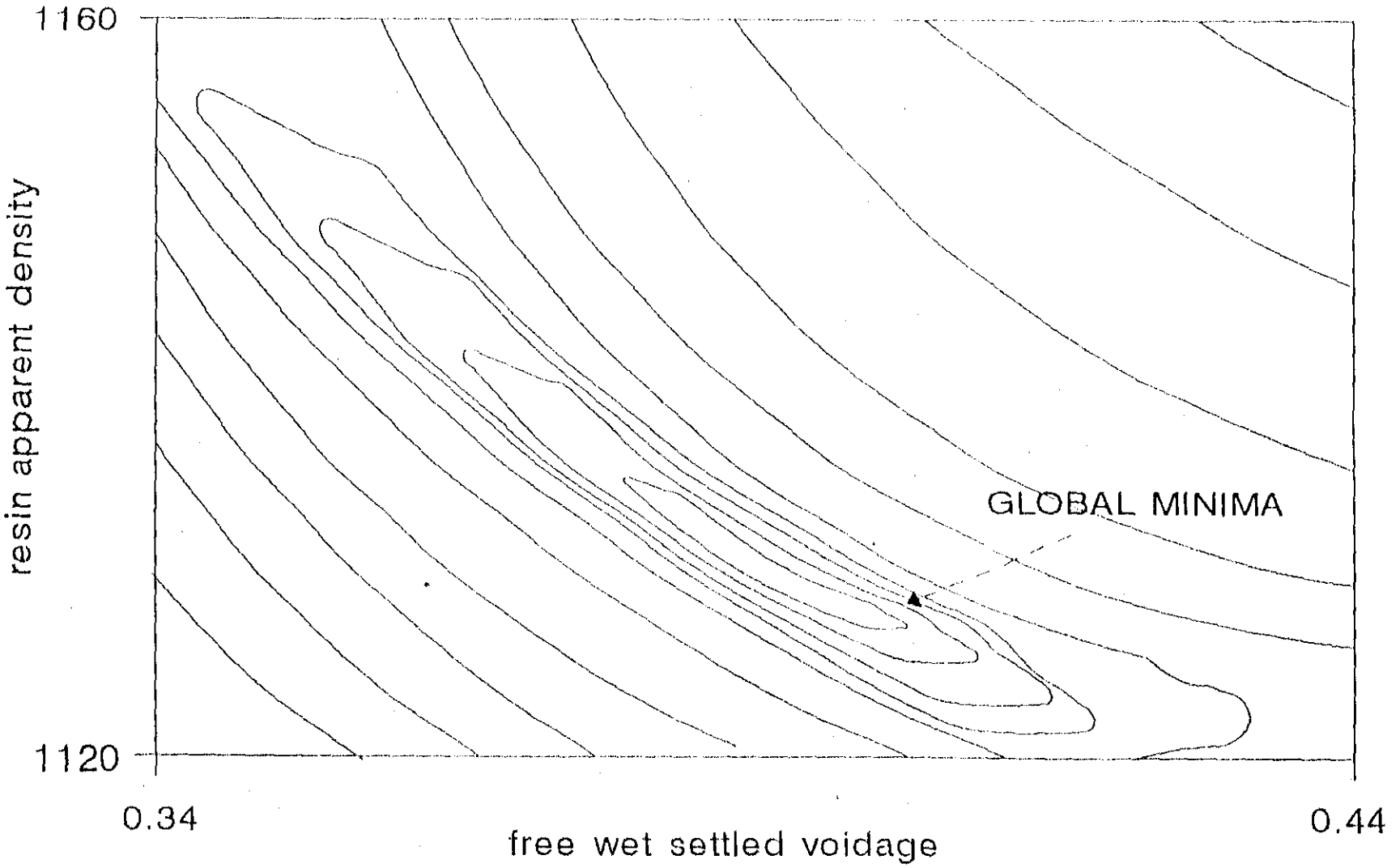
1160
1120
resin apparent density
GLOBAL MINIMA
0.34
0.44
free wet settled voidage

FIG. 8

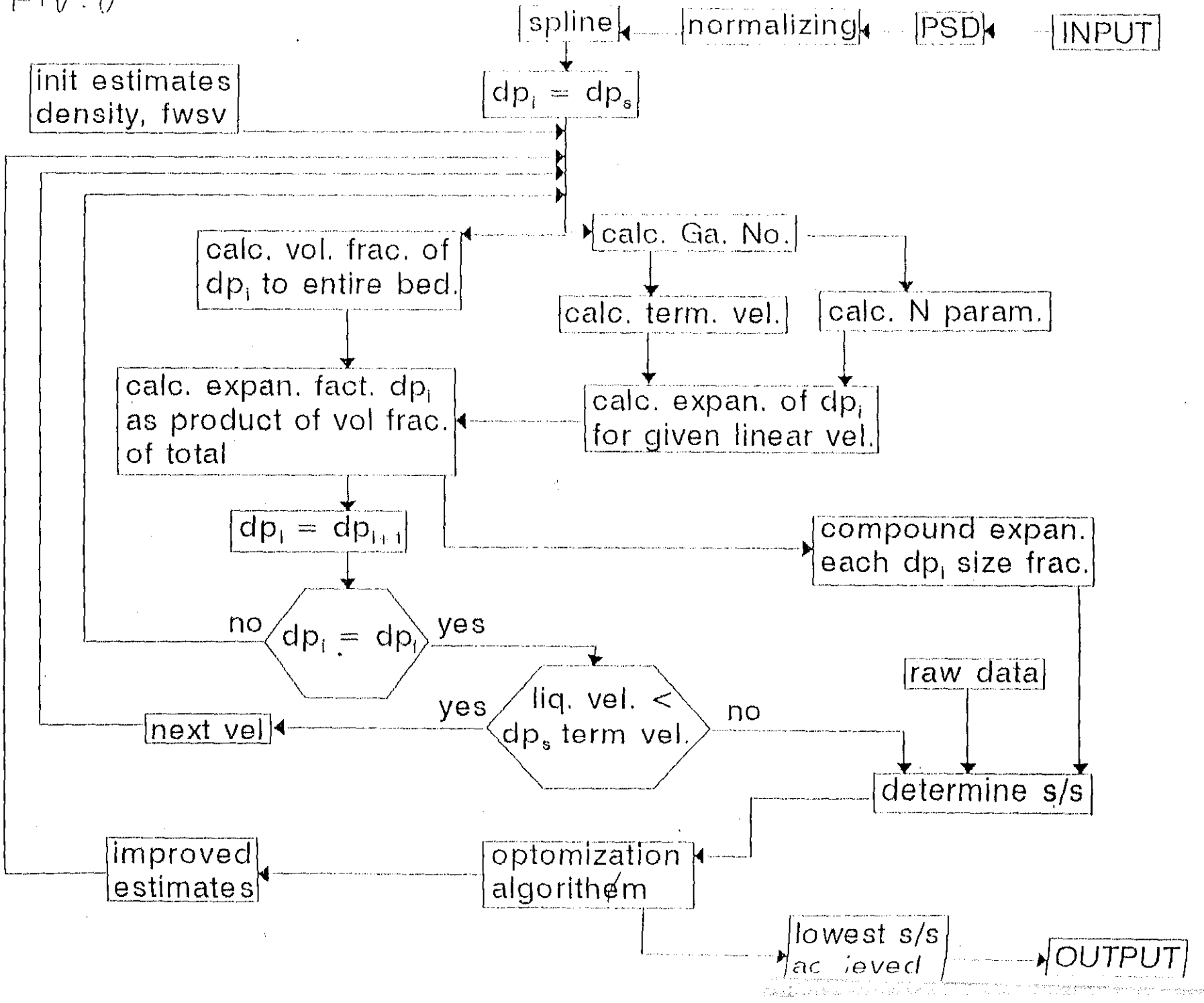
spline
normalizing
PSD
INPUT
init estimates density, fwsv
$dp_i = dp_s$
calc. Ga. No.
calc. vol. frac. of dp_i to entire bed.
calc. term. vel.
calc. N param.
calc. expan. fact. dp_i as product of vol frac. of total
calc. expan. of dp_i for given linear vel.
$dp_i = dp_{i+1}$
compound expan. each dp_i size frac.
no
$dp_i = dp_l$
yes
raw data
yes
liq. vel. < dp_s term vel.
no
next vel
determine s/s
improved estimates
optomization algorithem
lowest s/s achieved
OUTPUT